CELL AUTONOMOUS AND NON-CELL AUTONOMOUS REGULATION OF BETA CELL MASS EXPANSION

By

Jennifer Lynn Plank

Dissertation

Submitted to the Faculty of the

Graduate School of Vanderbilt University

in partial fulfillment of the requirements

for the degree of

DOCTOR OF PHILOSOPHY

in

Cell and Developmental Biology

December, 2011

Nashville, Tennessee

Approved:

Professor Christopher Wright, Chair

Professor Maureen Gannon

Professor David Piston

Professor Roland Stein

Professor Patricia Labosky

To my grandfather for his constant encouragement

And

To my mom and dad for making me the person I have become

ACKNOWLEDGEMENTS

This work would not be possible without the financial support of the Juvenile Diabetes Research Foundation, the University of Georgia Pilot Program Grant, Vanderbilt University Diabetes Research Training Center, and Vanderbilt University Academic Program Support. My training was funded by the Molecular Endocrinology Training Program and an American Heart Association predoctoral fellowship. I was also fortunate enough to receive funding to attend conferences from the Vanderbilt Graduate School, the Vanderbilt Program in Developmental Biology, and the American Society for Cell Biology.

Next, I would like to thank my thesis committee: Chris, Maureen, Dave, and Roland. The members of my committee were incredibly helpful in providing feedback on each of my projects and allowing me to discuss data and experiments with them at any time. The members of my committee were also instrumental in advising me on experimental techniques. I learned the majority of the physiological assays with the help of the Gannon lab. In addition, attending the Gannon lab meetings for the first few years of graduate school was a fantastic opportunity to learn pancreas development. Members of the Wright lab completed the *Xenopus* cap assays used to determine the functionality of Foxd3 fusion proteins. Chris was always willing to meet with me and advise me on the directions of my project and my career path and I'm very grateful for these one-on-one interactions. Roland, and members of his lab, taught me how to do ChIP assays and allowed me to regularly use their sonicator.

Several collaborators within and outside of Vanderbilt were instrumental on my success during graduate school. The department of CDB, the Program in Developmental Biology, and the VCSCB were a fantastic environment to present and discuss research within the university. I'd like to thank Mark Magnuson and his lab for allowing me to use several instruments including the real time PCR machine, Nanodrop, centrifuges, and microscopes. Without these instruments, I would not have been able to achieve nearly as much scientifically. I'd also like to thank several shared resource cores at Vanderbilt including the Islet Procurement and Analysis Core, the Cell Imaging Shared Resource Core, and the Transgenic Mouse and ES cell shared resource core. Several of the experiments were completed by or in collaboration with these various cores. The *Pdx1-Cre* mice were generated by Dave Tuveson and Andy Lowy and the *Wnt1-Cre* mice were generated by Dave Rowitch and Andy McMahon. Steve Dalton from the University of Georgia provided me with human ES cells and Michael Kyba from the University of Minnesota provided me with the vectors and cells for Induced Cassette Exchange. Lastly, I'd like to thank Anna Means for her encouragement, feedback, and support.

The Labosky lab was an ideal environment for me to complete my Ph.D. Audrey Frist was an excellent source of technical support. Previous and current lab members, Ying Liu, Brian Nelms, Nathan Mundell, Elise Pfaltzgraff, and Michael Suflita have provided a significant amount of both technical and moral support. Without the help of Alison LeGrone, who is a coworker and also a friend, our mouse colony would not have run nearly as smoothly! Alison's calmness and willingness to help was invaluable, especially during the last 6 months to a year of research. Working for Trish has been a wonderful experience. She has been supportive on so many levels- scientifically,

professionally, and personally. Without her support and encouragement I would not have been as successful. She's been an example that you can balance life in the lab as well as a healthy life at home, something I will strive to achieve in my career.

Lastly, I need to thank my family and friends, specifically my mom and grandfather. Although many of them did not understand what I did on a daily basis, they were always willing to listen to me vent and congratulate me when something major happened. Without their moral support, this journey would not have been as enjoyable.

TABLE OF CONTENTS

LIST OF TABLES

LIST OF FIGURES

LIST OF ABBREVIATIONS

AAALAC	Association for Accredidation and Assessment of Laboratory Animal Care
ACS	American Cancer Society
ADA	American Diabetes Association
Akt1	Thymoma Viral Proto-oncogene 1
Akt2	Thymoma Viral Proto-oncogene 2
Alb1	Albumin1
ANOVA	Analysis of Variance
Arx	Aristaless related homeobox
Bmi1	Bmi1 Polycomb Ring Finger Oncogene
BrdU	5-bromo-2'-deoxyuridine
BSA	Bovine Serum Albumin
°C	Degrees Celsius
CD	Compact Disc
Cdc123	Cell Division Cycle homolog 123
CDK4	Cyclin Dependent Kinase 4
Cdkn	Cyclin Dependent Kinase Inhibitor
cDNA	Complementary DNA
ChIP	Chromatin Immunoprecipitation
CHO	Chinese Hamster Ovary
Ct	Critical Threshold
Cy	Cyanine
DAB	3,3'-Diaminobenzidine
DAPI	4',6-diamidino-2-phenylindole
DMF	Dimethylformamide
DMSO	Dimethyl Sulfoxide
DNA	Deoxyribonucleic Acid
DP	Dorsal Pancreas
dpc	Days Post Coitum
EB	Embryoid Body
Ednrb	Endothelin receptor type b
EDTA	Ethylenediaminetetraacetic Acid
EGTA	Ethylene Glycol Tetraacetic Acid
ELISA	Enzyme-Linked Immunosorbent Assay
ES	Embryonic Stem
ESC	Embryonic Stem Cell
Ezh2	Enhancer of Zeste Homolog 2
FABP7	Fatty Acid Binding Protein 7
FBS	Fetal Bovine Serum

FGF	Fibroblast Growth Factor
Flk1	Fetal liver kinase 1
Foxd	Forkhead box
FS	Frozen section
Gata4	GATA binding protein 4
Gcg	Glucagon
GDM	Gestational Diabetes Mellitus
Glut2	Glucose Transporter 2
HNF4a	Hepatic Nuclear Factor 4a
HPRT	Hypoxanthine-Guanine Phosphoribosyl Transferase
IACUC	Institutional Animal Care and Use Committee
ICC	Immunocytochemistry
IEQ	Islet Equivalents
IGRP	Islet Specific Glucose-6-Phosphate Catalytic Subunit Specific Protein
Ins1	Insulin1
Ins2	Insulin2
IPGTT	Intraperitoneal Glucose Tolerance Test
iPS cell	Induced pluripotent stem cell
KCl	Potassium Chloride
LB	Luria Broth
Lepr	Leptin Receptor
LIF	Leukemia Inhibitory Factor
LPM	Lateral Plate Mesoderm
Mafa	Musculoaponeurotic Fibrosarcoma Oncogene Homolog A
Mafb	Musculoaponeurotic Fibrosarcoma Oncogene Homolog B
MEF	Mouse Embryonic Fibroblast
Menin1	Multiple Endocrine Neoplasia 1
MIP	Mouse Insulin Promoter
Mnx1	Motor Neuron and Pancreas Homeobox1
NaCl	Sodium Chloride
NC	Neural Crest
Neo	Neomycin Resistant
Neurog3	Neurogenin3
Nkx2.2	Neurokinin2 Transcription Factor Related, Locus 2
OCT	Opitmal Cooling Temperature
p5PolII	Phosphorylated serine 5 RNA Polymerase II
Pax	Paired box gene
PBS	Phosphate Buffered Saline
PCR	Polymerase Chain Reaction
PDGF	Platelet Derived Growth Factor
Pdx1	Pancreatic and Duodenal Homeobox 1
PE	Paraffin Embedded

PFA	Paraformaldehyde
PGK	Phosphoglycerate Kinase
Pgp9.5	Protein Gene Product 9.5
Phox2b	Paired-like Homeobox 2b
PL	Placental Lactogen
PP	Pancreatic Polypeptide
PRC2	Polycomb repressive complex 2
Ptf1a	Pancreas Transcription Factor 1a
qPCR	Quantitative PCR
qRT-PCR	Quantitative Reverse Transcription PCR
RNA	Ribonucleic Acid
rpm	Revolutions Per Minute
rtTA	Tetracycline Reverse Transciptional Activator
SEM	Standard Error of the Mean
Skp2	S-phase Kinase Associated Protein 2
Sox	SRY-related HMG box
St5	Suppressor of tumorigenicity 5
T2D	Type 2 Diabetes
TBST	Tris Buffered Saline with 1 percent Tween-20
TCF7L2	Transcription factor 7 like 2
TE	Tris EDTA
TEM	Transmission Electron Microscopy
TM	Tamoxifen
TSA	Tyramide Signal Amplification
TUNEL	Terminal Deoxynucleotidyl Transferase dUTP Nick End Labeling
Vamp2	Vesicle Associated Membrane Protein 2
VP	Ventral Pancreas
WM	Whole Mount
X-gal	5-bromo-4-chloro-3-indolyl- beta-D-galactopyranoside
YFP	Yellow Fluorescent Protein

CHAPTER I

INTRODUCTION

Abstract

Diabetes mellitus affects approximately 150 million people worldwide. This disease is characterized by hyperglycemia resulting from dysfunctional pancreatic beta cells. Current treatments for diabetics are inadequate because they often do not prevent complications associated with the disease; therefore, considerable efforts are focused on derivation of beta cells from embryonic stem cells. Accomplishing this requires a precise understanding of beta cell development and the molecular control of beta cell expansion *in vivo.* We addressed these approaches in two ways: first, we analyzed the requirement for neural crest (NC) derivatives in regulating beta cell maturation and second, we determined that the transcription factor Foxd3 is required for beta cell mass expansion during pregnancy.

The pancreas develops through a coordinated system of signals from both the endoderm and surrounding mesoderm. Little effort has been devoted to analyzing the role of ectodermally-derived NC that innervates the pancreas during embryogenesis. Our work illustrated that NC enters the pancreatic primordium around 10.25 dpc, shortly after pancreatic evagination from the foregut epithelium. Using a genetic ablation of NC derivatives in the pancreas, we showed, in agreement with published data, increased beta cell proliferation and insulin-positive area. Additionally, our work illustrated a novel requirement for this lineage; NC derivatives are required for beta cell maturation.

Beta cell proliferation in adult mice is rare unless the mice are metabolically challenged, such as during pregnancy. Therefore, I chose to analyze the requirement for Foxd3 during pregnancy. Foxd3 is expressed in the pancreatic primordium beginning at 10.5 dpc and is localized predominantly to beta cells after birth. Virgin mice carrying a pancreas-specific deletion of Foxd3 are euglycemic; however, during pregnancy these mice become glucose intolerant. Several genes required for cell proliferation are misregulated in the absence of Foxd3 resulting in decreased beta cell proliferation and beta cell mass during pregnancy.

Together, my thesis research illustrated the requirement for NC derivatives in controlling beta cell maturation and demonstrated a novel role for Foxd3 in beta cell mass expansion during pregnancy. The findings from both studies can be applied to cell-based therapies to treat diabetics.

Pancreas anatomy and function

Pancreas anatomy and function: The pancreas is a glandular organ responsible for secreting hormones to regulate blood glucose levels and enzymes to aid digestion (Berne, 1993). In humans, the head of the pancreas (ventral pancreas) is located adjacent to the duodenum while the tail of the pancreas (dorsal) is located adjacent to the stomach and spleen. The pancreas is connected to the duodenum by the ampulla of Vater, the location where the pancreatic duct connects to the common bile duct (Figure 1.1, reviewed in (Slack, 1995)).

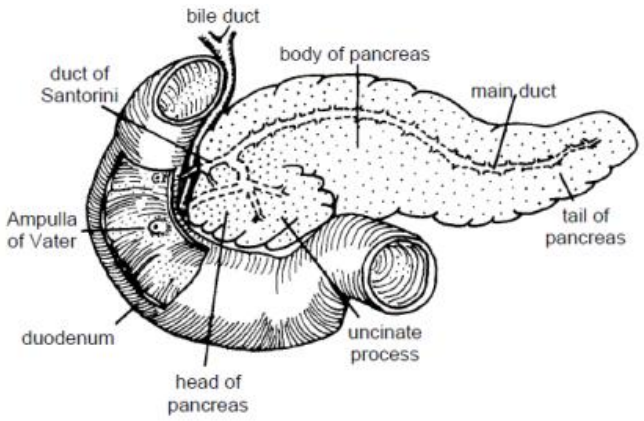

Figure 1.1: Diagram of the human pancreas. The head of the pancreas (ventral pancreas) is attached to the duodenum at the Ampulla of Vater. The main pancreatic duct connects to the bile duct. The tail of the pancreas (dorsal pancreas) is adjacent to the stomach and spleen. This image was taken from (Slack, 1995).

The endodermally-derived pancreas consists of 2 cell types: the exocrine pancreas that is responsible for secreting enzymes required for digestion and the endocrine pancreas that secretes hormones to regulate blood glucose levels (Figure 1.2, reviewed in (Slack, 1995)). Approximately 98 percent of the pancreatic mass is comprised of exocrine tissue consisting of acinar and ductal cells. The acinar cells produce enzymes including proteases, amylases, lipases, and nucleases that aid in digestion. These pancreatic enzymes are secreted by the acinar cells into the ducts as immature proteins in zymogen granules and eventually drain into the duodenum where they are activated (Bruno, 1995). Additionally, centroacinar cells adjacent to the pancreatic duct produce and secrete bicarbonate to neutralize acidic chyme located in the stomach while the goblet cells located within the ductal epithelium produce and secrete mucin (Berne, 1993; Grapin-Botton, 2005).

This essential organ is conserved among all vertebrates, although the structure and organization of the pancreas is different in some fish. Additionally, while most invertebrates do not have a pancreas, some have endocrine cells similar to beta cells located in the gut or brain (reviewed in (Slack, 1995)).

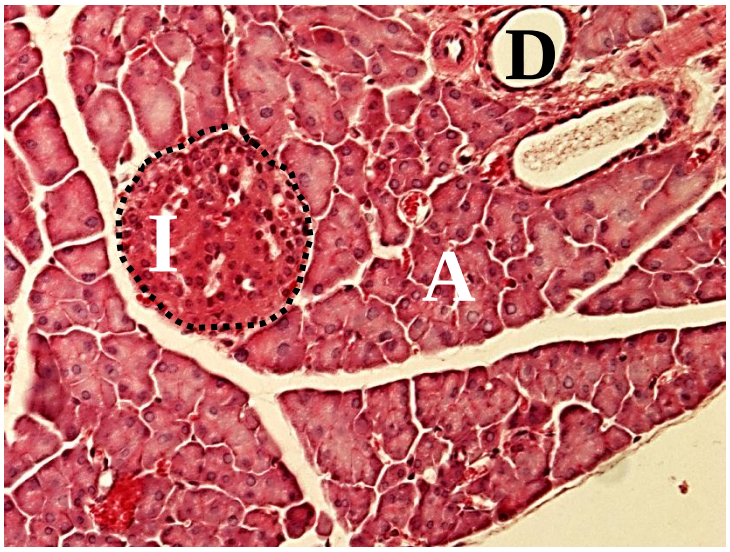

Figure 1.2: The acinar cells of the pancreas (A) which produce enzymes to aid in digestion and ductal cells (D) which facilitate draining of enzymes into the duodenum form the exocrine pancreas. The endocrine cells are located in the islets of Langerhans (I). Cell types within the pancreas can be distinguished histologically using hematoxylin and eosin staining.

Pancreatic endocrine cells comprise approximately 2 percent of the entire pancreatic mass and are responsible for producing hormones that regulate blood glucose levels. The endocrine cells are organized into spherical microorgans called the islets of Langerhans consisting of 5 different endocrine cell types (Figure 1.3A reviewed in

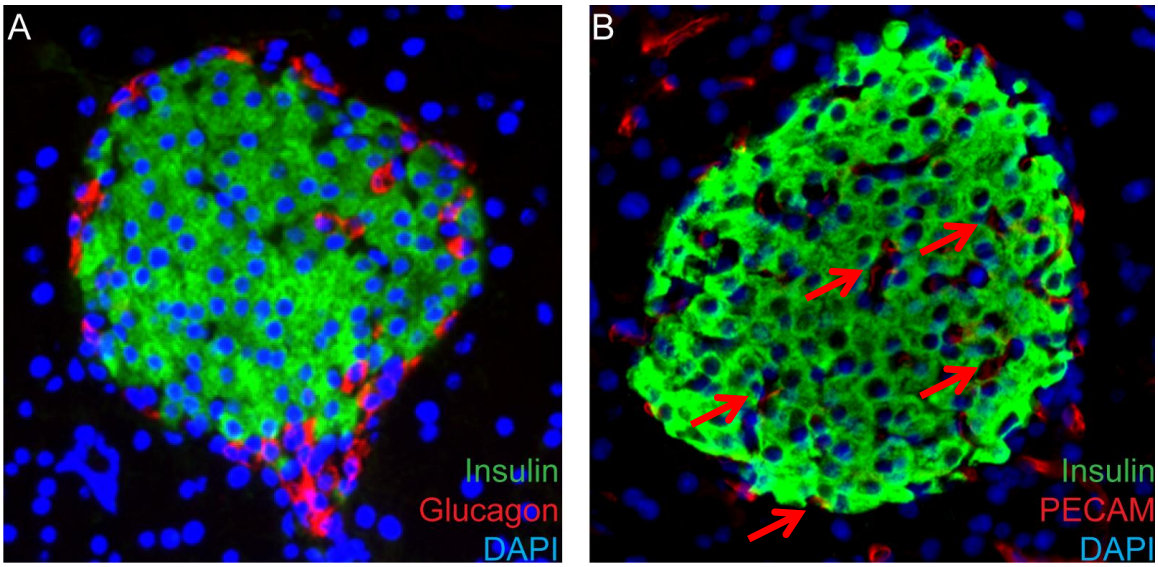

Figure 1.3: Images of murine islets. A. In murine islets, beta cells (indicated by insulin immunofluorescence, green) are located at the core of the islets of Langerhans while other endocrine cell types are primarily located at the periphery of the islets. In this image, alpha cells (indicated by glucagon immunofluorescence, red) are located at the periphery of the islets. B. Islets are highly vascularized; many blood vessels (indicated by PECAM immunofluorescence, red) are detected in the islets (indicated by insulin immunofluorescence, green). Red arrows, PECAM-positive endothelial cells.

(Edlund, 2002; Murtaugh and Melton, 2003)). The islets are highly vascularized mediating secretion of hormones into the blood flow (Figure 1.3B,(Lifson et al., 1985)). The most abundant islet cell type in most mammals, including rodents, primates, camels, bats, whales, and seals, is the beta cell (Steiner et al., 2010); beta cells are the only cell in the body capable of secreting insulin in response to blood glucose levels. When blood glucose levels are high insulin is secreted into the blood stimulating glucose uptake by peripheral tissues such as the liver, skeletal muscle, or adipose cells (Berne, 1993). The second most abundant cell type in the islets is the glucagon-producing alpha cell. Glucagon function opposes insulin; glucagon is secreted when blood sugar is low causing the liver to convert glycogen to glucose (Berne, 1993). The third most abundant cell type

in the islets is the somatostatin-producing delta cells that secrete somatostatin to inhibit secretion of both glucagon and insulin. The pancreatic polypeptide (PP) cells secrete PP to regulate endocrine and exocrine cell secretion (Lonovics et al., 1981). Finally, the least abundant endocrine cell is the ghrelin-producing epsilon cell. Epsilon cells are abundant in the islets during embryogenesis and in the adult under certain circumstances (Prado et al., 2004). While ghrelin secreted from the stomach is known to stimulate hunger, the function of ghrelin in the islets is less understood although some investigators suggest that ghrelin regulates proliferation and survival of beta cells (Prado et al., 2004; Sussel et al., 1998). Together, the endocrine cells in the pancreas function to precisely control blood glucose levels.

Pancreatic dysfunction: Dysfunction of either the exocrine or endocrine pancreas results in serious clinical complications. Diabetes mellitus results from insufficient production of insulin to compensate for blood glucose levels. Approximately 25.8 million people in the United States, or 8.3 percent of the population, has diabetes and another 79 million are considered to be pre-diabetic resulting in an economic burden of 218 billion dollars per year (ADA, 2011). To properly control diabetes, treatments such as exogenous insulin injections are used to lower blood glucose levels. However, even slight hyperglycemia can result in secondary complications such as heart disease, stroke, high blood pressure, blindness, kidney disease, neuropathy, and amputation of extremities demonstrating the importance of precisely controlling the disease (Genuth, 2006).

There are three major classes of diabetes: type 1, type 2, and gestational diabetes (GDM). Type 1 diabetes, formerly called juvenile diabetes, is an autoimmune disorder that results in destruction of pancreatic beta cells (Devendra et al., 2004). Type 1 diabetes

is most commonly developed during childhood although patients can develop the disease at any age. The most common treatment for type 1 diabetic patients is exogenous insulin injections. Type 2 diabetes is characterized by insulin resistance followed by beta cell failure. In early stages of type 2 diabetes, patients can be treated with oral medication such as sulfonylurea drugs; however, late stage type 2 diabetic patients ultimately become dependent on exogenous insulin injections (Laybutt et al., 2007; Scheuner et al., 2001; Scheuner et al., 2005). During pregnancy, peripheral tissues become insulin resistant and the beta cell population must expand to compensate for increased metabolic demand. GDM occurs in patients whose beta cells are unable to overcome the increased need for insulin due insulin resistance in peripheral tissues (Parsons et al., 1992). Normally, GDM patients are euglycemic following parturition; however, they have an increased risk of developing type 2 diabetes later in life (Bellamy et al., 2009).

In addition to diseases of the endocrine pancreas, dysfunction in the exocrine pancreas can result in severe clinical implications. Pancreatic cancer is the fourth most common cause of cancer related deaths (Hariharan et al., 2008). Additionally, patients diagnosed with pancreatic cancer have a very poor prognosis; only 6 percent of patients diagnosed with pancreatic cancer survive 5 years with a median survival from diagnosis of 6 to 10 months. The majority of pancreatic cancers (95 percent) are ductal adenocarcinomas; ductal adenocarcinomas occur as a result of pancreatic intraepithelial neoplasias that acquire an oncogenic mutation (ACS, 2005). Primary ductal adenocarcinomas are largely asymptomatic until they metastasize resulting in poor prognosis. A rarer form of pancreatic cancer is neuroendocrine tumors or tumors that originate from the islets. Because neuroendocrine tumors produce high concentrations of

hormones, patients may be more symptomatic than patients with ductal adenocarcinoma and seek treatment earlier resulting in a better prognosis (Ekeblad et al., 2008). Additionally, neuroendocrine tumors are often less aggressive than exocrine tumors resulting in a median survival from diagnosis of 38 to 104 months (Yao, 2007). In addition to tumors that arise from exocrine or endocrine cells, neuroblastomas are an incredibly rare form of pancreatic cancer that results from increased proliferation of NC derivatives that innervate the pancreas during embryogenesis (Vouriot et al., 1985). Neuroblastomas normally originate from sympathetic ganglia, however, in rare cases neuroblastomas can originate from another location within the body. In fact, a recent case study identified a primary neuroblastoma that originated from NC derivatives that innervated the pancreas of a 22 year old female patient and resulted in a fatal outcome (Abdou et al., 2011).

Pancreas and beta cell development

Overview of murine pancreas development: Pancreas development in the mouse begins at approximately 9.5 dpc and occurs by responding to a series of intrinsic factors and extrinsic signaling molecules. At 9.5 dpc, the dorsal foregut epithelium thickens and evaginates to form the presumptive dorsal pancreas. After the evagination of the dorsal pancreatic bud, the ventral foregut epithelium thickens and evaginates to form the ventral pancreatic bud at approximately 10.0 dpc (reviewed in (Pan and Wright, 2011)). Immature endocrine cells expressing glucagon and insulin can be detected at this time (Herrera, 2000). From around 9.5 dpc until around 12.5 dpc, the pancreatic epithelium

undergoes extreme proliferation and branching. The secondary transition, a wave of extensive differentiation of endocrine cells, occurs from 12.5 to 15.5 dpc (reviewed in (Slack, 1995)). During this period, the branching epithelium can be divided into 2 distinct domains: tip and trunk cells (reviewed in (Pan and Wright, 2011)). The cells located in the tip are multipotent progenitor cells that can give rise to endocrine, acinar, or duct cells while cells adjacent to the tips in the trunk are duct-endocrine bipotent progenitor cells (Zhou et al., 2007). The cells that remain at the tip of the branches will form the acinar cells. The endocrine cells produced during the secondary transition will mature and form the glucose-responsive endocrine cells in the adult animal (Herrera, 2000). During late embryonic and early postnatal stages, the endocrine cells form clusters and delaminate from the ductal epithelium to form the mature islets of Langerhans (Rukstalis and Habener, 2007).

Endoderm derivatives: The developing pancreatic endoderm is initially demarcated by three transcription factors that are critical for pancreas development: pancreatic and duodenal homeobox 1 (Pdx1), pancreatic transcription factor 1a (Ptf1a), and motor neuron and pancreas homeobox 1 (Mnx1, formerly called Hb9). In fact, a deletion in any of these factors is catastrophic for pancreas development; *Pdx1* and/or *Ptf1a* null embryos are largely lacking a functional pancreas with only a small dorsal pancreatic rudiment present at 9.5 dpc while *Mnx1* null embryos lack a dorsal pancreas (Harrison et al., 1999; Jonsson et al., 1994; Kawaguchi et al., 2002; Krapp et al., 1998; Offield et al., 1996; Stoffers et al., 1997b). Conversely, a deletion of *Gata4*, a transcription factor expressed in the pancreatic endoderm results in the absence of the ventral pancreas while the dorsal pancreas develops normally (Watt et al., 2007). Additionally, the transcription factors

hepatocyte nuclear factor 1 homeobox beta (Hnf1beta) and SRY-box 9 (Sox9) expressed in the pancreas are critical for initial pancreas development; *Hnf1beta* null embryos do not form a ventral pancreas and dorsal pancreas development is arrested early while *Sox9* null embryos have smaller pancreata than control littermates (Haumaitre et al., 2005; Seymour et al., 2007).

Following the initial specification and outgrowth of the pancreatic buds, the pancreas undergoes extensive proliferation and branching. At around 12.5 dpc, cells in the branching epithelium can be characterized as "tip" or "trunk" cells. The cells located at the "tip" of the branching epithelium are multipotent progenitor cells that express low levels of Ptf1a, Pdx1, Sox9, and Hnf4beta while maintaining high levels of Gata4. Cells at the "tips" lose multipotency between 13.5 and 14.5 dpc, obtain a proacinar fate, and express high levels of Ptf1a and Gata4. Cells that are located within the "trunk" of the branching epithelium are bipotent progenitor cells that can give rise to ductal or endocrine cells. These bipotent progenitors express low levels of Pdx1 and high levels of Sox9 and Hnf1beta. The cells fated to become ductal cells maintain expression of Sox9 and Hnf1beta while Pdx1 expression is decreased. Alternatively, the progenitors fated to become endocrine cells express high levels of the proendocrine factor Neurog3, NeuroD, and Islet1 (reviewed in (Pan and Wright, 2011)). Expression of all 3 factors is required for pancreatic endocrine cell development.

A complicated network of transcription factors is required for specification of beta cells from the endocrine cell progenitors (Figure 1.4). Beta cell specification requires repressive activity of the transcription factor Nkx2.2 (Papizan et al., 2011; Sussel et al., 1998; Wang et al., 2004). *Nkx2.2* null mice develop diabetes due to arrested development of

the pancreatic beta cell (Sussel et al., 1998). Additionally, cells fated to become beta cells express high levels of Pdx1 and the transcription factors v-maf musculoaponeurotic fibrosarcoma oncogene homolog A and B (MafA and MafB), paired box gene 4 (Pax4), and NeuroD. These early insulin-expressing cells are not fully mature or competent to secrete insulin in response to glucose concentration (Herrera, 2000). Towards the end of embryogenesis, the insulin-expressing cells undergo maturation and MafB expression decreases while MafA expression persists (Artner et al., 2010). Additionally, the cells maintain expression of Pdx1 and begin to express the glucose transporter Glut2, islet-specific glucose-6-phosphatase catalytic subunit specific protein (IGRP), and glucokinase to mediate glucose stimulated insulin secretion (Aramata et al., 2005; Artner et al., 2007; Raum et al., 2006; Zhao et al., 2005). Much less is known about the transcriptional profiles of the other endocrine cell types; developing alpha cells express MafB and aristaless related homeobox (Arx), PP cells express Arx, and delta cells express Pdx1 (Artner et al., 2006; Collombat et al., 2005; Collombat et al., 2003).

Mesodermal contributions: The pancreas develops through a series of inductive and permissive signals from the surrounding mesoderm. Both prospective pancreatic buds are adjacent to mesoderm prior to pancreas induction; the prospective dorsal pancreas is adjacent to the notochord and the dorsal aorta while the prospective ventral pancreas is adjacent to the lateral plate mesoderm (reviewed in (Slack, 1995)). Prior to pancreas specification, FGF2 and activin-beta2 signaling from the notochord is required to suppress Shh within the dorsal foregut (Kim et al., 1997). Additionally, retinoic acid secreted from the paraxial mesoderm is required to establish the prospective dorsal

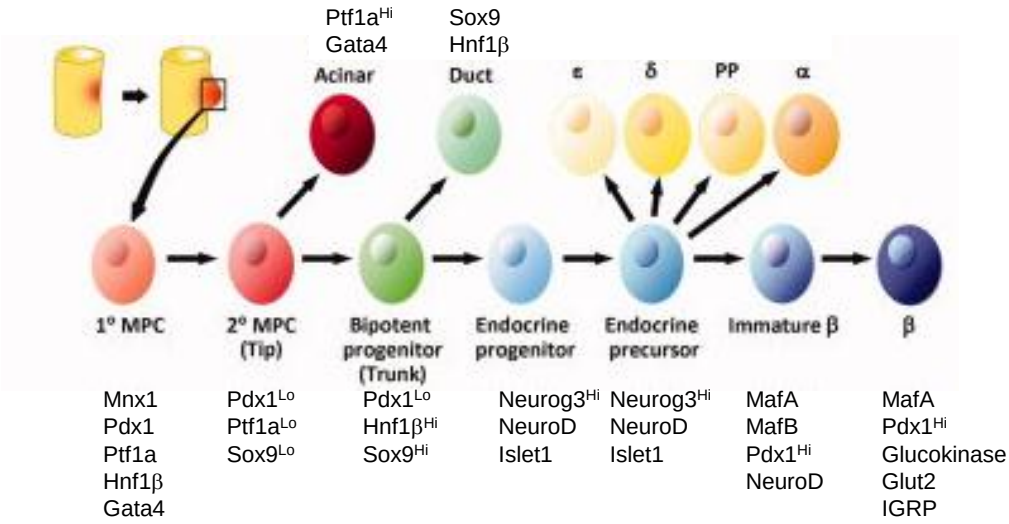

Figure 1.4: Schematic of gene regulatory networks required for pancreas and beta cell development. Details are outlined in the text. Figure adapted from (Pan and Wright, 2011).

pancreatic bud (Martin et al., 2005; Molotkov et al., 2005). Slightly later, the dorsal aorta and the vitelline veins contact the foregut endoderm and induce Pdx1, Ptf1a, and insulin expression in the developing pancreas (Lammert et al., 2001, 2003). *Fetal liver kinase 1 (Flk1)* null mice that lack endothelial cells do not induce Ptf1a expression in the dorsal pancreas (Yoshitomi and Zaret, 2004). Later in development, connective tissue growth factor (CTGF) secreted from endothelial cells results in decreased vascularization reducing beta cell mass expansion; mice carrying a *Tie1-Cre* allele to delete *CTGF* from the endothelial cells have decreased beta cell proliferation compared to littermate controls (Guney et al., 2011).The lateral plate mesoderm (LPM) provides instructive signals to the prospective ventral pancreas bud, although the signal secreted from the LPM remains elusive (Kumar et al., 2003).

As the pancreatic buds grow, the pancreatic mesenchyme condenses around the branching epithelium. Several factors expressed within the pancreatic mesenchyme are essential for pancreas development. Pancreatic buds dissected from embryos at 11.5 dpc and cultured without pancreatic mesenchyme were unable to develop further (Golosow and Grobstein, 1962). Fibroblast growth factor (Fgf10) secreted by the pancreatic mesenchyme recognized by the Fgf receptor 2b (Fgfr2b) in the pancreatic epithelium is required for pancreas development; mice lacking either Fgf10 or Fgfr2b do not form a pancreas (Bhushan et al., 2001; Hart et al., 2003; Miralles et al., 1999). Similarly, bone morphogenetic protein (BMP) signaling from the mesenchyme and recognized by the Alk2/3 receptors in the pancreatic epithelium is required for pancreas development (Ahnfelt-Ronne et al., 2010). A null mutation of *Islet1* results in loss of mesenchyme surrounding the dorsal pancreas resulting in loss of the dorsal exocrine pancreas. Additionally, there is a complete loss of islet cell differentiation (Ahlgren et al., 1997). Similarly, the cell adhesion molecule N-cadherin, which is expressed in the pancreatic mesenchyme but not pancreatic endoderm during early pancreas development, is required for dorsal pancreas outgrowth (Esni et al., 2001). Together, all of these data demonstrate that signals from the developing mesoderm are absolutely required for pancreas development and a complex network of intrinsic and extrinsic signals mediate pancreatic outgrowth and beta cell development. Additionally, my dissertation research demonstrates that the ectodermally-derived NC is a critical regulator of beta cell mass expansion and maturation (Plank et al., 2011b).

Establishing and maintaining pancreatic beta cell mass

An organism's beta cell mass is obtained and maintained by a careful balance of beta cell proliferation, neogenesis, cell size, apoptosis, and atrophy (reviewed in (Ackermann and Gannon, 2007)). While beta cell mass increases significantly during embryogenesis and early postnatal periods in both humans and rodents, following adolescence (or weaning in the case of rodents), beta cell mass increases at a much slower rate than during early postnatal stages (Bonner-Weir, 2000; Bonner-Weir et al., 2010; Bouwens and Rooman, 2005; Finegood et al., 1995). In rodents, beta cell mass expansion is most commonly a result of increased beta cell proliferation (Dor et al., 2004; Teta et al., 2007). Beta cells undergo low levels of proliferation in young animals and as the animals age, beta cell proliferation becomes even more rare under basal physiological conditions (Desgraz and Herrera, 2009; Scaglia et al., 1997; Teta et al., 2007). However, in some instances of metabolic challenge such as obesity or pregnancy, beta cells regain the ability to proliferate (Butler et al., 2007; Rhodes, 2005; Teta et al., 2007; Zhang et al., 2010). Another mechanism for increasing beta cell mass is beta cell neogenesis. Beta cell neogenesis is most robust during embryogenesis; however, it is unclear if beta cell neogenesis can occur in postnatal animals. Some studies indicate that beta cell neogenesis in rodents also occurs perinatally and up to approximately 2 to 3 weeks of age (Finegood et al., 1995). In addition to beta cell proliferation and neogenesis, beta cell hypertrophy regulates beta cell mass in humans and rodents. While beta cell size does not usually change drastically, beta cells can increase in size to compensate for increases in body mass (Montanya et al., 2000; Park et al., 2008; Scaglia et al., 1997). To avoid decreasing an organism's beta cell mass, negative regulators of beta cell mass expansion such as

apoptosis and atrophy are rarely observed in healthy animals, although a wave of apoptosis occurs in postnatal rats around 3 weeks of age (Scaglia et al., 1997). Together these mechanisms tightly regulate beta cell mass in healthy animals.

Postnatal beta cell mass expansion is maintained by a complex system of transcription factors, cell cycle regulators, tumor suppressors, growth factors, and cytokines. Some of the key regulators of beta cell mass are highlighted in this section. Loss of one copy of *Pdx1* results in decreased beta cell mass and increased beta cell apoptosis (Johnson et al., 2003). Similarly, a beta cell specific deletion of *Pdx1* results in the loss of beta cell identity. Specifically, Pdx1 is required to regulate expression of *Glut2* which is essential for glucose stimulated insulin secretion (Ahlgren et al., 1998; Gannon et al., 2008). Importantly, the requirement for PDX1 is conserved in humans; a missense mutation of PDX1 results in mature onset diabetes of the young (MODY) (Stoffers et al., 1997a).

Placental lactogen (PL) signaling also regulates beta cell mass expansion. Mice over expressing PL exhibit increased beta cell mass, proliferation and hypertrophy (Cozar-Castellano et al., 2006; Vasavada et al., 2000). Conversely, a null mutation of the PL receptor results in decreased beta cell mass (Freemark et al., 2002). The transcription factor Foxm1 functions downstream of PL signaling (Zhang et al., 2010), and it is a critical regulator of beta cell mass expansion (Ackermann-Misfeldt et al., 2008; Zhang et al., 2006; Zhang et al., 2010). Mice lacking Foxm1 in the pancreas have reduced beta cell mass by 6 weeks of age due to decreased proliferation and male mutant mice have overt diabetes by 9 weeks of age (Zhang et al., 2006). The S-phase kinase associated protein 2 (Skp2) functions downstream of Foxm1; *Skp2* null mice have decreased beta cell mass

and proliferation but increased beta cell size (Zhong et al., 2007). The cell cycle inhibitor Cdkn1b ($p27^{kip1}$) functions downstream of Foxm1 and Skp2, and in the absence of Foxm1, Cdkn1b accumulates in beta cells (Zhang et al., 2006). A null mutation of *Cdkn1b* results in increased beta cell proliferation and mass (Georgia and Bhushan, 2006) while ectopic expression of Cdkn1b in the beta cell results in decreased beta cell proliferation and mass (Uchida et al., 2005).

Another growth factor implicated in beta cell mass expansion is platelet derived growth factor (PDGF). In rodents and humans, expression of PDGF receptor (PDGFr) in the islets decreases with age coincident with decreasing beta cell proliferation. A beta cell-specific deletion of *PDGFr* results in decreased beta cell proliferation and beta cell mass. Alternatively, over expression of human PDGFr-alpha in mouse beta cells results in increased beta call mass expansion and proliferation. Additionally, juvenile human islets cultured with PDGF-AA ligand showed increased beta cell proliferation (Chen et al., 2011). Together these data suggest that PDGF signaling is a potent regulator of beta cell proliferation in humans and rodents. The enhancer of zeste homolog 2 (Ezh2) is a downstream target of PDGF signaling (Chen et al., 2011). Ezh2 is the histone methyltransferase of the polycomb repressor complex 2 (PRC2) (Cao et al., 2002; van der Vlag and Otte, 1999). Similar to expression of PDGFr, expression of Ezh2 in the islets decreases upon aging (Chen et al., 2011). A beta cell specific mutation of Ezh2 results in glucose intolerance; in the absence of Ezh2, the cell cycle inhibitor Cdkn2a ($p16^{Ink4a}$) accumulates in the beta cell inhibiting proliferation and beta cell mass expansion (Chen et al., 2009a). A null mutation of *Cdkn2a* results in increased beta cell proliferation while ectopic expression results in impaired beta cell proliferation (Krishnamurthy et al., 2006).

These data demonstrate that PDGF regulates beta cell proliferation upstream of Ezh2 and Cdkn2a.

Another regulator of beta cell mass expansion is the multiple endocrine neoplasia 1 (Menin1) tumor suppressor gene. Menin1 promotes expression of the cell cycle inhibitors Cdkn2c and Cdkn1b ($p18^{Ink4c}$ and $p27^{Kip1}$) (Milne et al., 2005). Mice that are heterozygous for *Menin1* have increased beta cell proliferation and beta cell mass but develop islet tumors (Karnik et al., 2005). Similarly, a beta cell specific deletion of *Menin1* results in increased beta cell mass and beta cell proliferation (Crabtree et al., 2003). Conversely, ectopic expression of Menin1 in beta cells results in decreased beta cell mass (Karnik et al., 2007). A null mutation of *Cdkn2c*, a target of Menin1, results in increased beta cell mass (Pei et al., 2004), presumably through increased beta cell proliferation. Together, all of these data demonstrate that regulation of beta cell mass expansion and maintenance is a tightly regulated process requiring several gene regulatory networks to ensure the organism's beta cells are sufficient to secrete insulin in response to blood glucose levels and prevent hyperglycemia A model based on date from the literature indicating a subset of factors required to establish and maintain beta cell mass is depicted in Figure 1.5.

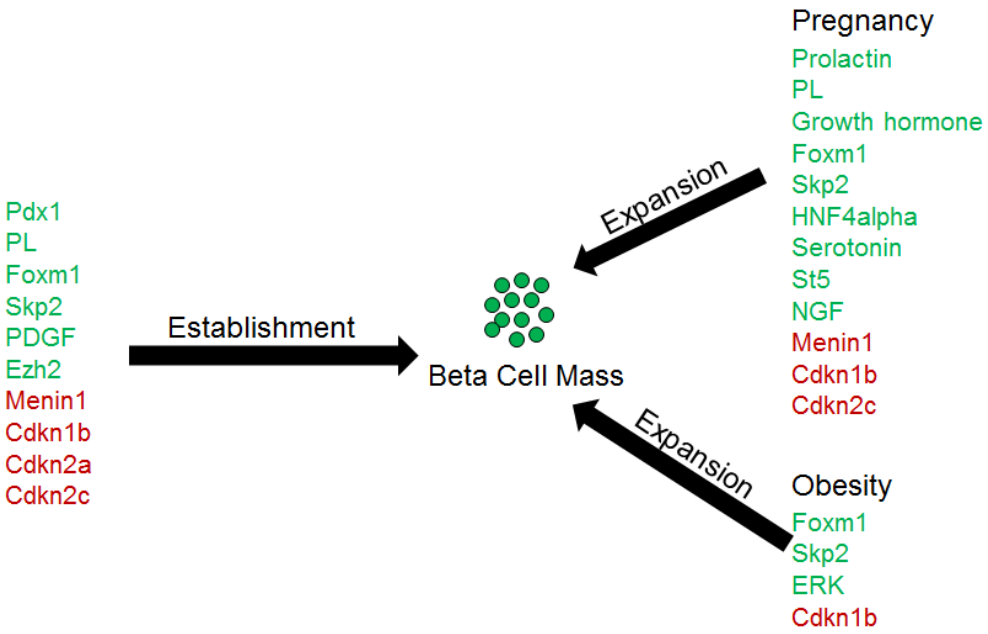

Figure 1.5: Genes and pathways required for beta cell mass establishment and expansion. Positive regulators of beta cell mass/establishment are indicated in green while negative regulators are indicated in red. Some conserved factors, including Foxm1, Skp2, and Cdkn1b are utilized in all three scenarios. This implies similarities in regulating beta cell mass expansion and ultimately glucose homeostasis in multiple physiological contexts.

The impact of metabolic challenge on beta cell mass expansion

During physiological states of increased insulin resistance, such as pregnancy and obesity, beta cell mass must expand to meet the increased metabolic demand. Failure to adequately increase beta cell mass results in diabetes: type 2 in the case of obesity and gestational diabetes (GDM) in the case of pregnancy. Because 70 percent of women who develop GDM go on to develop type 2 diabetes, it is likely that the factors contributing to GDM are conserved in the onset of type 2 diabetes (Rieck and Kaestner, 2010). Additionally, at the onset of type 1 diabetes, an autoimmune response destroys the majority of beta cells; however, the remaining beta cells proliferate in an attempt to compensate. Ultimately, this attempt will be unsuccessful and the majority of the beta

cell population (greater than 99 percent) will be lost (Meier et al., 2005). A model of factors required for beta cell mass expansion during periods of metabolic challenge are depicted in Figure 1.5.

Pregnancy: During pregnancy, peripheral tissues become insulin resistant necessitating increased insulin production and secretion during this metabolically challenging time (Brelje et al., 1993; Parsons et al., 1992; Sorenson and Brelje, 1997). During rodent pregnancy, there is a 3 to 4 fold increase in beta cell mass through increased proliferation and hypertrophy (Brelje et al., 1993; Parsons et al., 1992; Rieck et al., 2009; Sorenson and Brelje, 1997). Specifically, this increase in proliferation peaks approximately two-thirds of the way through gestation (Karnik et al., 2007; Rieck et al., 2009). Following parturition, the beta cell mass returns to normal through decreased proliferation, increased atrophy, and increased apoptosis (Scaglia et al., 1995). A schematic of beta cell mass dynamics during pregnancy is depicted in Figure 1.6.

Regulation of beta cell mass expansion during pregnancy occurs through coordination of several gene regulatory networks. Factors required for beta cell proliferation and beta cell survival are both critical for beta cell mass expansion. PL, prolactin, and growth hormone signaling positively regulate beta cell proliferation during pregnancy. Over expression of PL in beta cells results in increased beta cell proliferation and hypoglycemia (Vasavada et al., 2000). Alternatively, a null deletion of the prolactin receptor which mediates PL and prolactin signaling results in decreased beta cell mass and decreased insulin secretion (Freemark et al., 2002). The transcription factor Foxm1 functions downstream of PL signaling and is required for beta cell mass expansion during

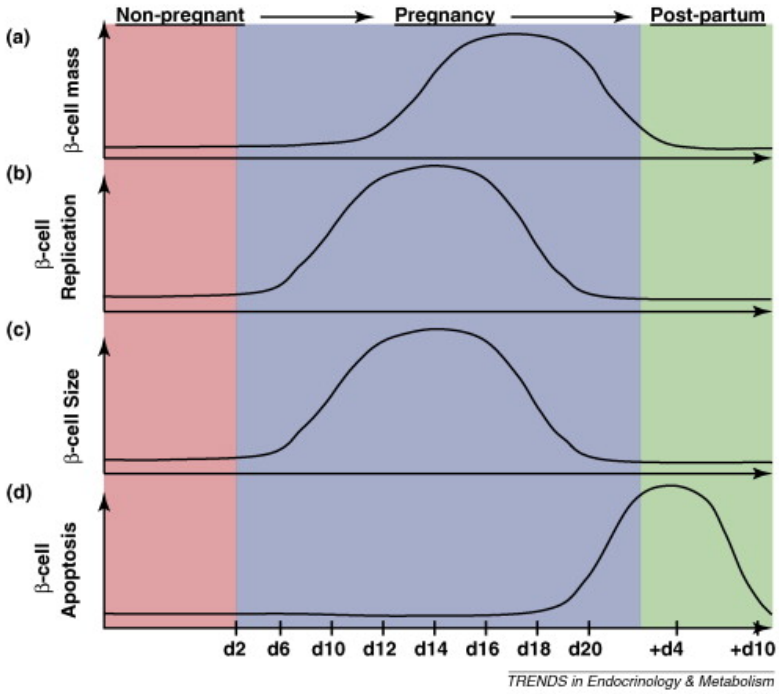

Figure 1.6: A schematic of beta cell mass dynamics during and following rodent pregnancy. The peak of beta cell proliferation and hypertrophy occurs approximately two thirds of the way through pregnancy (b,c) resulting in increased beta cell mass (a). Following parturition, a wave of apoptosis occurs (d) resulting in the beta cell mass returning to pre-pregnancy levels (a). Image taken from (Rieck and Kaestner, 2010).

pregnancy; a pancreas-specific deletion of *Foxm1* results in gestational diabetes (Zhang et al., 2010). In addition, inhibition of serotonin synthesis, normally increased in response to PL signaling, results in decreased beta cell mass expansion and glucose intolerance during pregnancy (Kim et al., 2010). A gene misregulated in mature onset diabetes of the young (MODY1), Hepatic nuclear factor alpha (Hnf4alpha (Stoffel and Duncan, 1997)), is required for beta cell mass expansion. A beta cell-specific deletion of *Hnf4alpha* results in decreased beta cell proliferation, beta cell mass, pancreatic insulin content, and islet size resulting in impaired glucose tolerance. Hnf4alpha is required for transcription of *suppression of tumorigenicity 5 (St5*), encoding a protein that mediates ERK

phosphorylation (Gupta et al., 2007). An additional mechanism for glucose homeostasis regulation and beta cell proliferation is at the epigenetic level. Menin1 functions as part of a histone methyltransferase complex to promote tri-methylation of histone 3 lysine 4 (H3K4), thereby maintaining expression of cell cycle inhibitors Cdkn1b and Cdkn2c. Menin1 is normally downregulated in beta cells during pregnancy, and artificially maintained expression during pregnancy causes decreased beta cell proliferation and maternal hyperglycemia (Karnik et al., 2007).

In addition to factors that regulate beta cell proliferation, factors regulating beta cell survival are also required for beta cell mass expansion during pregnancy. The transcription factor c-myc regulates both proliferation and survival. Ectopic expression of c-myc in the beta cell results in increased proliferation and apoptosis, thereby resulting in diabetes reinforcing the importance of the properly balancing proliferation and apoptosis (Laybutt et al., 2002). Additionally, inhibiting caspase 3 while over expressing c-myc results in increased beta cell proliferation and beta cell mass (Radziszewska et al., 2009). A signaling cascade required for beta cell survival is neural growth factor (NGF) signaling. Expression of neural growth factor receptor (NGFr, p75) in islets increases during pregnancy (Rieck et al., 2009), and NGF signaling contributes to beta cell survival (Navarro-Tableros et al., 2004). Together, this work suggests that the delicate balance of beta cell proliferation and survival is regulated by a complicated network of signaling pathways and transcription factors.

Obesity: Another physiological cause of insulin resistance is obesity. Obese humans and rodents must expand their beta cell mass to compensate for obesity-induced insulin resistance and failure to do so results in type 2 diabetes. Several factors and pathways

required for beta cell mass expansion during pregnancy are utilized in the obese state. For example, Foxm1 is required for beta cell mass expansion in both instances; islets isolated from obese, non-diabetic C57BL/6 *Leptin*$^{ob/ob}$ mice express higher levels of Foxm1 than islets isolated from obese, diabetic BTBR *Leptin*$^{ob/ob}$ mice. In the non-diabetic mice, Foxm1 activates a transcriptional network required for beta cell proliferation. Additionally, a study was conducted where islets were isolated from non-diabetic cadaveric donors with a body mass index (BMI) ranging from 24 to 51 (a BMI of 30 or greater is considered obese) and the expression levels of *FOXM1* increased with body mass (Davis et al., 2010). These data suggest a correlative relationship between *Foxm1* expression and obesity and suggest that Foxm1 is required to prevent obesity induced diabetes. Further supporting this notion, Skp2, a target of Foxm1, is responsible for degradation of the cell cycle inhibitor Cdkn1b and is required for beta cell proliferation. A null mutation of *Skp2* limits beta cell mass expansion following a high fat diet (Zhong et al., 2007).

In addition to intrinsic factors controlling beta cell mass expansion in obese animals, extrinsic factors also regulate beta cell proliferation in this metabolic state. Neurons from the liver are responsible for non-cell autonomously activating ERK signaling in the beta cells. Additionally, ectopic activation of ERK signaling restores beta cell proliferation and blood glucose levels in mouse models of diabetes (Imai et al., 2008; Imai et al., 2009). These data demonstrate that ERK signaling is required for beta cell mass expansion during pregnancy and in the obese state. Additionally, this work indicates the importance of ectodermally-derived cells in regulation of beta cell mass expansion.

Differences in beta cell mass expansion between humans and rodents: In both humans and rodents beta cell mass expands in younger organisms through beta cell proliferation (Dor et al., 2004; Kassem et al., 2000; Teta et al., 2007). Additionally, beta cell mass expands in response to physiological stresses such as pregnancy and obesity; however, the mechanisms by which the beta cell population expands differ between rodents and humans (Butler et al., 2007). In mice and rats, beta cell mass expands due to increased beta cell proliferation and hypertrophy with no discernable changes in cell death. Conversely, in humans, beta cell mass expands in the obese state approximately 50 percent and this increase in mass occurs through increased beta cell hypertrophy (Butler et al., 2003). Intriguingly, during pregnancy, beta cell mass increases approximately 1.5 fold although no changes in proliferation, hypertrophy, or cell death could be detected although an increased number of small islets were identified suggesting increased beta cell neogenesis during human pregnancy (Butler et al., 2010). However, this work is not without caveats. It is well known that murine beta cells undergo a discrete proliferation response within a defined time window and it is likely that the 18 pregnant human donors examined were not within an analogous gestational age (Karnik et al., 2007; Rieck and Kaestner, 2010). This study also included donors with inflammatory disease that may have adversely affected beta cell mass expansion (Genevay et al., 2010). It is important to note that the pregnancy associated hormones prolactin, PL, and human growth hormone all stimulate beta cell proliferation in islets isolated from mice, rats, and humans suggesting that proliferation could be a conserved mechanism of beta cell mass expansion during pregnancy (Brelje et al., 1993). Additionally, while the study identified no changes in proliferation during pregnancy, it is critical to note that low levels of beta cell

proliferation does, in fact, occur in humans (approximately 1 percent) suggesting that beta cells in adult humans are capable of proliferating (Butler et al., 2010).

There are several reasons why increased beta cell proliferation does not occur to the same extent in rodents and humans. One difference among species that may result in decreased beta cell proliferation in humans is the length of telomeres. As cells replicate, telomeres shorten decreasing the capacity for further replication. In adult humans, active telomerase is rarely detected resulting in cellular senescence. Conversely, in the mouse, while telomeres do become shorter in the adult, active telomerase can be detected in many adult tissues allowing for continued extension of telomeres and replication of adult cells (Prowse and Greider, 1995). Additionally, most human studies are conducted in pancreata from adult donors while most murine studies are conducted in relatively young mice. In both species, epigenetic modifications increase with age rendering the beta cells unable to replicate (Chen et al., 2009a; Dhawan et al., 2009). Therefore, this inability to standardize the relative ages in humans and rodents poses difficulty in analyzing data.

While some fundamental differences exist between beta cell mass expansion in rodents versus humans, several factors required for beta cell mass expansion in rodents are conserved in humans. Beta cell proliferation in mice requires CyclinD and Cyclin Dependent Kinase 4 (CDK4). Similarly, beta cell proliferation in humans requires CyclinD, CDK4, and CDK6 (Georgia and Bhushan, 2004; Kushner et al., 2005; Rane et al., 1999). Several factors regulating beta cell proliferation in mice including Cdkn2a, Cdkn2b ($p15^{Ink4b}$), cell division cycle homolog 123 (CDC123), and CDK11A have been identified as genes that are misregulated in type 2 diabetes genome wide association studies (Saxena et al., 2007; Scott et al., 2007; Zeggini et al., 2007). Furthermore,

epigenetic modifications at the *Cdkn2a/Cdkn2d* (*p16*^{Ink4a}/*p19*^{Arf}) locus increase with age in both mice and humans resulting in inhibition of the cell cycle suggesting a conserved epigenetic mechanism for negatively regulating beta cell proliferation (Chen et al., 2009a; Dhawan et al., 2009). Additionally, Wnt signaling has been implicated in the onset of diabetes in both mice and humans. Recent genome wide association studies indicate that variants of transcription factor 7-like 2 (TCF7L2), a transcription factor that functions downstream of Wnt signaling, increase susceptibility for the onset of type 2 diabetes (Chandak et al., 2007; Dahlgren et al., 2007; van Vliet-Ostaptchouk et al., 2007). Depletion of TCF7L2 in cultured human islets decreases beta cell proliferation and increases beta cell apoptosis suggesting that Wnt signaling regulates beta cell mass expansion in humans (Liu and Habener, 2008; Lyssenko et al., 2007; Shu et al., 2008). Wnt signaling also regulates beta cell mass expansion in rodents. Expression of the transcription factor Sox6 is decreased in mice fed a high fat diet in *Leptin*$^{ob/ob}$ mice (Iguchi et al., 2005). Sox6 interacts with beta catenin, a downstream mediator of Wnt signaling, to negatively regulate *CyclinD* expression and beta cell proliferation (Iguchi et al., 2007). A recent study identified the association between Foxm1 and Wnt signaling; Foxm1 is required for beta catenin translocation to the nucleus and controls expression of Wnt target genes in gliomas (Zhang et al., 2011). Together, these data suggest that factors required for beta cell mass expansion are conserved in rodents and humans.

Mechanisms of beta cell mass expansion for cell-based therapies: In the case of type 1 diabetes or late stage type 2 diabetes, the most common medical treatment is exogenous insulin injections which are exceedingly effective but come with the caveat that they do not precisely regulate glucose levels, a caveat that can lead to secondary complications.

In non-insulin dependent type 2 diabetic patients, several drugs are used to decrease beta cell hypoplasia. Treatments such as exenatide, gastrin, various growth factors and glitazones are used to preserve and/or increase the beta cell mass. These treatments, however, are also hindered by significant side effects. For example, patients who take Pioglitazone to treat diabetes have an increased risk of heart failure, bone loss, and myocardial infarction (Buchanan et al., 2002; Lin et al., 2005). Additionally, the use of sulfonylurea drugs decreases blood glucose levels but accelerates loss of beta cell mass necessitating exogenous insulin injections (Maedler et al., 2005; Matthews et al., 1998). Because of the complications associated with current treatments for diabetic patients, considerable effort has been devoted to replacement of beta cells.

Several cellular sources of functional beta cells for diabetic patients have been considered including islet transplantations from cadaveric donors, directed differentiation of beta cells from embryonic stem cells (ES cells) or induced pluripotent stem cells (iPS cells), transdifferentation of other adult cell lineages into beta cells, and increased replication of beta cells *in vivo* (Figure 1.7). Islet transplantation from cadaveric donors is greatly hindered by the lack of available donors; approximately 3 donors are required to treat each diabetic patient (Shapiro et al., 2000). Additionally, because of the autoimmune response that resulted in beta cell destruction in the case of type 1 diabetes, patients receiving islet transplantation require immunosuppressive drugs. Unfortunately, immunosuppression inhibits beta cell proliferation in a diabetic setting indicating that the transplanted islets will be unable to expand their beta cell mass (Nir et al., 2007).

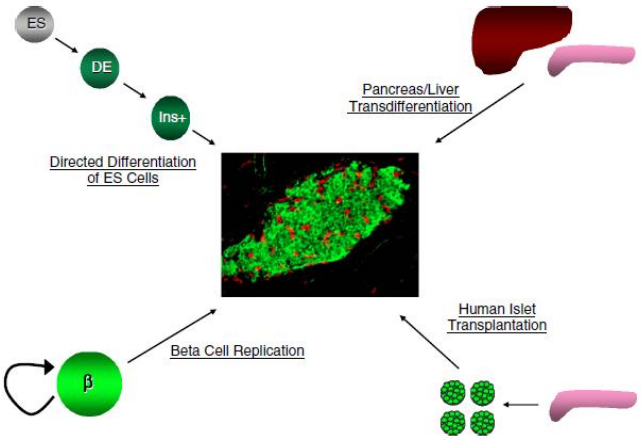

Figure 1.7: A schematic of alternative sources for developing beta cells. Currently, the only source of cells for beta cell transplantation is human islets from cadaveric donors. Considerable effort has been devoted to understanding the gene regulatory networks required for *in vivo* beta cell replication and beta cell mass expansion. Additionally, several groups have identified factors that promote transdifferentiation of liver or other pancreatic cell lineages into beta cells. Lastly, very promising studies have demonstrated that ES cells and iPS cells can be differentiated into beta-like cells that are responsive to blood glucose *in vivo.* Image taken from (Claiborn and Stoffers, 2008).

Another mechanism of generating beta cells for transplantation in diabetic patients is directed differentiation of pluripotent cells into functional beta cells or beta cell precursors. However, to date, this approach has not been successfully executed. *In vitro* differentiation of ES cells towards a beta cell fate resulted in the production of insulin-expressing beta-like cells. These cells, however, were unable to secrete insulin in response to glucose concentration (D'Amour et al., 2006). Further refinement of this directed differentiation paradigm allowed the same group to generate ES cell-derived pancreatic endoderm progenitors. When these progenitors were transplanted into the fat pads or kidney capsules of mice, they were able to mature and generate glucose-responsive beta cells that rescued hyperglycemia in diabetic mice (Kroon et al., 2008). These data suggest that *in vivo* cell types, such as endothelial cells, neurons, and/or other

endocrine cell lineages, are required to improve maturation. Unfortunately, transplantation of an impure population of progenitor cells has the potential to lead to teratoma formation (Kroon et al., 2008).

Induced pluripotent stem cells (iPS cells) function similarly to ES cells in terms of pluripotency and differentiation potential providing patients with an autologous source of cells for transplantation without the ethical considerations of ES cells (Maehr et al., 2009; Takahashi and Yamanaka, 2006; Wernig et al., 2007; Yu et al., 2007). Recently, investigators used a directed differentiation paradigm to generate beta-like cells from iPS cells and transplanted the cells into the liver of hyperglycemic mice. The transplanted cells secreted insulin and reduced blood glucose levels in a dose-dependent manner (Alipio et al., 2010). In this study, the injected cellular population was predominantly beta-like cells, however, other cell lineages were detected, and the investigators did not conduct a careful analysis of teratoma formation. Therefore, careful analysis of tumor formation needs to be conducted before this treatment is considered clinically relevant. In addition to the inherent risk of tumor formation in these studies, obtaining a sufficient number of beta cells for transplantation may be difficult because derivation of beta cells from pluripotent stem cells is inefficient and mature beta cells replicate at low rates. Approximately 420,000 beta cells will be required for each transplantation (Shapiro et al., 2000). Therefore, future efforts should be devoted to generating a pure population of beta-like cells and understanding mechanisms for beta cell mass expansion in order to produce enough beta-like cells for transplantation.

Although these efforts at generating beta cells from pluripotent cells is promising, another mechanism for increasing beta cell mass is by expanding the existing beta cell

population through increased proliferation and augmented beta cell survival. One controversial source for adult-stem cell derived beta cells is the bone marrow. One group injected recipient mice with GFP-positive bone marrow cells and sacrificed the animals 6 weeks later. At this time, the group observed GFP-positive beta-like cells that incorporated into the existing islets suggesting that bone marrow stem cells could be an autologous source for generating beta cells (Ianus et al., 2003). However, at the same time other groups found that the GFP-positive bone marrow did not give rise to GFP-positive beta like cells (Choi et al., 2003; Hess et al., 2003). Interestingly, although differentiation of bone marrow into beta-like cells could not be repeated, several groups determined that bone marrow transplantation increased beta cell proliferation and could ameliorate hyperglycemia following pancreatic injury (Choi et al., 2003; Hasegawa et al., 2007; Hess et al., 2003). Additionally, bone marrow transplantation improves vascularization of islets (Mathews et al., 2004). Together these data suggest that bone marrow transplantation may contribute to *in vivo* expansion of endogenous pancreatic beta cells. In fact, in a recent study, patients that were newly diagnosed with type 1 diabetes were treated with immunosuppressive drugs followed by bone marrow transplantation and more than half the patients in this study remained insulin-independent for more than a year (Voltarelli et al., 2007).

Transdifferentiation from multiple cell lineages into pancreatic beta cells is also a promising avenue to pursue. Ectopic expression of three transcription factors MafA, Neuorg3, and Pdx1 in the exocrine pancreas results in transdifferentiation of cells into what appeared to be mature beta cells. These exocrine-derived beta cells express markers of mature beta cells and contained mature insulin granules (Zhou et al., 2008).

Additionally, ectopic expression of either Neurog3 or NeuroD in the liver induced reprogramming of hepatic progenitor cells in pancreatic cell lineages, specifically beta cells. In this model, the newly produced beta cells can reduce hyperglycemia in animals treated with streptozotocin, a drug that is toxic to beta cells (Kojima et al., 2003; Yechoor et al., 2009). While this approach is promising, considerable research will be required for this to become clinically relevant. In both approaches, the newly produced beta cells do not form clusters or undergo morphogenesis into islets, suggesting they may not function as well as endogenous beta cells. Additionally, viral delivery of transcription factors is not clinically feasible.

Generation of new pancreatic beta cells remains a very promising treatment for both type 1 and type 2 diabetic patients. My thesis research has identified two factors that may be applied to current paradigms for generated beta cells. First, NC derivatives are required for beta cell maturation (Plank et al., 2011b). Second, the transcription factor Foxd3 regulates beta cell mass expansion during pregnancy (Plank et al., 2011a).

Dissertation research

Function of Foxd3 in progenitor cells: Foxd3, a Forkhead transcriptional regulator, is required for the maintenance of every progenitor cell lineage tested to date. Foxd3 is expressed in the progenitors of early embryo as early as the 4 cell stage and expression persists in the inner cell mass and trophectoderm cells at the blastocyst stage and in the epiblast at 6.5 dpc (Hanna et al., 2002; Tompers et al., 2005). *Foxd3* null blastocysts are indistinguishable from controls and maintain expression of pluripotency markers such as

Oct4, *Sox2*, and *Fgf4*. However, these embryos die around 6.5 dpc due to a catastrophic loss of epiblast cells and an expansion of extra embryonic tissue (Hanna et al., 2002). Foxd3 is also required in the extraembryonic tissues; *Foxd3* null extraembryonic tissues precociously differentiate into trophoblast giant cells at the expense of spongiotrophoblast cells and labyrinthine cells, lineages that appear slightly later in placental development (Tompers et al., 2005). Additionally *Foxd3* null embryonic stem cells (ES cells) and trophoblast stem cells cannot be established *de novo* from embryos demonstrating the requirement for Foxd3 in maintaining progenitor cell lineages (Hanna et al., 2002; Tompers et al., 2005). Together these data demonstrate and absolute requirement for Foxd3 in the early mammalian embryo.

To characterize the function of Foxd3 in ES cells, our lab generated an allele of *Foxd3* where the entire coding sequence is flanked by LoxP sites ($Foxd3^{Lby.3}$, called $Foxd3^{fl}$). Using the appropriate mouse line expressing Cre recombinase, *Foxd3* can be deleted in the desired temporal or spatial manner. In order to conditionally delete *Foxd3* from ES cells, we generated ES cells from blastocysts carrying a Tamoxifen-inducible, ubiquitously expressed Cre recombinase (CAAG-Cre^{ER}) and 2 $Foxd^{fl}$ alleles. The entire Foxd3 coding sequence was deleted upon addition of 2 μM of Tamoxifen (TM) (Liu and Labosky, 2008). After 12 hours of culture with TM, Foxd3 protein was reduced but could still be detected. However, 24 hours after TM addition, Foxd3 protein was rarely detected (Figure 1.8). In the absence of Foxd3, stem cell proteins and their mRNAs including Oct4, Sox2, and Nanog are maintained at relatively normal levels suggesting that Foxd3 is not required for their expression. Although these proteins required for pluripotency are maintained, ES cells lacking Foxd3 lose key stem cell properties. They

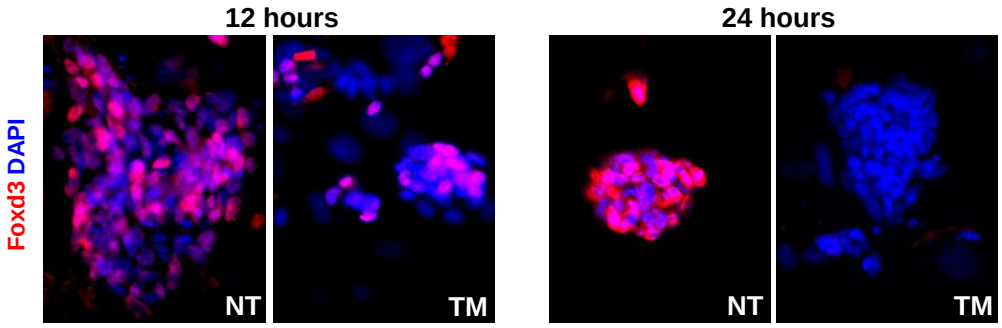

Figure 1.8: Generation of Foxd3 mutant ES cells. ES cells were derived from blastocysts carrying 2 alleles of *Foxd3* that were flanked by LoxP sites (Flox) and a ubiquitous CreER. When cultured with Tamoxifen (TM) to induce Cre activity, the entire Foxd3 coding sequence was excised. Using immunocytochemistry we demonstrated that Foxd3 protein (red) can still be detected after 12 hours of TM treatment. However, by 24 hours after TM addition Foxd3 protein is rarely detected in ES cells. NT, not treated (control).

are no longer pluripotent as they differentiate into mesendoderm and trophectoderm lineages while cultured in conditions that normally maintain pluripotency. Additionally, inducible-mutant ES cells lose self-renewal capacity and undergo aberrant apoptosis (Liu and Labosky, 2008). Due to the multiple issues surrounding the feasibility and ethical considerations of using ES cells from humans, one focus of stem cell biologists is determining the transcriptional networks controlling stem cell properties in both ES cells and iPS cells. While Foxd3 is not one of the "core" transcription factors sufficient for reprogramming somatic cells into iPS cells (Yu et al., 2007), it is indispensible for generating iPS cells; mouse embryonic fibroblasts (Mefs) lacking Foxd3 cannot be reprogrammed in pluripotent stem cells (Suflita, Ess, and Labosky, 2011 unpublished data). Together, these data demonstrate that Foxd3 functions downstream of, or in a pathway parallel to, other stem cell factors and is required for self-renewal and pluripotency of ES cells.

In addition to expression in the early embryo, Foxd3 is also one of the earliest markers of the NC lineage (Hromas et al., 1999; Labosky and Kaestner, 1998). NC cells are a multipotent, transient migratory cell lineage derived from the dorsal neural tube; as the neural tube closes, NC cells located at the dorsal aspect of the neural tube undergo an epithelial to mesenchymal transition (EMT) and migrate to various regions in the embryo giving rise to disparate cell types such as neurons, glia, craniofacial mesenchyme, melanocytes, and vascular smooth muscle (Le Douarin, 1999). In combination with the *Flox*^{fl} mice mentioned above, Cre recombinase driven by the *Wnt1* promoter was used to delete *Foxd3* in the NC. *Foxd3*$^{fl/-}$*; Wnt1-Cre* mice die perinatally, likely due to lack of innervation of the diaphragm (Mundell and Labosky, 2011; Teng et al., 2008). NC progenitors cannot be maintained in the absence of Foxd3 leading to a catastrophic loss of craniofacial mesenchyme and lack of peripheral, and specifically, enteric nervous system derivatives (Teng et al., 2008). Additionally, in the absence of Foxd3, individual NC progenitors aberrantly differentiate into mesenchymal derivatives at the expense of neural and glial lineages (Mundell and Labosky, 2011). This mouse model was used extensively in my thesis work. Altogether, data from our lab indicates that Foxd3 is required to maintain progenitor cell properties in multiple disparate progenitor cell lineages.

Although the requirement for Foxd3 in progenitor cell lineages is well established, the mechanism by which Foxd3 functions is less clear. In *Xenopus*, Foxd3 functions as a transcriptional repressor and interacts with the Groucho related protein, Grg4, to induce mesoderm (Steiner et al., 2006; Yaklichkin et al., 2007). However, data obtained using other experimental systems suggests that Foxd3 can function as both a

repressor and activator in different biological contexts (Lee et al., 2006; Pan et al., 2006; Thomas and Erickson, 2009). Additionally, data from two independent groups suggests that Foxd3 may function in ES cells to "poise" loci for transcription. A relay-model has been suggested based on the evidence that Foxd3 binds to target genes and/or their regulatory regions to inhibit transcription in ES cells. As the cell differentiate into B cells, Foxd3 is replaced by Foxp1 and transcription of target genes ensues (Liber et al., 2010). Similarly, a complementary model suggests that Foxd3 functions as a "pioneer factor" and occupies the *Albumin1* locus in ES cells thereby maintaining the unmethylated state of a single CpG residue. Upon differentiation into endoderm, Foxd3 is replaced by a Foxa family member resulting in activation of *Albumin1* expression (Xu et al., 2007). Both models suggest that Foxd3 is required prior to activation of target genes to maintain a binding site for other Forkhead proteins.

Summary of findings: While there is an established literature detailing the requirement for mesodermal and endodermal cues in pancreas and beta cell development, the role of ectodermal derivatives is less clear. A recent study demonstrated that NC inhibits proliferation of insulin-expressing cells (Nekrep et al., 2008). We sought to characterize the precise timing of NC migration to the pancreas and to further analyze the effect of NC derivatives in the pancreas on beta cell development and maturation. Our work demonstrated that NC reaches the dorsal pancreatic bud between the 26 and 27 somite stage and reaches the ventral pancreatic between the 27 and 28 somite stage (approximately 10.25 dpc), much earlier than was previously thought (Horb and Slack, 2000; Percival and Slack, 1999). To determine the effect of NC derivatives on developing beta cells, we used the NC specific deletion of *Foxd3*; ENS progenitors, including those

that innervate the pancreas, are absent in embryos lacking Foxd3 in the NC (Teng et al., 2008). In agreement with previous data, we found that proliferation of insulin-expressing cells and insulin-positive area were increased in mutant embryos. Additionally, using a combination of gene expression analysis and transmission electron microscopy, we determined that NC is required for beta cell maturation. Together, these data suggest that NC negatively regulates beta cell proliferation while positively regulating beta cell maturation.

Unexpectedly, our laboratory showed that Foxd3 is also expressed in the pancreatic primordium beginning at 10.5 dpc and becomes predominantly localized to the beta cells in the adult (Perera et al., 2006). To determine the role of Foxd3 in the pancreatic epithelium, we generated *Foxd3*$^{fl/-}$*; Pdx1-Cre* mice to characterize the phenotype of mice lacking Foxd3 in the entire Pdx1 expression domain including the pancreatic epithelium. Pancreata from pancreas-specific Foxd3 mutant mice developed normally and the mice were euglycemic under basal physiological conditions. To determine if Foxd3 is required for beta cell mass expansion, we analyzed the requirement for Foxd3 in the pancreas during pregnancy. In the absence of Foxd3, beta cell proliferation was decreased resulting in decreased beta cell mass and glucose intolerance at 15.5 days gestation.

Together, my work has generated data regarding cell autonomous and non-cell autonomous regulators of beta cell mass expansion during embryogenesis and in the adult mouse. Identification of signaling molecules from the NC required for beta cell maturation and this information can be utilized to improve directed differentiation paradigms to generate beta cells from pluripotent stem cells. Ideally, these molecules will

be sufficient for beta cell maturation *in vitro* eliminating the need to transplant an impure population of cells. Additionally, identifying and inhibiting the signaling factor in the NC that restricts beta cell proliferation may also aid in the generation of a large number of beta cells. I have also demonstrated that expression of Foxd3 within the pancreatic epithelium is required for beta cell mass expansion and the proposed future directions will elucidate the function of Foxd3 in beta cells. Identification and manipulation of extracellular signaling pathways and/or cell surface markers functioning upstream or downstream of Foxd3 may lead to the generation of small molecules that can be used to facilitate the expansion of beta cell mass *in vivo.*

CHAPTER II

INFLUENCE AND TIMING OF ARRIVAL OF MURINE NEURAL CREST ON PANCREATIC BETA CELL DEVELOPMENT AND MATURATION

This work was published in its entirety under the same title in the January 15, 2011 issue of *Developmental logy* (Plank et al., 2011b).

Introduction

A fundamental question in the field of developmental biology is how cells from one germ layer regulate normal development of a separate germ layer. Organ development is synchronously regulated to assure proper postnatal function, and coordination of innervation with morphogenesis is critical to this process. This issue is of particular interest to investigators studying pancreatic development; it is well known that endoderm development is dependent upon signaling from surrounding mesoderm tissues. Factors secreted by the mesoderm-derived notochord are largely responsible for development of the dorsal pancreas bud; in the absence of the notochord, expression of pancreas and endocrine cells markers are eliminated (Kim et al., 1997). In addition to the notochord, the developing vasculature produces inductive cues to influence early endoderm differentiation (Jung et al., 1999; Lammert et al., 2001). Subsequent to this induction, signals from mesodermally-derived pancreatic mesenchyme regulate proliferation of pancreatic progenitors to promote pancreatic outgrowth (Golosow and Grobstein, 1962; Wessells, 1967). Specifically, FGF10 signaling from pancreatic mesenchyme maintains *Ptf1a* expression in the dorsal pancreatic bud and is required for

growth, differentiation, and branching morphogenesis of the developing pancreas (Bhushan et al., 2001; Jacquemin et al., 2006).

In addition to mesodermally-derived tissues, a role for ectodermally-derived tissues in pancreas development was recently described. While ectodermally-derived neural signals had been implicated in growth and/or function of adult endocrine pancreas (Edvell and Lindstrom, 1998; Imai et al., 2008; Razavi et al., 2006), a recent study demonstrated for the first time that the ectodermally-derived neural crest regulates embryonic development of the pancreas (Nekrep et al., 2008). However, the relationship between neural crest populating the pancreas and the developmental switch between immature Insulin-expressing cells to mature beta cells remained unclear. Neural crest is a multipotent embryonic cell lineage that migrates ventrally from the dorsal neural tube and, among other functions, generates enteric nervous system derivatives that innervate endodermally-derived organs of the gut (Le Douarin, 1999). Molecular control of specification, maintenance, migration and function of the neural crest is at least partially controlled by the transcription factors Sox10 and Foxd3 (Labosky and Kaestner, 1998; Nelms, 2010; Sauka-Spengler and Bronner-Fraser, 2008; Southard-Smith et al., 1998). *Phox2b* is a downstream target of Sox10, and both Phox2b and Sox10 are required for neural and glial differentiation in the gut (Herbarth et al., 1998; Pattyn et al., 1999; Southard-Smith et al., 1998). *Phox2b*$^{-/-}$ embryos lack neural crest cells within the pancreas, resulting in a profound increase in proliferation of Insulin-expressing cells (Nekrep et al., 2008). To date, this model of neural crest regulation of beta cell proliferation has not been validated in an independent neural crest-deficient system, and the timing of neural crest arrival into the pancreatic primordium had not been described.

The transcription factor Foxd3, one of the earliest markers of neural crest (Labosky and Kaestner, 1998), is required for maintenance of neural crest progenitors. In the absence of neural crest expression of Foxd3, there is a catastrophic loss of this lineage including the entire enteric nervous system (Teng et al., 2008). Using neural crest-specific lineage labeling, we determined the timing and patterning of neural crest arrival at the developing pancreas. In addition, with a genetic manipulation that disrupts neural crest, we demonstrate that pancreatic beta cell development and maturation depends on interactions with neural crest derivatives.

Materials and methods

Mouse lines: *Tg(Wnt1-Cre)11Rth* (referred to as *Wnt1-Cre*), two independent *Foxd3* null alleles, $Foxd3^{tm1.Lby}$ and $Foxd3^{tm2.Lby}$ ($Foxd3^{-}$), and $Foxd3^{tm3.Lby}$ ($Foxd3^{fl}$) mice were interbred to generate $Foxd3^{fl/+}$ (control) and $Foxd3^{fl/-}$*; Wnt1-Cre* (mutant) embryos. These mouse lines and genotyping were previously described (Danielian et al., 1998; Hanna et al., 2002; Teng et al., 2008). For lineage analyses, a reporter allele, $Gt(ROSA)26Sor^{tm1(EYFP)Cos}$ ($R26R^{YFP}$, (Srinivas et al., 2001)), was also used. Mice were maintained on an outbred genetic background consisting of CD-1, 129S6 and C57BL/6J. All mouse lines were maintained under protocols approved by the Vanderbilt University Institutional Animal Care and Use Committee (IACUC). To generate embryos for dissections and further analysis, mice of the appropriate genotypes were mated, dams checked daily for the presence of a vaginal plug, and noon on the day of the plug considered 0.5 days post coitum (dpc). To measure BrdU incorporation, pregnant dams were injected with 50 mg BrdU/kg body weight one hour before sacrifice.

Histology and Immunohistochemistry: At 11.5 dpc or younger, embryos were dissected from the placenta and surrounding maternal tissues and fixed in 4% paraformaldehyde (PFA) in PBS for 4 hours. For embryos aged 13.5 dpc or older, the pancreas, duodenum, stomach, and spleen were dissected from the embryo in cold PBS and fixed in 4% PFA in PBS for 4 hours. Yolk sacs or embryonic tissues were removed for DNA extraction and PCR genotyping. Tissues were processed, embedded, and sectioned following standard procedures (Presnell, 1997). For whole mount immunohistochemistry, 9.5 to 10.25 dpc embryos were fixed and then permeabilized in 0.5 % Triton X-100 at room temperature for 30 minutes. Non-specific antigen recognition was minimized by blocking in 1% BSA, 10% normal donkey serum and 0.1% Triton X-100 in PBS. Embryos were then incubated with primary antibodies, washed, and subsequently incubated with secondary antibodies; each step was performed overnight at 4°C. Finally, samples were washed overnight in PBS with 0.1% Triton X-100. For 9.5-10.25 dpc embryos, the hindlimb and surface ectoderm were removed and the gut tube was separated from the neural tube to facilitate imaging. The following primary antibodies were used: chicken anti-GFP (1:500, Abcam), mouse anti-β-III Tubulin (1:500, Covance,TUJ1), rabbit anti-PGP9.5 (1:1000, AbD Serotec) rabbit anti-Fabp7 (1:1000, a kind gift from Dr. Thomas Muller, (Kurtz et al., 1994; Schnutgen et al., 1996)), guinea pig anti-Pdx1 (1:2500) and goat anti-Pdx1 (1:10000, both Pdx1 antibodies were kind gift from Dr. Christopher Wright, (Boyer et al., 2006; Hingorani et al., 2003)), guinea pig anti-Insulin (1:500, Millipore), rabbit anti-Glucagon (1:500, Millipore), rabbit anti-Pancreatic Polypeptide (1:100, Millipore), rat anti-Somatostatin (1:100, Millipore), rabbit anti-Ghrelin (1:100, Phoenix Pharmaceuticals), rabbit anti-Glut2 (1:1000, Millipore), rat anti-BrdU (1:250, Accurate

Biochemical), mouse anti-Neurog3 (1:1000, Developmental Studies Hybridoma Bank), rabbit anti-Foxd3 (1:1000, (Tompers et al., 2005)). The secondary antibodies used were: biotin donkey anti-chicken (1:500), biotin donkey anti-mouse (1:500), Cy2 donkey anti-mouse (1:500), Cy2 donkey anti-guinea pig (1:500), Cy2 donkey anti-rabbit (1:500), Cy3 donkey anti-mouse (1:500), Cy3 donkey anti-guinea pig (1:500), Cy3 donkey anti-rabbit (1:500), Cy3 donkey anti-rat (1:500), Cy3 donkey anti-goat (1:800), Cy5 donkey anti-rabbit (1:500), Cy5 donkey anti-mouse (1:500), and Cy5 donkey anti-guinea pig (1:500). All secondary antibodies were purchased from Jackson ImmunoResearch. To detect YFP and Neurog3 protein, tyramide signal amplification was used (Invitrogen). BrdU was detected as previously described (Plank et al., 2011a; Teta et al., 2007). Tissue sections were imaged using either a Zeiss Axioskop2 plus with a Q-Imaging Retiga 2000R Fast 1394 camera or an Olympus FV1000 Confocal Laser Scanning Microscope. Transmission electron microscope (TEM) analyses were completed with the assistance of the Vanderbilt Cell Imaging and Shared Resource using standard procedures (Tweedie et al., 2006).

Quantification and Statistical Analysis: To quantify pancreatic alpha, beta, delta, epsilon, and PP cell area, the Glucagon-, Insulin-, Somatostatin-, Ghrelin-, or PP-positive area was determined using ImageJ (NIH) and divided by the total pancreatic area from 5-7 evenly spaced sections throughout the pancreas. Approximately 10 percent of the total pancreatic area was quantified for each cell type. Similarly, Neurog3-positive cells were quantified: the number of Neurog3-positive cells per section was divided by the pancreatic area. The percent of Glut2- and/or Pdx1-positive Insulin-expressing cells was calculated by counting the number of Insulin-expressing cells co-expressing Glut2 and/or

Pdx1 divided by the total number of Insulin-expressing cells. Two endocrine cell clusters from 5 evenly spaced sections throughout the pancreas were analyzed (10 clusters total at each age). At least 250 Insulin-positive cells from each animal were counted. The percent of endocrine cell clusters in contact with neurons was calculated by determining the number of endocrine cell clusters (in this assay, a cluster was defined as having more than 5 cells) in contact with neurons divided by the total number of endocrine cell clusters per section. At least 4 evenly spaced sections throughout the pancreas were analyzed per embryo or mouse, accounting for approximately 5 to 8% of the total pancreatic area. Statistical significance for each assay was determined using a two-tailed Student's t-test.

RNA Isolation and Real Time PCR: The pancreatic primordium was dissected and stored in RNA Later (Ambion). RNA was isolated using QIAshredder columns and the RNeasy Mini Kit (Qiagen) and contaminating genomic DNA removed with Turbo DNase (Ambion). cDNA was generated using the Superscript First Strand Synthesis (Invitrogen) and 2 ng of cDNA was amplified using Power SYBR Green PCR Master Mix (Applied Biosystems). All samples were run in duplicate and 4-6 biological replicates were used in each case. The relative amount of mRNA was determined by comparison to *Hypoxanthine Phosphoribosyl Transferase (Hprt)* and a two-tailed Student's t-test was used to determine statistical significance. Primer sequences are in Table 2.1.

Table 2.1- qRT-PCR Primer Sequences

Gene Name	Forward Primer Sequence (5'→3')	Reverse Primer Sequence (5'→3')
Gcg	AGGAATTCATTGCGTGGCTG	CAATGGCGACTTCTTCTGGG
Ins1	CAGCAAGCAGGTCATTGTTT	GGGACCACAAAGATGCTGTT
Mafa	TCGACCTGATGAAGTTCGAG	CAGAAGCTGGGCGAAGAG
Mafb	CCCACACATTGGCAACTAAC	AACGGAAGGGACTTGAACAC
Neurog3	ATCCATCACTTTTTCCAGGGTG	TCATCTATGGGCCAAGAGCTG
Nkx2.2	GCAGCGACAACCCCTACA	ATTTGGAGCTCGAGTCTTGG
Pdx1	CTGAGGGACAAAGATGCAGA	TTCTAATTCAGGGCGTTGTG

Neural crest arrival at the pancreatic primordium occurs between the 26 and 27 somite stages

Signals from the neural crest regulate proliferation of Insulin-expressing cells that in turn influence initial beta cell mass (Nekrep et al., 2008); however, the timing of interactions between neural crest and the pancreatic primordium has not been carefully defined. By 9.0 days post coitum (dpc, 13-15 somites) the endoderm-derived gut epithelium forms two outpocketings that will become the dorsal and ventral pancreatic buds. Mesoderm-derived pancreatic mesenchyme surrounds both buds, and interactions between these tissues are required for subsequent branching morphogenesis (Gittes et al., 1996; Golosow and Grobstein, 1962). To determine when migratory neural crest first makes physical contact with the pancreatic primordium, we analyzed the neural crest lineage in *Wnt1-Cre; R26R*$^{YFP/+}$ (control) embryos from 9.5 dpc-10.25 dpc. At the 26 somite stage (10.0 dpc), YFP-positive neural crest cells were detected in the anterior foregut (Figure 2.1A) but were not in the vicinity of the pancreatic primordium (Figure 2.1D). The pancreatic epithelium was identified by Pdx1 expression. However, by the 27 somite stage and afterwards (Figure 2.1B-C), YFP-positive neural crest cells were present within the pancreatic mesenchyme adjacent to the epithelium. This demonstrated that

neural crest arrival at the pancreatic primordium begins between the 26 and 27 somite stages (approximately 10.0 dpc). Additionally, because a new pair of somites is formed approximately every 2 hours in the mouse embryo (Tam, 1981), these data provide, for the first time, a precise characterization of the timing of neural crest migration to the pancreatic primordium. These data suggest that neural crest is proximal to the pancreatic epithelium well in advance of significant branching and the secondary transition, a key developmental stage initiating around 13.5 dpc that marks a wave of Insulin-positive cell differentiation. In addition, this contradicts previous studies concluding that only mesodermally- and endodermally-derived tissues were present in dorsal pancreatic buds at 11.5 dpc (Horb and Slack, 2000; Percival and Slack, 1999). We also observed that NC enters the mesenchyme surrounding the dorsal pancreas prior to the ventral pancreas; YFP-positive NC cells are present in the mesenchyme surrounding the dorsal pancreas by the 27 somite stage (Figure 2.1E-F) while YFP-positive cells are not detected adjacent to the ventral pancreas until the 28 somite stage (Figure 2.1 G-H). This timing confirms that NC arrival at the pancreatic buds parallels the timing of pancreas development as the dorsal bud undergoes branching morphogenesis and expansion slightly earlier than the ventral bud (Jorgensen et al., 2007).

Foxd3 is required for NC arrival at the developing pancreas

Loss of Foxd3 in the NC results in a loss of most NC derivatives, however, some regions of the embryo, such as the outflow tract, are only mildly perturbed (Teng et al., 2008). To determine if Foxd3 function in the NC is required for the NC that migrates to

Figure 2.1: NC cells enter the pancreatic primordium between the 26 and 27 somite stages. **(**A-C). Whole mount immunofluorescence for Pdx1 marking the pancreatic epithelium (red), and YFP marking NC cells (green), illustrates the path and timing of NC migration. In these samples NC was lineage labeled with Wnt1-Cre driven recombination of $R26R^{YFP}$ in control embryos (*Wnt1-Cre;* $R26R^{YFP/+}$). NC cells have not reached the pancreatic primordium by the 26 (A) somite stage, by the 27 somite stage (B) migrating NC cells had just reached the pancreatic epithelium, and at the 28 somite stage (C), the leading edge of the NC migratory stream was past the pancreatic primordium. (D-F) Higher magnification of the dorsal and ventral pancreatic buds illustrate that the YFP-positive NC cells have not reached the dorsal bud at the 26 somite stage (D) but have arrived at the dorsal bud at the 27 somite stage (E) and the ventral bud at the 28 somite stage (F). (G-H) Higher magnification images of the ventral bud demonstrate no YFP-positive NC cells present near the ventral bud at the 27 somite stage (G) but NC are at the ventral bud at the 28 somite stage (H). The cartoon illustrates the orientation of the embryos with the boxed region corresponding to the area shown in A-C. VP, ventral pancreas; DP, dorsal pancreas; *, sympathetic ganglia. N=2-3 embryos per time somite stage. Imaging done by Nathan Mundell.

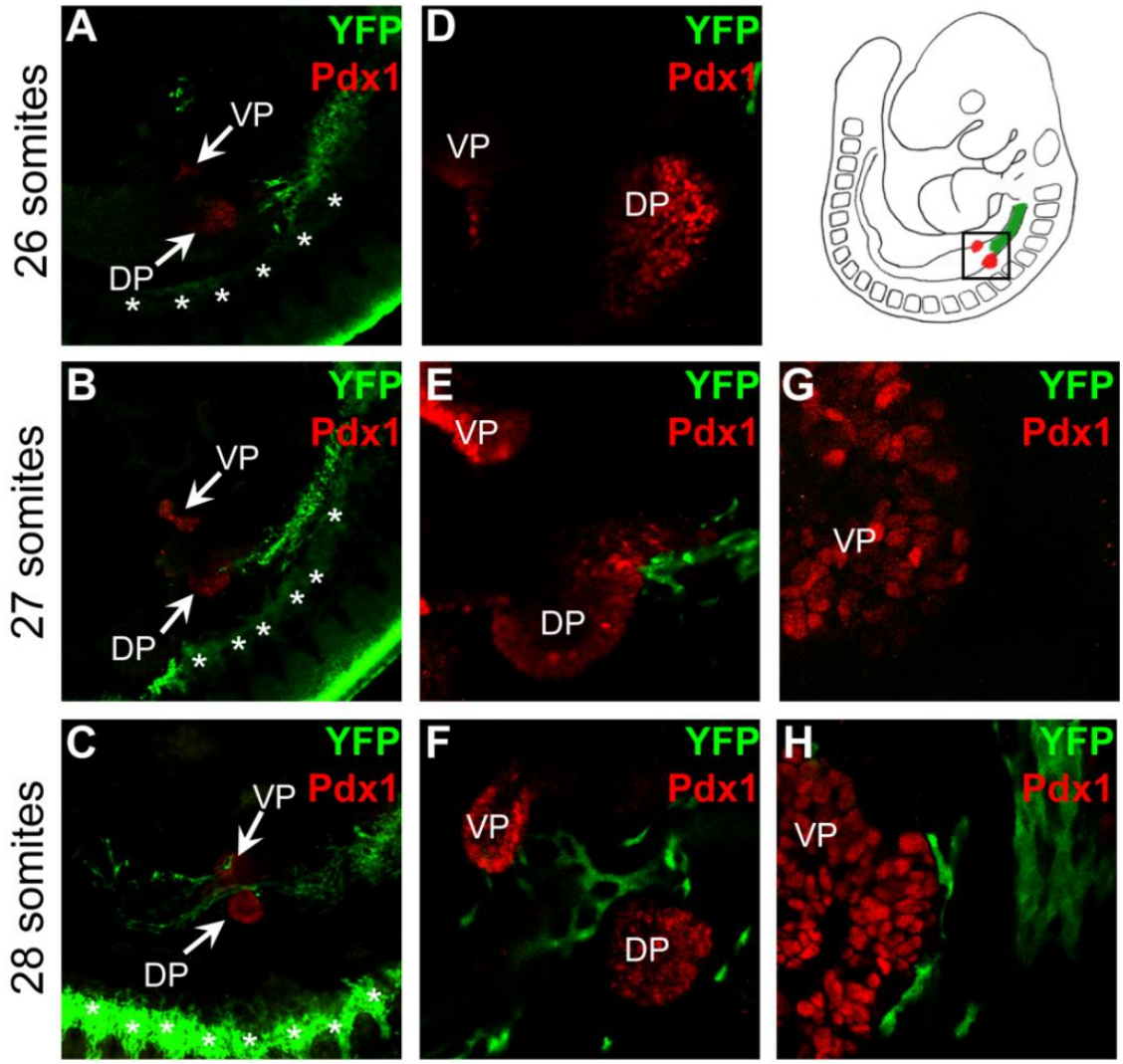
26 somites
27 somites
28 somites
A
B
C
D
E
F
G
H
YFP
Pdx1
VP
DP

the developing pancreas, we analyzed the NC lineage in control and mutant embryos with a Cre-activatable lineage label, *R26R*$^{YFP/+}$. In contrast to controls (Figure 2.2A-B), mutant NC cells, identified with YFP expression, were not found near the pancreatic epithelium, identified by Pdx1 and Glucagon expression, at 10.5 or 11.5 dpc (Figure 2.2E-F). These data confirm a cell autonomous requirement for Foxd3 within NC fated to enter the pancreas.

To further characterize NC in control embryos and determine if NC cells were present in the pancreata of mutant embryos at later developmental time points, we analyzed the NC lineage at 15.5 and 17.5 dpc. As pancreatic development progresses, the branches of pancreatic epithelium, identified by Pdx1 expression, invade the surrounding mesenchyme, and we observed NC cells interspersed throughout the developing pancreas (Figure 2.2C- D). However, NC cells were never present near the pancreas in mutant embryos (Figure 2.2G-H) supporting our earlier observations that Foxd3 expression in the NC is required for maintenance of NC (Teng et al., 2008), including NC derivatives in the pancreas.

Neurons and glia are absent in mutant pancreata

Normally, NC cells differentiate to form neurons and glia of the sensory, sympathetic, and enteric nervous systems (Adams and Bronner-Fraser, 2009) and in a previous report using mouse embryos homozygous for a null mutation in *Phox2b* (*Phox2b*$^{-/-}$) lacking much of the NC, neurons and glia are absent from the

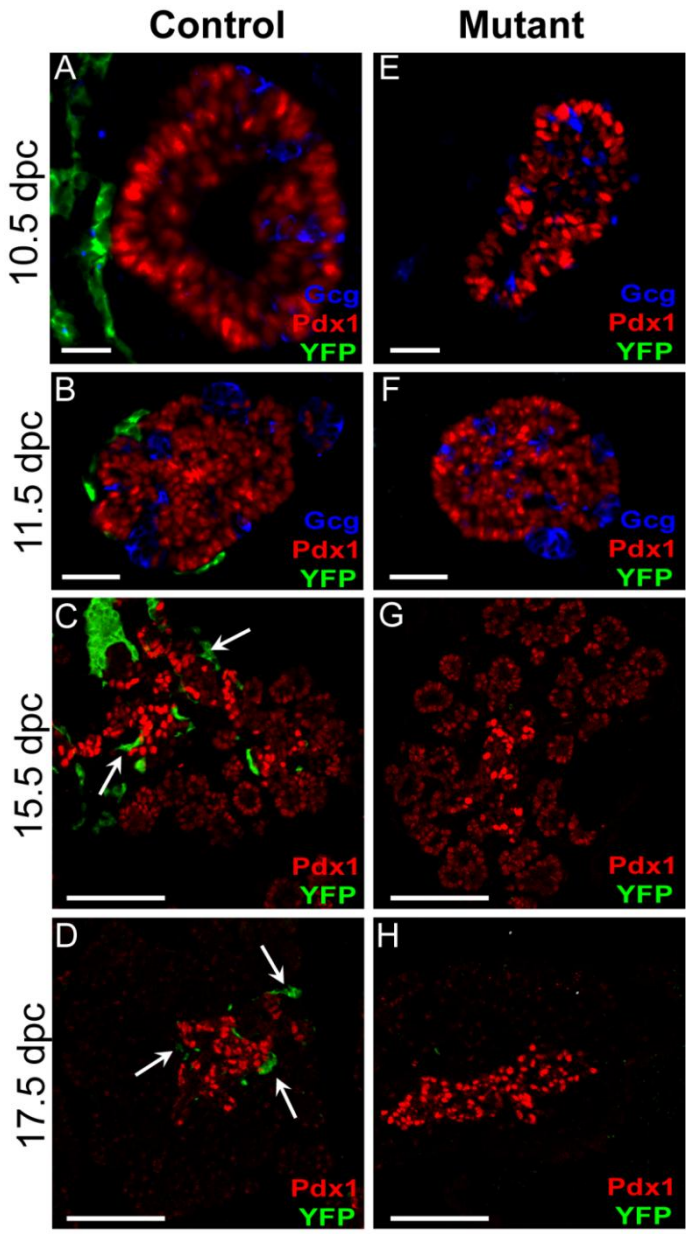

Figure 2.2: The NC does not populate the pancreas in the absence of *Foxd3*. **(**A-B) Immunofluorescence on sections of embryonic tissue demonstrated that YFP-positive NC cells (green) are adjacent to the Pdx1-positive pancreatic epithelium (red) at 10.5 (A) and 11.5 dpc (B) in control embryos (*Wnt1-Cre; Foxd3*$^{flox/+}$*; R26R*$^{YFP/+}$). (C-D) As pancreatic branching ensues, YFP-positive NC cells (green) become intermingled with pancreatic epithelial cells (red) and are closely associated with cells expressing higher levels of Pdx1 at 15.5 (C) and 17.5 dpc (D). (E-H) YFP-positive cells were not detected in the pancreatic primordium of mutant embryos (*Wnt1-Cre; Foxd3*$^{flox/}$*; R26R*$^{YFP/+}$) at any developmental time point. Arrows illustrate YFP-expressing cells. Scale bars, 100 μm. N=3-4 embryos in each group.

pancreas (Nekrep et al., 2008). To further characterize this finding using a NC-specific mutation, we analyzed the timing of neural and glial differentiation in pancreata from control embryos at various developmental stages. Very few TUJ1-positive neurons and no FABP7-positive glia were present at 13.5 dpc (data not shown). However, by 15.5 and 17.5 dpc, both neurons and glia were intermingled with pancreatic epithelial cells, identified by Pdx1 expression (Figure 2.3A-B), suggesting that neural and glial differentiation in the pancreas began between 13.5 and 15.5 dpc and NC derivatives are in position to affect beta cell development by the beginning of the secondary transition. In addition, by 17.5 dpc, neurons and glia are closely associated with cells expressing high levels of Pdx1, indicative of endocrine cells. Consistent with our earlier observations (Figure 2.1-2.2), *Foxd3* mutant embryos completely lacked neurons and glia in the pancreas (Figure 2.3C-D) supporting our conclusion that pancreatic neurons and glia are derived from the NC.

NC cells regulate proliferation of Insulin-expressing cells and Insulin-positive area

Analysis of the *Phox2b*$^{-/-}$ embryos lacking NC demonstrated that signals from the NC regulate insulin-expressing cell proliferation and the total number of Insulin-expressing cells (Nekrep et al., 2008). In *Phox2b*$^{-/-}$ embryos, NC cells migrate to the endoderm of the foregut but then undergo apoptosis prior to differentiating into enteric neurons (Pattyn et al., 1999). Because the NC is more significantly ablated in *Foxd3* NC-conditional null embryos (no NC cells migrate into the foregut in mutants, (Teng et al., 2008)), it leaves open the possibility that beta cell development may be more severely

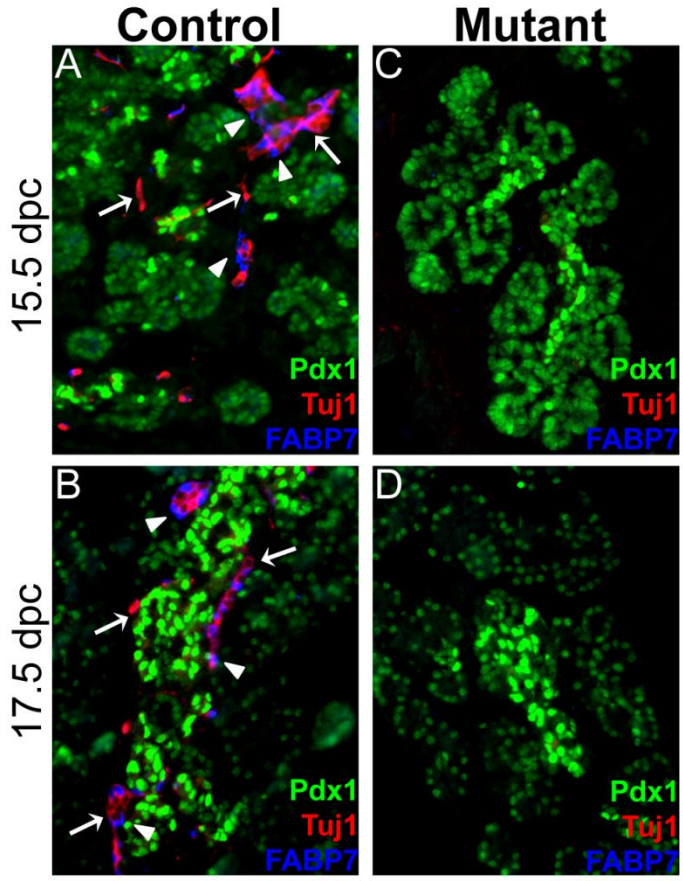

Figure 2.3: Neurons and glia are absent in pancreata from embryos with a NC specific deletion of *Foxd3*. (A-B) Immunofluorescent analyses of sections of embryonic pancreata demonstrated that TUJ1-expressing neurons (red) and FABP7-expressing glia (blue) were present in control pancreata at 15.5 (A) and 17.5 (B) dpc. TUJ1- and FABP7-expressing cells were not detected at any stages in mutant pancreata (C-D). The pancreas was indicated by Pdx1-positive cells (green). Arrows, TUJ1-positive cells; arrowheads, FABP7-positive cells. N=3-4 embryos in each group.

altered in this genetic model. To determine if the insulin-expressing cell area is greater in Foxd3 NC mutant embryos, we assayed insulin- and glucagon-positive area in mutant and control pancreata at 17.5 dpc. Similar to the previous study, the area occupied by insulin-expressing cells in the pancreas was increased approximately 1.5 fold (Figure 2.4A) while glucagon-positive area was unchanged (Figure 2.4B) in mutants compared to controls. In addition, we analyzed PP-, Somatostatin-, and Ghrelin-positive area and found that the area of these endocrine cell lineages was similar between mutant and control embryos (Figure 2.4C). To determine if *Nkx2.2* expression, a transcription factor required for initial beta cell differentiation and, to a lesser extent, alpha and PP cell differentiation was altered in our system (Sussel et al., 1998), we used real time PCR (qPCR) to analyze *Nkx2.2* mRNA expression. At both 13.5 and 15.5 dpc, *Nkx2.2* was significantly increased (Figure 2.4D), consistent with previous findings (Nekrep et al., 2008). To resolve whether the increase in Insulin-positive area was due to changes in cell proliferation, we assayed BrdU incorporation in mutant and control pancreata. In both 15.5 and 17.5 dpc embryos, BrdU incorporation was increased (85% at 15.5 dpc and 29% at 17.5 dpc) in Insulin-expressing cells from embryos lacking Foxd3 in the NC (Figure 2.4E). These results suggested that NC-derived cells negatively regulate proliferation in Insulin-expressing cells. In contrast, BrdU incorporation in Glucagon-expressing cells of control and mutant embryos was unchanged at both times (Figure 2.4F). These data agree with the previous report that signals from the NC regulate Insulin-expressing, but not Glucagon-expressing, cell area and proliferation (Nekrep et al., 2008).

Figure 2.4: NC-derived cells regulate Insulin-expressing cell expansion. (A) The Insulin (Ins)-positive area from mutants and controls was calculated and indicated that mutants have a greater Ins-positive area than controls at 17.5 dpc. (B) The Glucagon (Gcg)-positive area was similar between mutants and controls at 17.5 dpc. (C) The Pancreatic Polypeptide (Ppy), Somatostatin (Sst), and Ghrelin (Ghrl)-positive areas were slightly increased but not to a statistically significant level in mutants compared to controls at 17.5 dpc. (D) qPCR analyses indicated that *Nkx2.2* mRNA expression was increased in mutants compared to controls at 13.5 and 15.5 dpc. (E) BrdU incorporation in Insulin-positive cells was greater in mutants than controls at 15.5 and 17.5 dpc. (F) BrdU incorporation in Gcg-positive cells was unchanged in mutants and controls at 15.5 and 17.5 dpc. (G) qPCR analyses indicated *Neurog3* mRNA expression was increased in mutants compared to controls at 13.5 and 15.5 dpc. (H) The total number of Neurog3-positive cells per pancreatic area was unchanged between mutants and controls at 13.5 and 15.5 dpc. Purple lines and bars represent control embryos; red bars, represent mutant embryos. Error bars indicate SEM. * $p < 0.05$, ** $p < 0.01$. N= 3-5 embryos per group.

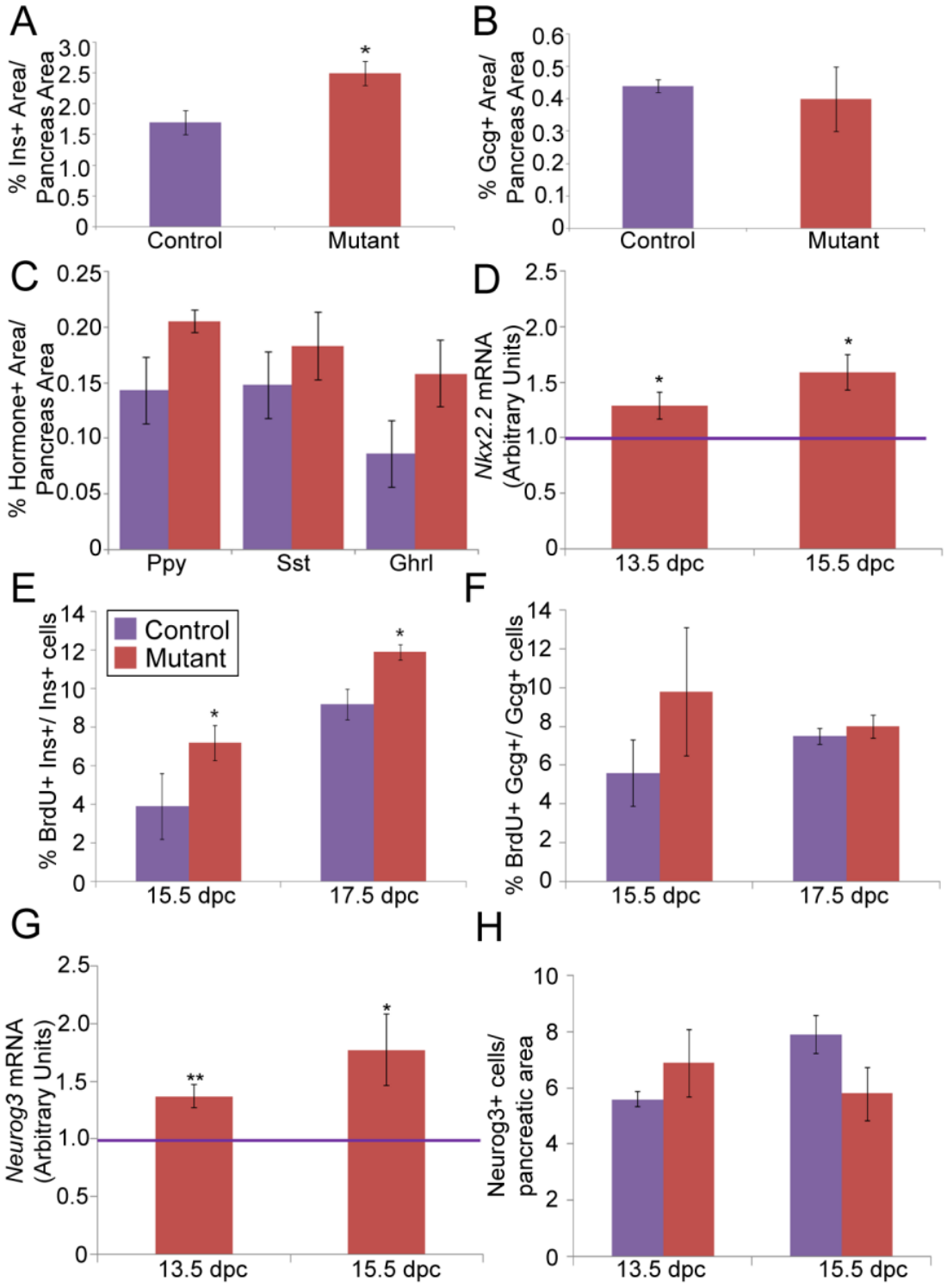
A
% Ins+ Area/ Pancreas Area
3.0
2.5
2.0
1.5
1.0
0.5
0
*
Control
Mutant
B
% Gcg+ Area/ Pancreas Area
0.6
0.5
0.4
0.3
0.2
0.1
0
Control
Mutant
C
% Hormone+ Area/ Pancreas Area
0.25
0.20
0.15
0.10
0.05
0
Ppy
Sst
Ghrl
D
Nkx2.2 mRNA (Arbitrary Units)
2.5
2.0
1.5
1.0
0.5
0
*
*
13.5 dpc
15.5 dpc
E
% BrdU+ Ins+/ Ins+ cells
14
12
10
8
6
4
2
0
Control
Mutant
*
*
15.5 dpc
17.5 dpc
F
% BrdU+ Gcg+/ Gcg+ cells
14
12
10
8
6
4
2
0
15.5 dpc
17.5 dpc
G
Neurog3 mRNA (Arbitrary Units)
2.5
2.0
1.5
1.0
0.5
0
**
*
13.5 dpc
15.5 dpc
H
Neurog3+ cells/ pancreatic area
10
8
6
4
2
0
13.5 dpc
15.5 dpc

NC cells do not regulate beta cell neogenesis

While proliferation changes profoundly influence the final number of beta cells, endocrine cell neogenesis also plays a significant role. To analyze beta cell neogenesis, we quantified *Neurog3* mRNA expression, an indicator of endocrine cell neogenesis (Gu et al., 2002; Schwitzgebel et al., 2000). qPCR analyses demonstrated increased *Neurog3* expression in pancreata from mutant embryos at both 13.5 and 15.5 dpc (Figure 2.4G), when Neurog3 is playing a profound role in the generation of new beta cells (Gu et al., 2002). This result is consistent with 2 possibilities: 1) an increase in *Neurog3* mRNA expression per individual cell or 2) an increase in the number of cells expressing *Neurog3*, suggesting increased endocrine cell neogenesis. To distinguish between these two explanations, we used immunohistochemistry and quantified the total number of Neurog3-positive cells per pancreatic area and discovered that the number of cells expressing Neurog3 was similar between mutants and controls (Figure 2.4H) suggesting that NC cells are not required for endocrine cell neogenesis, but that regulation of *Neurog3* levels on a per cell basis was disrupted. During embryogenesis, Neurog3-positive precursors are unipotent (Desgraz and Herrera, 2009); therefore, it is possible that individual endocrine progenitors expressing high levels of Neurog3 may be mis-specified to a beta cell fate resulting in increased Insulin-positive area. Because we did not detect changes in the proportion of other pancreatic endocrine cells in mutant embryos (Figure 2.4B-C), it is unlikely that endocrine progenitors are reallocated to a beta cell fate. However, the possibility remains open that Neurog3 may regulate other aspects of beta cell development such as self-renewal and maturation.

NC cells regulate beta cell maturation

Although increased Insulin-expressing cell area is significant, it is more physiologically important that the Insulin-expressing cells are capable of responding to glucose stimulation. Unfortunately, embryos with a NC-specific deletion of *Foxd3* or a homozygous null mutation in *Phox2b* result in perinatal lethality, so beta cell function cannot be tested in postnatal animals. As an alternative, we first examined expression of definitive markers of mature beta cells. The transcription factor MafA is a key regulator of glucose stimulated Insulin secretion and is expressed upon maturation (Zhang et al., 2005). Similarly, Pdx1 is strongly expressed in mature beta cells (Ohlsson et al., 1993). Alternatively, MafB is expressed in immature Insulin-expressing cells and immature and mature Glucagon-expressing cells while Glucagon (Gcg) is expressed in all alpha cells (Artner et al., 2006; Matsuoka et al., 2003). Therefore, to determine if signals from NC-derivatives are required for beta cell maturation, we analyzed mRNA expression of *MafA* and *Pdx1* in addition to *MafB, Ins1*, and *Gcg* at 17.5 dpc. Expression of *MafB* and *Gcg* were unchanged in mutant embryos while expression of *Ins1* appeared increased in mutant embryos, although this trend was not statistically significant. Importantly, expression of both *MafA* and *Pdx1* mRNA was significantly decreased, suggesting that signals from NC derivatives positively regulate beta cell maturation (Figure 2.5A). To examine beta cell maturation on a more cell biological level, we analyzed protein expression of Pdx1 and Glut2, the glucose transporter utilized by beta cells that is critical for glucose stimulated Insulin secretion (Guillam et al., 1997). There was a significant decrease (approximately 6 percent) in the percentage of Insulin-positive cells co-expressing Glut2 and Pdx1 (Figure 2.5B-D). Additionally, there was an increase

(approximately 15 percent) in the percentage of Insulin-positive cells that do not express Pdx1 or Glut2, further suggesting a decrease in beta cell maturation (Figure 2.5B-D). We extended this analysis of Pdx1 and Glut2 expression to 18.5 dpc and found similar results. Again, we observed an increase the percentage of cells expressing Insulin but not Pdx1 or Glut2 (Figure 2.5E-G). Our data demonstrate that although the majority of Insulin-expressing cells co-express Pdx1 and Glut2, there is a significant fraction of Insulin-expressing cells that do not express Pdx1 or Glut2. The presence of this small but significant population of cells supports the conclusion that signals from NC derivatives are critical for beta cell maturation.

To analyze beta cell maturation at higher resolution, we used transmission electron microscopy (TEM). Mature Insulin containing granules can be identified by the presence of electron dense cargo surrounded by an electron-free halo (Figure 2.5H-I, black arrows) while immature Insulin containing granules can be identified by the presence of less dense cargo surrounded by the characteristic halo (Figure 2.5H-I, white arrows). These criteria were applied for the identification of Insulin-expressing cells. Our TEM analyses revealed striking defects within the Insulin-expressing cells from mutant embryos (Figure 2.5I). First, the number of granules in all cells analyzed from mutant embryos was decreased compared to controls (Figure 2.5H). Second, although some granules from mutant embryos had the morphology characteristic of Insulin granules, a significant proportion of the granules in 3 out of 6 cells from mutant embryos were abnormal. These abnormal granules were less dense than Insulin granules and were not surrounded by the characteristic halo (Figure 2.5I, arrowheads). Previous data, together with our data here (Figure 2.4-5) suggest that NC-derived cells regulate beta cell

Figure 2.5: Beta cell maturation is impaired in the absence of NC. (A) *MafA* and *Pdx1* mRNA was decreased in mutants (red bars) compared to controls (purple line) while *MafB, Ins,* and *Gcg* mRNA were similar between mutants and controls at 17.5 dpc. N= 5 pancreata in each group. (B-G). Immunofluorescent analyses of Pdx1 (blue) and Glut2 (red) expression in Insulin-positive cells (green) indicated that a greater proportion of Insulin-positive cells from mutant embryos (C, F) do not co-express Glut2 or Pdx1 compared to control littermates (B, E) at 17.5 (B-C) and 18.5 dpc (E-F). Quantification of immunofluorescent analyses at 17.5 dpc (D) indicated that the proportion of Ins-positive cells that do not express Glut2 or Pdx1 (blue portion of the graph) was increased while the proportion of Insulin-positive cells that co-expressed both Pdx1 and Glut2 (red) are decreased in mutant embryos. Quantification of immunofluorescent analyses at 18.5 (G) indicated that the proportion of Insulin-positive cells that do not co-express Glut2 or Pdx1 (blue) was increased in mutant embryos. Arrows indicate Insulin-positive cells that do not express Pdx1 or Glut2. N=3-4 embryos per group. * $p < 0.05$, ** $p < 0.01$, *** $p < 0.001$. Note the vertical y-axis extends from 80-100 %. (H-I) Transmission electron microscopy revealed there were fewer Insulin granules in pancreata from mutant embryos (I) compared to controls (H) at 17.5 dpc. Additionally, abnormal granules in Insulin-expressing cells were also present in mutant samples but not in controls. Black arrows indicate examples of mature Insulin granules, white arrows indicate examples of immature Insulin granules, and white arrowheads indicate examples of abnormal granules. n, nucleus; dashed line, nuclear membrane; solid line, cell membrane. Scale bars represent 500 nm. Error bars represent SEM.

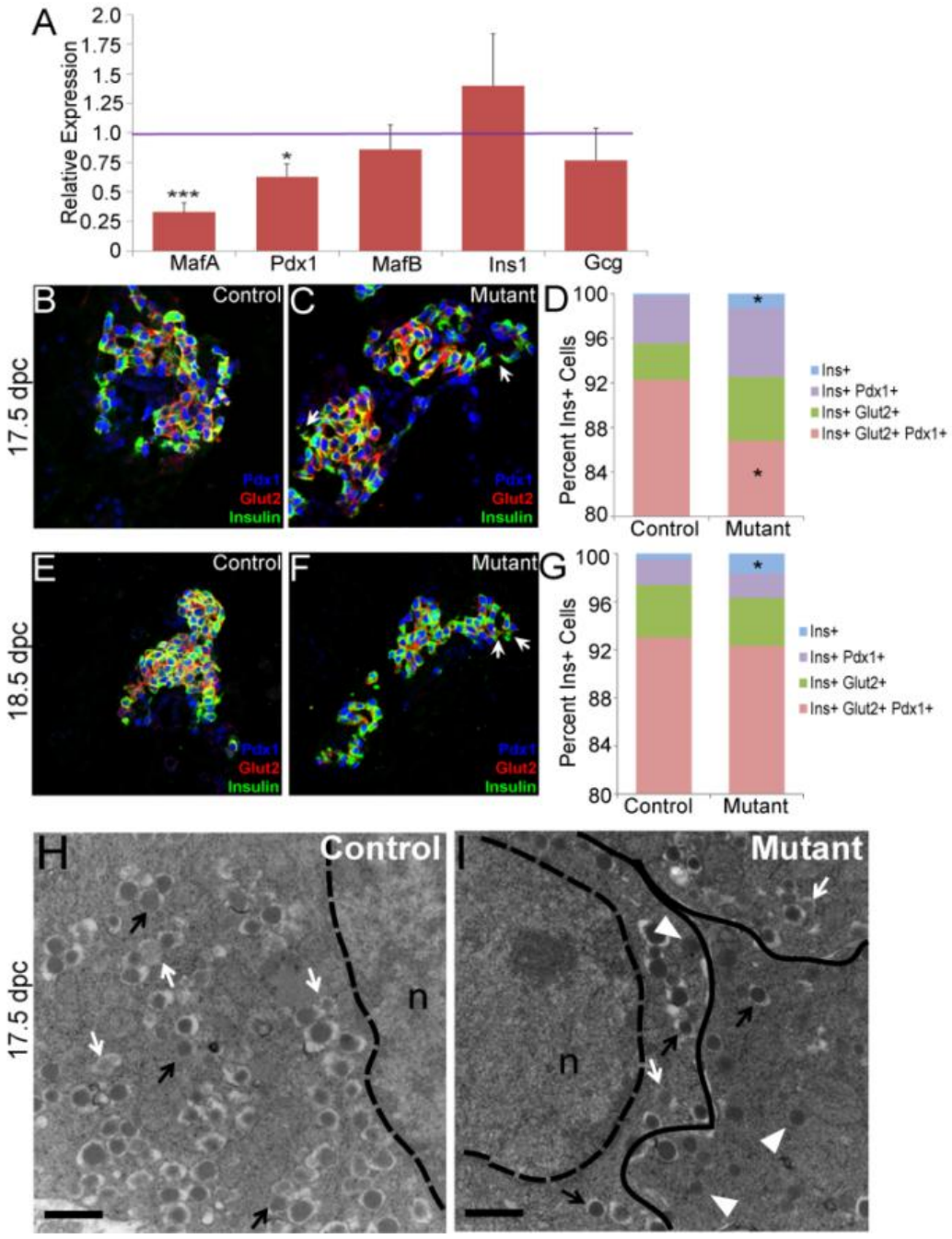
A
Relative Expression
2.0
1.75
1.5
1.25
1.0
0.75
0.5
0.25
0
***
*
MafA
Pdx1
MafB
Ins1
Gcg
B
Control
C
Mutant
17.5 dpc
Pdx1
Glut2
Insulin
D
Percent Ins+ Cells
100
96
92
88
84
80
Control
Mutant
Ins+
Ins+ Pdx1+
Ins+ Glut2+
Ins+ Glut2+ Pdx1+
E
Control
F
Mutant
18.5 dpc
G
H
Control
I
Mutant
17.5 dpc
n

development in two independent manners. First, NC cells regulate Nkx2.2 expression, proliferation of Insulin-expressing cells and Insulin-positive area (Figure 2.4), (Nekrep et al., 2008). Second, NC cells positively regulate expression of *MafA* and *Pdx1,* and thus, beta cell maturation (Figure 2.5).

NC-derived cells directly contact Insulin- and Glucagon-expressing cells

To determine whether NC derivatives signal to Insulin-expressing cells through juxtracrine or paracrine signaling, high magnification images of Insulin-expressing cell clusters from control animals were analyzed. By 15.5 dpc, approximately 55 percent of Insulin-expressing clusters were in direct contact with TUJ1-expressing neurons (Figure 2.6A, D). This increased to approximately 84 percent of Insulin-expressing clusters in contact with TUJ1-expressing neurons by 17.5 dpc (Figure 2.6 B, D), and continued until postnatal day 1 when nearly every Insulin- expressing cluster (98.9%) was contacted by TUJ1-expressing neurons (Figure 2.6C,D). In addition, by 17.5 dpc we detected TUJ1-positive projections between endocrine cells (Figure 2.6B, inset) demonstrating that by late embryogenesis, NC derivatives enter endocrine cell clusters. Together, these data suggest a model where NC-derived cells signal to the pancreas through juxtracrine signaling and this mechanism of regulation of beta cell development begins prior to 15.5 dpc.

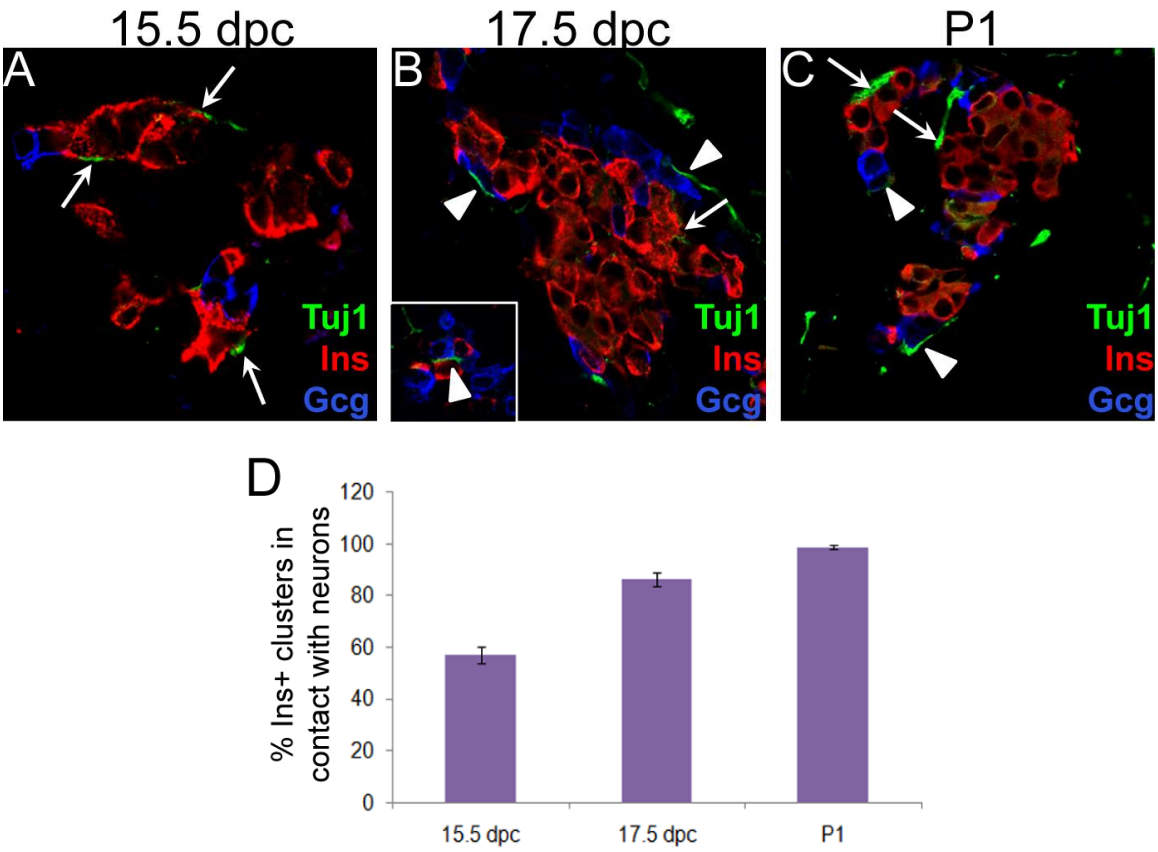

Figure 2.6: Neurons directly contact Insulin-expressing cells. (A-C) High-resolution (100X) confocal images of sections from control embryonic pancreata demonstrated that TUJ1-positive neurons (green) directly contact Insulin-expressing beta cells (red) at 15.5 dpc (A). TUJ1-positive neurons also contact both and Insulin (red)- and Glucagon (blue)-expressing beta and alpha cells at 17.5 dpc (B), and postnatal day 1 (C). The inset in B is an example of a TUJ1-positive cell that had a projection between a Glucagon (blue)- and an Insulin (red)- expressing cell at 17.5 dpc. Arrows indicate TUJ1-positive cells in direct contact with cells expressing Insulin and arrowheads indicate TUJ1-positive cells in direct contact with Glucagon (blue)-expressing cells. (D) Quantification of the number of Insulin-positive clusters that were in direct contact with neurons at each time examined. Error bars indicate SEM. N= 2-3 embryos/animals with at least 10 Insulin-positive clusters per sample.

Conclusion

To understand the importance of the NC on development of the pancreatic primordium, we first sought to precisely characterize the timing of NC arrival at the developing pancreas and determined that NC enters the pancreatic mesenchyme between the 26 and 27 somite stages (approximately 10.0 dpc, Model in Figure 2.7A). As the pancreatic epithelium branches and invades the surrounding mesenchyme, NC cells intermingle with acinar and pancreatic endocrine cells (Figure 2.7A). By 15.5 dpc, the majority of Insulin-expressing cell clusters were directly contacted by NC derivatives, suggesting that these cells may signal through direct cell-cell contact. This process is complete by postnatal day 1 when the overwhelming majority of Insulin-expressing cell clusters were contacted by NC derivatives. Our data, for the first time, precisely defines the stage at which this critical ectoderm-endoderm interaction is initiated, and confirms that NC is the sole source of pancreatic neurons and glia.

Earlier work demonstrated that loss of NC increased proliferation and, therefore increased the overall number of Insulin-expressing cells present in the embryonic pancreas (Nekrep et al., 2008). We show here, that in the absence of Foxd3, and therefore the NC, the Insulin-expressing area increased but, in addition, expression of beta cell maturation markers decreased, suggesting that NC promotes differentiation of Insulin-expressing cells to mature beta cells. In the absence of NC, increased proliferation of Insulin-expressing cells is associated with decreased or delayed beta cell maturation, suggesting that the immature beta cells are expanding (Figure 2.7B). Our work demonstrates a novel manner by which the ectodermally-derived NC influences development of the endodermally-derived beta cell and shows for the first time

Figure 2.7: Model of NC migration into the pancreatic primordium and regulation of beta cell development. (A) The pancreatic bud (blue) outpockets from the gut epithelium (red) between 9.0 and 9.5 dpc. Precisely by the 27 somite stage, migrating NC cells (green) enter the mesenchyme adjacent to the dorsal pancreatic bud (mesenchymal cells are not depicted here for simplicity), and by the 28 somite stage migrating NC cells enter the mesenchyme adjacent to the ventral pancreatic bud. As significant pancreatic branching ensues, NC cells become surrounded by the pancreatic epithelium. Between 13.5 and 15.5 dpc, endocrine cell clusters (purple) delaminate from the pancreatic epithelium and NC derivatives are found in direct contact with endocrine cells. (B) By 15.5 dpc and onwards, the majority of endocrine cell clusters are directly contacted by NC-derived TUJ1-positive neurons. Signals from NC derivatives positively regulate *MafA, Pdx1,* and Glut2 expression and, therefore, beta cell maturation while negatively regulating Insulin-expressing cell proliferation and Insulin-expressing cell area.

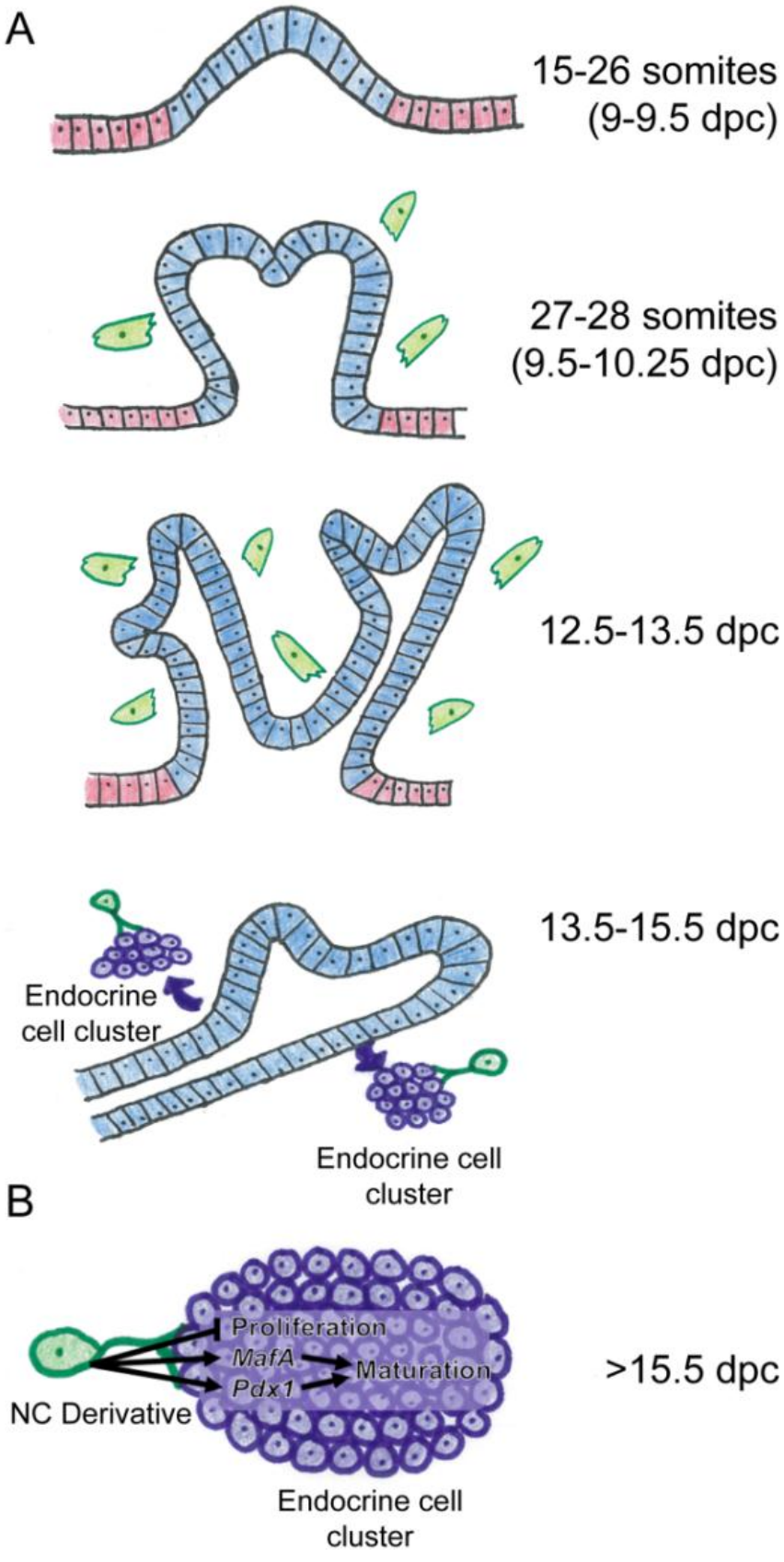
A
15-26 somites
(9-9.5 dpc)
27-28 somites
(9.5-10.25 dpc)
12.5-13.5 dpc
13.5-15.5 dpc
Endocrine
cell cluster
Endocrine cell
cluster
B
Proliferation
MafA
Maturation
Pdx1
NC Derivative
>15.5 dpc
Endocrine cell
cluster

that NC derivatives are critical regulators of beta cell development and maturation. This in turn suggests that identification of NC-derived signals may be important for the optimization of generation of glucose-responsive beta cells *in vitro*. Currently, in the most successful methods of producing human embryonic stem cell (hESC)-derived beta cells, the Insulin-expressing cells stall at an immature beta-cell stage (D'Amour et al., 2006). However, transplantation of a heterogeneous population of cells consisting mostly of pancreatic progenitor cells into adipose tissue or the kidney capsule of a host mouse provides a permissive environment for beta cell development and maturation, and transplanted cells become glucose responsive and can rescue glucose stimulated Insulin secretion in a beta cell ablated mouse model (Kroon et al., 2008). To our knowledge, no one has examined innervation in these models and it is possible that contaminating ectodermal cells were transplanted and/or that resident postnatal NC progenitor cells in the host may function to facilitate beta cell maturation in situ. Co-culture of NC stem cells and adult islets in vitro increases beta cell proliferation and function (Olerud et al., 2009), therefore, identification of NC-specific factors that augment beta-cell maturation has the potential to improve these directed differentiation schemes.

CHAPTER III

LOSS OF FOXD3 RESULTS IN DECREASED BETA CELL PROLIFERATION AND GLUCOSE INTOLERANCE DURING PREGNANCY

This work was published in its entirety under the same title in the December 2011 issue of *Endocrinology* (Plank et al., 2011b).

Introduction

Approximately 7 percent of pregnant women are affected by gestational diabetes mellitus (GDM), a disease resulting from the inability of the resident beta cell population to produce sufficient insulin during pregnancy (Parsons et al., 1992). GDM increases the risk of complications to both mother and newborn child; the mother is more likely to develop Type 2 diabetes (T2D) later in life and the child is more likely to be born with birth defects, macrosomia and an increased risk of developing T2D (Bellamy et al., 2009; Brelje et al., 1993; Feig et al., 2008; Lindsay, 2008; Mathiesen and Vaz, 2008). During normal murine pregnancy, beta cells proliferate, or self-renew, thereby expanding the total beta cell mass to meet the mother's increasing demand for insulin (Dor et al., 2004; Dor and Melton, 2008; Freemark et al., 2002; Parsons et al., 1992; Sorenson and Brelje, 1997; Teta et al., 2007; Vasavada et al., 2000). This mechanism of beta cell mass expansion during human pregnancy remains controversial. Analogous measurements are not ethically feasible in humans, however, morphological analyses of human pancreata indicate that beta cell mass is increased during pregnancy (Butler et al., 2007; Van Assche et al., 1978). Recent work analyzing pancreata from 38 cadaveric donors (18 pregnant, 20 controls) suggested that beta cells do not proliferate during human

pregnancy. Instead, an increased number of smaller islets and insulin-positive cells were observed within the ductal epithelium (Butler et al., 2010). However, this work is not without caveats. It is well known that murine beta cells proliferate within a defined time window and it is likely that the 18 pregnant human donors examined were not within an analogous gestational age (Karnik et al., 2007; Rieck and Kaestner, 2010). This study also included donors with inflammatory disease that may have adversely affected beta cell mass expansion (Genevay et al., 2010). It is important to note that the pregnancy associated hormones prolactin, placental lactogen (PL) and human growth hormone all stimulate beta cell proliferation in islets isolated from mice, rats, and humans suggesting that cell proliferation is a conserved mechanism of beta cell mass expansion during pregnancy (Brelje et al., 1993). While much of beta cell proliferation is controlled systemically (Porat et al., 2011), cell-autonomous control of beta cell proliferation is also a factor. Therefore, it is important to identify factors required for murine beta cell self-renewal because the associated gene regulatory networks controlling beta cell mass expansion are likely to be conserved in human beta cells.

To date, there are only a few existing mouse models of GDM. A heterozygous deletion of the Leptin receptor ($Lepr^{db/+}$) causes extreme insulin resistance, and during pregnancy this results in maternal hyperglycemia (Yamashita et al., 2001). A beta cell-specific deletion of *Hnf4α* results in decreased beta cell proliferation, beta cell mass, pancreatic insulin content, and islet size resulting in impaired glucose tolerance (Gupta et al., 2007). The transcription factor Foxm1 functions downstream of PL signaling. A pancreatic deletion of *Foxm1* results in decreased beta cell proliferation and beta cell mass in adult mice, and pregnant mutant mice have GDM by 15.5 days gestation, two-

thirds of the way through gestation (Zhang et al., 2010). In addition, inhibition of serotonin synthesis, normally increased in response to PL signaling, results in decreased beta cell mass expansion and glucose intolerance during pregnancy (Kim et al., 2010). An additional mechanism for glucose homeostasis regulation and beta cell proliferation is at the epigenetic level. Menin1 (Men1) functions as part of a histone methyltransferase complex to promote tri-methylation of histone 3 lysine 4 (H3K4), thereby maintaining expression of cell cycle inhibitors p27 and p18. Men1 is normally downregulated in beta cells during pregnancy, and artificially maintained expression during pregnancy causes decreased beta cell proliferation and maternal hyperglycemia (Karnik et al., 2007). Recent work highlights two proteins of the Polycomb complex required for beta cell proliferation: Ezh2 and Bmi1 facilitate epigenetic modifications permitting beta cell proliferation during basal physiological conditions (Chen et al., 2009a; Dhawan et al., 2009).

Foxd3, a Forkhead transcriptional regulator, is critical for self-renewal of multiple progenitor cells (Labosky and Kaestner, 1998; Nelms et al., 2011; Teng et al., 2008; Tompers et al., 2005; Xu et al., 2009). Foxd3 is expressed within the pancreatic primordium in two distinct cell populations: NC cells fated to innervate the pancreas (Plank et al., 2011b) and pancreatic beta cells (Perera et al., 2006). Pancreatic co-expression of Foxd3 and insulin begins by 15.5 dpc, and in adults, Foxd3 is expressed in beta cells (Perera et al., 2006). This expression is also observed in human and rat islets, suggesting a conserved function among mammalian species (Perera et al., 2006; White et al., 2008). Because Foxd3 is required for embryonic stem (ES) cell and NC progenitor cell self-renewal (Liu and Labosky, 2008; Mundell and Labosky, 2011; Nelms et al.,

2011; Teng et al., 2008), and beta cell mass expansion is primarily accomplished through self-renewal of existing beta cells (Dor et al., 2004; Dor and Melton, 2008; Teta et al., 2007), we hypothesized that Foxd3 is required for beta cell self-renewal, and by extension, beta cell mass expansion during pregnancy. Using a *Pdx1-Cre* transgenic mouse, we deleted *Foxd3* within the Pdx1-Cre expression domain, including the pancreas (Wicksteed et al., 2010). While these mice are unaffected under normal conditions, they suffer from glucose intolerance during pregnancy. In the absence of Foxd3 in the Pdx1 expression domain *Foxm1, Ezh2, Skp2, Akt2,* and *Cdkn1a* are misregulated and the mice suffer from pregnancy-associated defects in beta cell proliferation, beta cell mass, and hyperglycemia.

Materials and Methods

Mouse lines: Mice with a *Foxd3* null allele, $Foxd3^{tm2.Lby}$ (called $Foxd3^{-}$ throughout), and a conditional *Foxd3* allele, $Foxd3^{tm3.Lby}$ (called $Foxd3^{fl}$ throughout), were bred to mice carrying a *Pdx1-Cre* transgene (*Tg (Ipf1-cre) 1Tuv*) to generate mice lacking Foxd3 expression in the Pdx1-Cre expression domain ($Foxd3^{fl/-}$*; Pdx1-Cre*) and littermate controls ($Foxd3^{fl/+}$). The $Foxd3^{-}$ allele was used to minimize the number of recombination events mediated by Cre recombinase and allow direct comparisons between animals. These mouse lines and genotyping were previously described (Hanna et al., 2002; Hingorani et al., 2003; Teng et al., 2008). For timed matings, females were checked daily for presence of a vaginal plug; noon on the day of an observed plug was considered 0.5 days gestation. Mice were housed on ALPHA-Dri bedding (Shepherd

Specialty Papers) and fed Laboratory Rodent Diet 5001 (Labdiet). All mouse lines were maintained on an outbred genetic background consisting primarily of CD-1 and C57BL/6NHsd and handled in accordance with AAALAC standards and protocols with approval from the Vanderbilt University Institutional Animal Care and Use Committee (IACUC).

BrdU Incorporation and Immunohistochemistry: For BrdU incorporation analyses on pregnant mice, mice were injected with 50 mg 5-bromo-2-deoxyuridine (BrdU) per kg body weight at noon at 13.5 and 14.5 days gestation. Similarly, to analyze BrdU incorporation in postnatal day 14 mice, mice were injected with BrdU at 13 days of age. To assess BrdU incorporation in 8 week old mice, BrdU was placed in the drinking water (0.8 mg/mL) for 1 week and treated water replaced after 4 days to ensure BrdU activity. Pancreata were dissected and fixed overnight in 4 percent paraformaldehyde in phosphate buffered saline (PBS) and histological experiments performed using standard procedures (Tompers et al., 2005). For BrdU detection and beta cell size analyses, immunohistochemistry was performed as described (Teta et al., 2007) with rat anti-BrdU (1:250, Accurate Chemical), guinea pig anti-insulin (1:500, Millipore), Cy2-donkey anti-guinea pig (1:500, Jackson Immunoresearch), Cy3-donkey anti-rat (1:500, Jackson Immunoresearch), and Cy5-donkey anti guinea pig (1:500, Jackson Immunoresearch) antibodies. To detect Foxd3 protein, slides were incubated in citrate unmasking solution (Vector Laboratories) for 2 hours at high pressure. Antibody for Foxd3 was as described (Tompers et al., 2005) and detected with donkey anti-biotin secondary antibody (Jackson Immunoreserach) followed by Tyramide Signal Amplification (Invitrogen TSA Kit #22). Sections were counter-stained with 4', 6-diamidino-2-phenylindole (DAPI) (1:2000,

Sigma). For beta cell mass analyses, immunohistochemistry was performed using guinea pig anti-insulin (1:500, Millipore) and biotin-donkey anti-guinea pig (1:500, Jackson Immunoresearch) antibodies. The signal was amplified using RTU (Vector Laboratories) and 3'3 diaminobenzidine (DAB, Vector Laboratories). Sections were counterstained with Hematoxylin (Richard Allen Scientific). TUNEL analysis was completed with the In Situ Cell Death Kit (Roche).

Quantitative Analyses and Imaging: For BrdU incorporation, islets from 5 sections evenly spaced throughout the pancreas (accounting for approximately 5 to 8 percent of total pancreatic mass) were imaged using a Zeiss AxioSkop2 Plus equipped with a Q Imaging Retiga 2000R camera. The total number of BrdU-positive beta cells was divided by the total number of beta cells. For beta cell mass, the pancreas was embedded in a manner to ensure equal representation of the dorsal and ventral pancreas. Five evenly spaced pancreatic sections (accounting for 5 to 8 percent of the total pancreatic mass) were imaged using an Ariol SL-50 imaging system. Insulin-positive area and total pancreatic area were determined using ImageJ software (National Institutes of Health) and beta cell mass determined by dividing total beta cell-positive area by total pancreatic area multiplied by pancreatic wet weight. To determine beta cell size, every islet from 4 evenly spaced sections (accounting for approximately 4 to 6 percent of total pancreatic mass) was imaged as above (Crawford et al., 2009). The total insulin-positive area from each section was calculated using Adobe Photoshop. The area was then divided by the total number of beta cells per section. At least 5,000 β cells per animal were counted.

Gene Expression analyses by TaqMan Low Density Arrays and Quantitative Real Time PCR (qRT-PCR): Islets were isolated following standard procedures by the Vanderbilt

Islet Procurement and Isolation Core (Brissova et al., 2004). To assay *Foxd3* and *Skp2* expression in the presence of placental lactogen (PL), islets were cultured in 50 ng/mL PL for 4 days (Zhang et al., 2010). Total RNA was collected with the RNeasy Mini Kit (Qiagen), contaminating DNA removed with Turbo DNase (Ambion) and cDNA generated from 400 ng total RNA using the High Capacity cDNA Reverse Transcription kit (Applied Biosystems); genes included in this array are shown in Table 3.1. 100 ng of cDNA was prepared for analysis using TaqMan Universal PCR Master Mix (Applied Biosystems) and analyzed on a custom TaqMan Low Density Array (Applied Biosystems). The sequences for the primers and probes were previously published (Gu et al., 2011). The relative amount of RNA was determined with 18S rRNA as a reference. For qRT-PCR, 4 ng of cDNA per sample was prepared with Power SYBR Green PCR Master Mix (Applied Biosystems). All samples were run in duplicate, and the relative amount of RNA was determined by comparison to *Hypoxanthine guanine phosphoribosyl transferase (Hprt)* mRNA. The following primer sequences were used:

*Foxd3:*5'GTCCGCTGGGAATAACTTTCCGTA3'and 5'ATGTACAAAGAATGTCCCTCCCACCC3'

Skp2: 5'AGCCGAGGTGAATGAGAGTT3' and 5'AGCATGAATGCTCCACAAAG3'

*HPRT:*5'TACGAGGAGTCCTGTTGAATGTTGC3'and 5'GGGACGCAGCAACTGACATTTCTA3'.

Table 3.1: Genes assayed by TaqMan Low Density Array. Relative mRNA levels of the listed genes were assayed using a TaqMan Low Density array. Genes were clustered into groups based on the function of the produced protein. Note, some genes were included in multiple categories.

Insulin signaling	Cell Cycle	Beta Cell Function	Pancreas Development
Akt1	Akt1	Foxo1	Arx
Akt2	Akt2	Gjd2	Foxa2
Foxo1	Bmi1	Glut2	Gcg
Irs2	Ccnd2	Ins1	Hnf4a
Prkca	Cdc25a	Ins2	Isl1
Pten	Cdk4	MafA	MafA
Rictor	Cdkn1a	Nkx2.2	MafB
Sgk1	Cdkn1b	Pdx1	Neurog3
	Cdkn2a	Snap25	Nkx2.2
	Cdkn2b	Stx1	Nkx6.1
	Cdkn2c	Stxbp1	Pax6
	Ezh2	Vamp2	Pdx1
	Foxm1		Ptf1a
	Men1		
	Prdm16		
	Pten		
	Rictor		
	Skp2		

Intraperitoneal Glucose Tolerance Testing (IPGTT): Following a 16-hour fast, mice were subjected to an intraperitoneal injection of 2 mg dextrose per gram body weight. Glucose measurements were obtained with blood samples from the tail vein using a glucometer (FreeStyle) prior to injection and at 15, 30, 60, 90, and 120 minutes post injection.

Serum Insulin Assays: Blood samples obtained from the saphenous vein were collected in a Microvette CB 300 (Fisher Scientific) capillary tube prior to injection of dextrose, as above, and 15 and 30 minutes post-injection. Serum insulin content was measured using Insulin Ultra-Sensitive ELISA (Alpco Diagnostics). All samples were run in duplicate.

Islet Perifusions: Islet perifusions were performed as described using 16.7 mM glucose and 20 mM KCl in 5.6 mM glucose as stimuli (Tweedie et al., 2006). Insulin was extracted from perifusates in acid alcohol for 48 hours and insulin levels measured using

radioimmunoassays performed by the Vanderbilt Hormone Assay and Analytical Services Core. The total amount of insulin was normalized to 100 islet equivalents (IEQ) to standardize the data for comparison.

Statistical Significance: Two-tailed Student's t-tests were used to determine statistical significance for each assay except IPGTTs. In the case of IPGTTs, statistical significance was determined using "repeated measures ANOVAs with Bonferoni post-hoc tests".

Foxd3 is not required to maintain euglycemia under basal physiological conditions

To analyze the function of Foxd3 in beta cells, we used a *Pdx1-Cre* transgene to generate mice lacking pancreatic *Foxd3* (*Foxd3$^{fl/-}$; Pdx1-Cre*) along with control (*Foxd3$^{fl/+}$*) and heterozygous littermates *(Foxd3$^{fl/-}$* and *Foxd3$^{fl/+}$; Pdx1-Cre*) (Hanna et al., 2002; Hingorani et al., 2003; Teng et al., 2008), referred to as mutant, control, and heterozygote, respectively. We chose *Pdx1-Cre* to delete *Foxd3* because *Pdx1-Cre* mice are euglycemic (Ackermann-Misfeldt et al., 2008; Morioka et al., 2007; Xie et al., 2010; Zhang et al., 2010). All Foxd3 expressing cells within the pancreatic endoderm are contained within the Pdx1 expression domain (Perera et al., 2006). Using quantitative real time PCR (qRT-PCR), we verified that *Foxd3* mRNA was decreased approximately 3-fold in mutant islets, confirming that *Pdx1-Cre* deleted the *Foxd3* coding region (Figure 3.1A). It is important to note that Foxd3 is also expressed in NC derivatives that innervate the islets (Mundell and Labosky, 2011; Plank et al., 2011b; Teng et al., 2008), therefore, residual Foxd3 expression is likely due to expression within this lineage. Additionally, using immunofluorescence analysis of Foxd3 protein expression, we could

Figure 3.1: Validation of loss of Foxd3 and Foxd3 expression in pancreatic islets during pregnancy. A. qRT-PCR data showed that *Foxd3* expression was decreased in mutant islets (white bars) using *Pdx1-Cre* (left graph). *Foxd3* mRNA levels were decreased in islets isolated from 15.5 days gestation (D.G.) control (black bars) and mutant (white bars) mice compared to islets from control virgin mice (right graph). *Foxd3* expression in virgin controls was arbitrarily set to 1. There was no statistical difference between the *Foxd3* mRNA levels in virgin mutants compare to controls or mutants at 15 D.G. B-E. Immunohistochemistry for Foxd3 demonstrated that Foxd3 (red) was detected in the nuclei of insulin-expressing β cells (green) from control animals (B). B' and C' show the red channel alone. Foxd3 protein was not detected in β cell nuclei in mutant animals (C). Nuclear expression of Foxd3 is indicated by arrows (B' inset) and non-specific cytoplasmic staining is indicated by arrowheads (C' inset). Additionally, immunofluorescent analyses confirmed that Foxd3 is not expressed in beta cells during pregnancy. Foxd3 protein (red) was not detected in the nuclei of beta cells (insulin, green) in mutant (E and E') or control animals (D and D') at 15.5 D.G. F. *Foxd3* expression decreased while *Skp2* expression increased in islets isolated from wild type females cultured with human PL (white bars). *Foxd3* and *Skp2* mRNA levels in islets cultured without PL was arbitrarily set to 1 (black bars). n=3-4 mice in each group. Error bars indicate standard error of the mean (SEM). * $p < 0.05$, ** $p < 0.01$. Abbreviations: D.G., days gestation; PL, human placental lactogen.

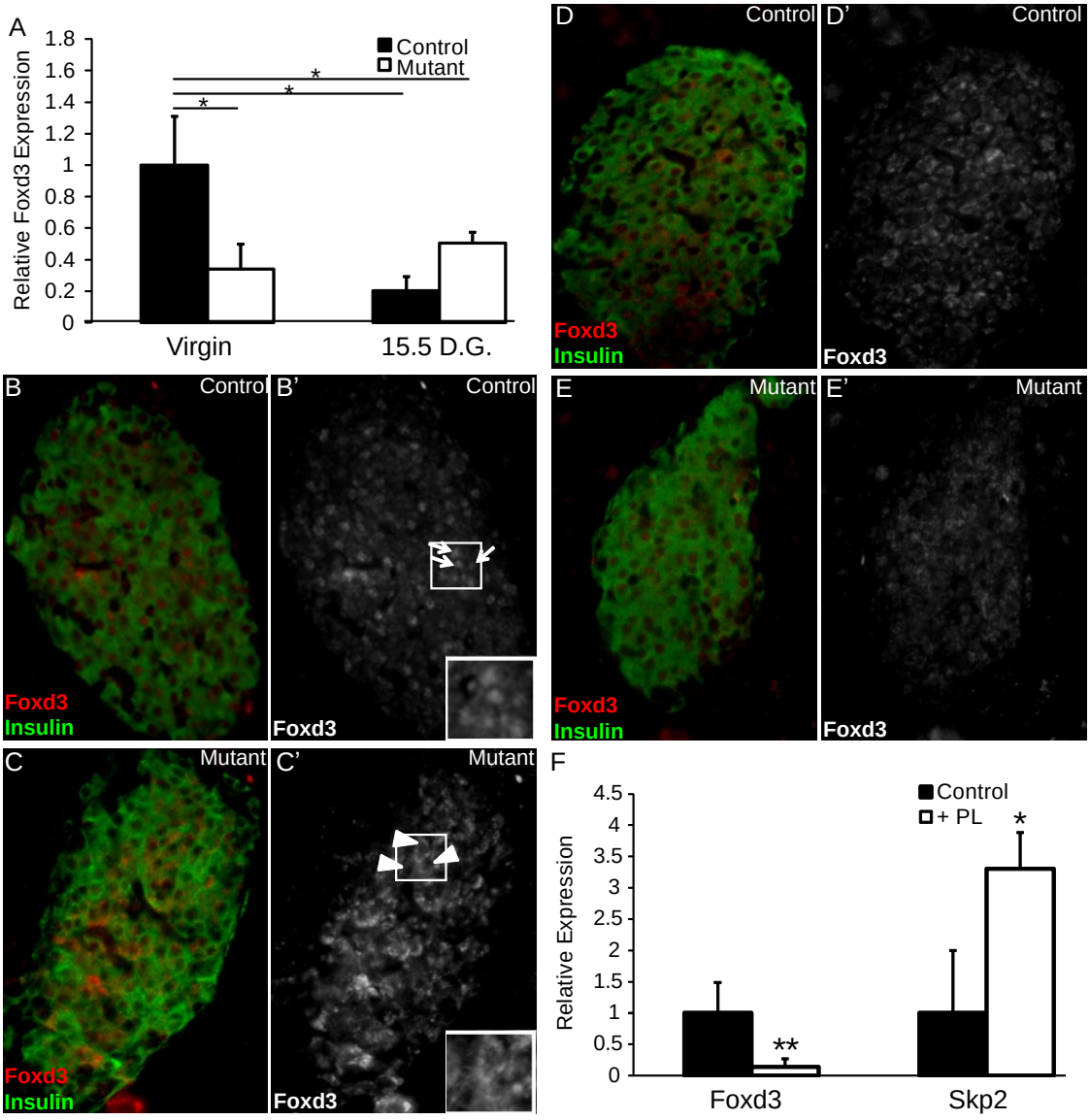
A
Relative Foxd3 Expression
1.8
1.6
1.4
1.2
1
0.8
0.6
0.4
0.2
0
Control
Mutant
*
*
*
Virgin
15.5 D.G.
B
Control
Foxd3
Insulin
B'
Control
Foxd3
C
Mutant
Foxd3
Insulin
C'
Mutant
Foxd3
D
Control
Foxd3
Insulin
D'
Control
Foxd3
E
Mutant
Foxd3
Insulin
E'
Mutant
Foxd3
F
Relative Expression
4.5
4
3.5
3
2.5
2
1.5
1
0.5
0
Control
+ PL
**
*
Foxd3
Skp2

not detect the protein in the nucleus of the islets from mutant mice (Figure 3.1C) compared to controls (Figure 3.1B). Because *Pdx1-Cre* is active in the hypothalamus (Honig et al., 2010; Song et al., 2010; Wicksteed et al., 2010), a region of the central nervous system critical for metabolic control, we analyzed *Foxd3* mRNA expression in the hypothalamus of control animals using RT-PCR and determined that *Foxd3* mRNA was not detectable in this region (Figure 3.2).

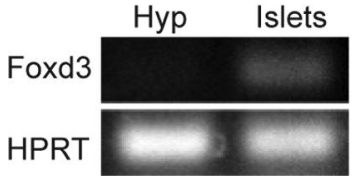

Figure 3.2: *Foxd3* expression was not detected in the hypothalamus. RT-PCR specific for *Foxd3* mRNA indicated that *Foxd3* was not expressed in the hypothalamus but was expressed in islets as expected. *HPRT* is a housekeeping gene that serves as a loading control. Note: 30 PCR cycles were needed to detect *Foxd3* while 25 PCR cycles were used to detect *HPRT*.

Additionally, *Foxd3* expression in both forms of heterozygous mice ($Foxd3^{fl/-}$ and $Foxd3^{fl/+}$*; Pdx1-Cre)* is not statistically different than $Foxd3^{fl/+}$ controls (Figure 3.3). The observation that Foxd3 expression in heterozygotes is similar to control mice is consistent with previous reports suggesting that Foxd3 functions as a transcriptional repressor (Steiner et al., 2006), and our data suggest the hypothesis that Foxd3 can autoregulate its own transcription.

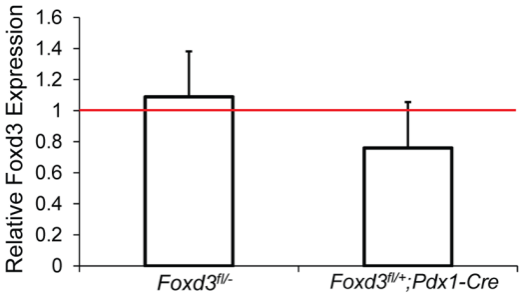

Figure 3.3: Foxd3 is expressed at normal levels in heterozygous mice. Expression of *Foxd3* in islets isolated from *Foxd3*$^{fl/-}$ and *Foxd3*$^{fl/+}$*; Pdx1-Cre* animals was similar to *Foxd3* expression in *Foxd3*$^{fl/+}$ controls. The expression in heterozygous animals was normalized to the expression in *Foxd3*$^{fl/+}$ controls and this value was arbitrarily set to 1 (red line). n=3 animals per group.

To determine the requirement for Foxd3 in maintaining euglycemia under basal physiological conditions, we performed IPGTTs on 38-week (data not shown) and 52-week old mice (Figure 3.4) fed a normal chow (5.1% fat/kcal). At both ages and for both genders, glucose clearance curves showed no significant differences between mutants, heterozygotes, and controls, suggesting that Foxd3 is not required to maintain glucose tolerance under normal physiological conditions.

Figure 3.4: Aged mutant mice maintain glucose tolerance. IPGTTs on one-year old mice indicate mutant mice (Δ) had glucose tolerance curves similar to control littermates (●). n= 7-10 mice in each group. Error bars indicate SEM.

Differential expression of Foxd3 during pregnancy

Because Foxd3 is required for proliferation and/or self-renewal of other cell lineages (Hanna et al., 2002; Liu and Labosky, 2008; Mundell and Labosky, 2011; Teng et al., 2008; Tompers et al., 2005) and it is expressed in adult beta cells (Perera et al., 2006), we hypothesized that Foxd3 plays a similar role in beta cells. To test this, we used pregnancy as a model because during pregnancy, murine beta cells self-renew to expand beta cell mass (Karnik et al., 2007; Parsons et al., 1992; Rieck and Kaestner, 2010; Sorenson and Brelje, 1997). To determine if *Foxd3* is differentially regulated during pregnancy, we analyzed *Foxd3* expression in islets from control and mutant females at 15.5 days gestation and found that, surprisingly, *Foxd3* mRNA levels were approximately 5 fold downregulated in wild type females at 15.5 days gestation (Figure 3.1A). These levels were similar to the levels detected in the mutant tissue, suggesting an almost complete loss of Foxd3 transcription. Additionally, Foxd3 protein was not detected in the nucleus of beta cells from control or mutant mice during pregnancy (Figure 3.1D-E). These data indicate that *Foxd3* is negatively regulated in response to pregnancy cues. During pregnancy, PL, growth hormone, and prolactin are upregulated and stimulate beta cell mass expansion. Although prolactin and growth hormone regulate beta cell proliferation, the most potent stimulus for beta cell proliferation during pregnancy is PL (Nielsen et al., 2001; Parsons et al., 1992; Sorenson and Brelje, 1997). Therefore, to determine if *Foxd3* expression decreases in response to placental lactogen (PL), we cultured islets isolated from wild type mice in the presence and absence of PL. To establish that our culture system worked as expected, we analyzed expression of *Skp2* after 4 days in culture. *Skp2* is a target of Foxm1 that increases expression in response to

PL (Zhang et al., 2010). We found that *Skp2* expression was increased, thereby validating this system (Figure 3.1F). At the same time, *Foxd3* mRNA levels were decreased approximately 6.7 fold supporting the notion that PL is a potent regulator of *Foxd3* expression during pregnancy (Figure 3.1F).

Requirement for Foxd3 to maintain euglycemia during pregnancy

To assess the ability of beta cells from mutant mice to meet the metabolic challenges of pregnancy, we analyzed pregnant females for their ability to clear glucose. To establish a baseline, IPGTTs on eight-week old virgin control and mutant mice demonstrated that, as expected, Foxd3 was not required to maintain glucose tolerance (Figure 3.5A). However, when the same mice were tested during pregnancy, mutants showed severe defects in glucose tolerance at 15.5 days gestation compared to controls, illustrated by both glucose tolerance curves and the calculated area under the curve (Figure 3.5 B and C). There were no defects observed in heterozygous mice at either stage (Figure 3.6 A and B).

To determine if impaired glucose tolerance in mutant mice resulted from reduced levels of secreted insulin, we measured serum insulin levels during an IPGTT from both virgin and pregnant mice. As expected, mutant and control serum insulin levels were similar prior to pregnancy (Figure 3.7A), confirming that insulin production and secretion is not impaired in virgin *Foxd3* mutant mice. However, during pregnancy, mutant mice had decreased serum insulin levels in response to a glucose stimulus (Figure 3.7B)

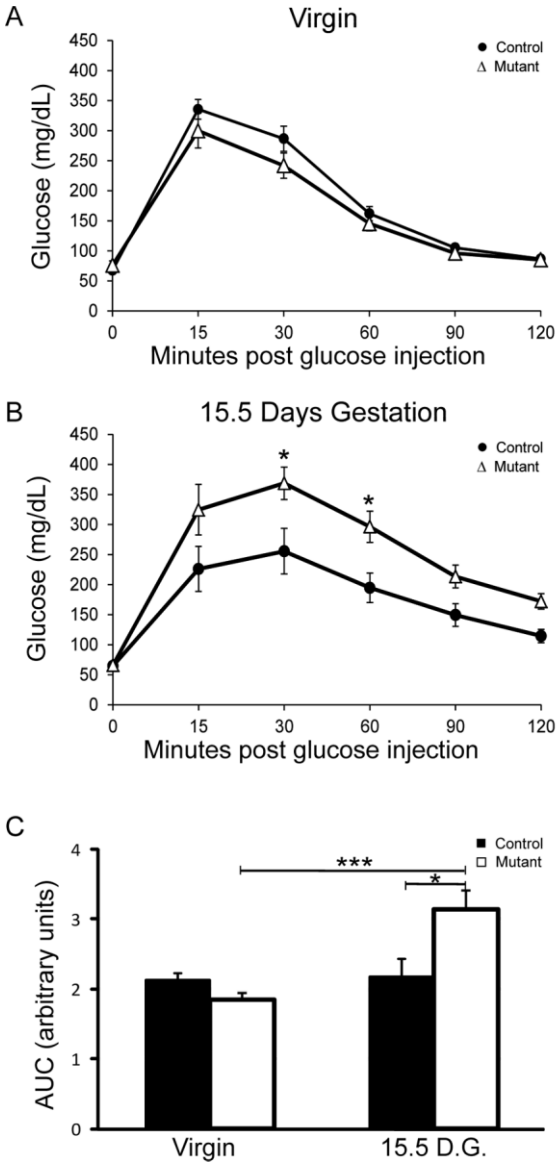

Figure 3.5: Glucose tolerance was impaired in *Foxd3$^{flox/-}$; Pdx1-Cre* mice during pregnancy. A. IPGTTs demonstrated that 8 week old virgin *Foxd3$^{flox/-}$; Pdx1-Cre* (Δ, mutant) and *Foxd3$^{flox/+}$* (●, control) female mice exhibited normal glucose tolerance. B. IPGTTs on the same mice at 15.5 days gestation showed mutant mice had impaired glucose tolerance while controls did not. C. The area under the curve of mutant mice (white bars) at 15.5 days gestation was greater than pregnant control (black bars) mice and virgin control and mutant mice. n= 10 mice in each group. Error bars indicate SEM. * $p< 0.05$, *** $p< 0.001$. Abbreviations: A.U.C., area under the curve; D.G., days gestation.

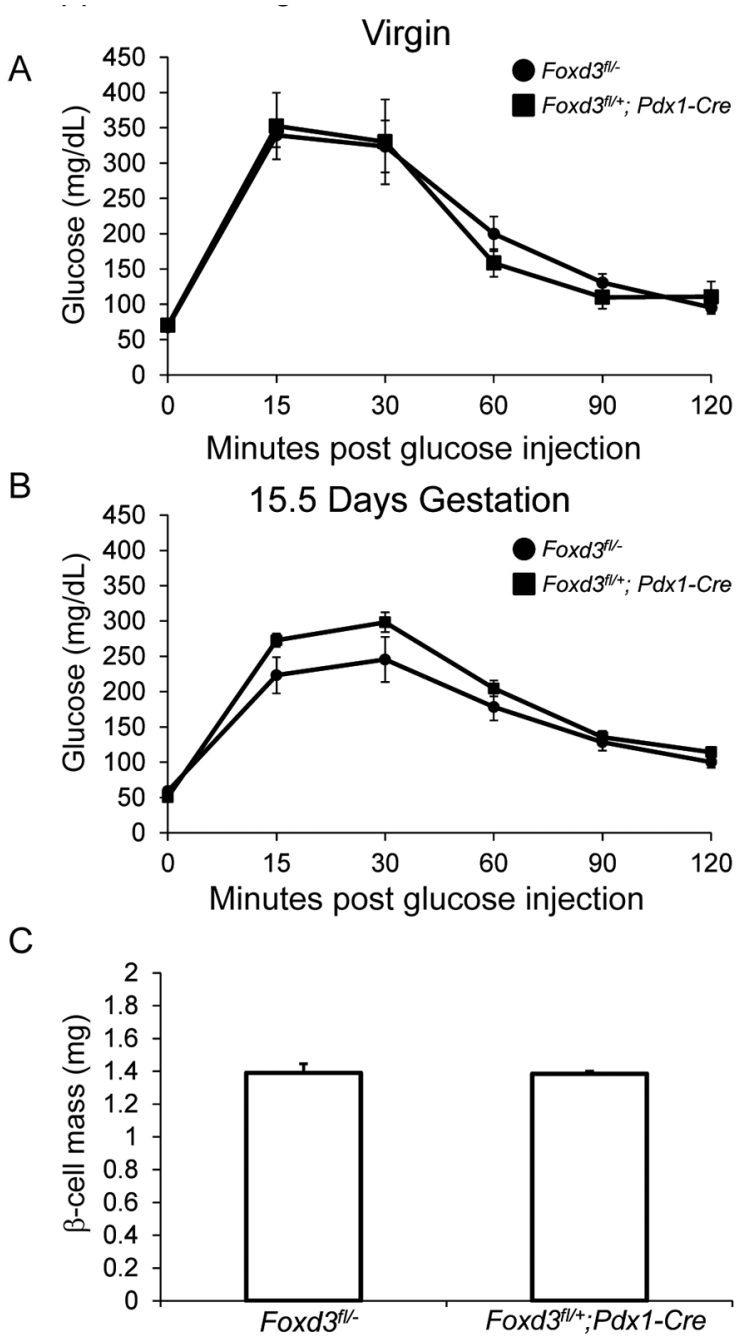

Figure 3.6: *Foxd3* heterozygous animals are phenotypically indistinguishable from control littermates. A-B. IPGTTs on *Foxd3*$^{fl/-}$ (●) and *Foxd3*$^{fl/+}$*; Pdx1-Cre* (■) animals each carrying one intact *Foxd3* locus in the pancreas demonstrated that mice heterozygous for *Foxd3* were euglycemic prior to pregnancy (A) and at 15.5 days gestation (B). n=8-12 animals per group. C. The β-cell mass in pregnant heterozygous females at 15.5 days gestation was not statistically different from *Foxd3*$^{fl/+}$ controls at the same time (compared to 1.53 mg for controls as shown in Figure 3.8). n=3 animals in each group. Error bars indicate SEM.

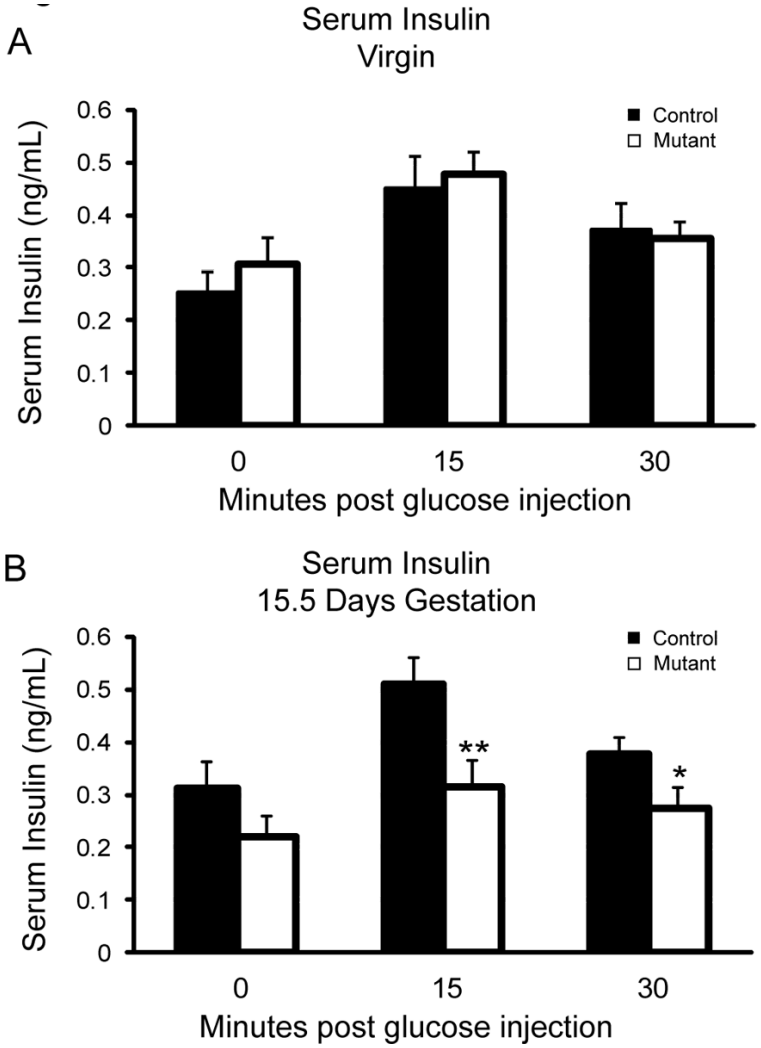

Figure 3.7: Serum insulin levels were decreased in mutant mice at 15.5 days gestation. A. ELISAs using serum collected from mutant and control virgin mice demonstrated that virgin mutant mice (white bars) had serum insulin levels similar to control mice (black bars). n=9-10 animals in each group. B. In contrast, mutant mice at 15.5 days gestation had reduced insulin serum levels 15 and 30 minutes after a glucose injection compared to controls. n= 9-10 animals in each group. Error bars indicate SEM. * $p< 0.05$, ** $p< 0.01$.

suggesting that Foxd3 is required to produce sufficient insulin levels to maintain glucose homeostasis in response to metabolic demand.

Genes required for cell proliferation and beta cell function are misregulated in Foxd3 mutant mice

To understand where Foxd3 functions in the known molecular pathways regulating glucose homeostasis, and to characterize genes misexpressed in mutant mice, we used TaqMan Low Density Arrays to evaluate expression of 47 genes (Table 3.1) implicated in either beta cell mass expansion/proliferation, beta cell function, insulin signaling and/or pancreas development (Figure 3.8). Several genes that regulate beta cell proliferation including *Cdkn1a, Cdkn2a, Ezh2, Foxm1,* and *Skp2* were misregulated in virgin mutant animals compared to virgin controls. There was a slight, but statistically significant, reduction in *Cdkn1b* expression. Additionally, *Ezh2* and *Akt2* were also severely downregulated in pregnant mutants compared to pregnant controls while *Skp2* was upregulated in pregnant mutants. These data suggest impaired beta cell proliferation that will impact beta cell mass expansion. In addition to expression changes in genes regulating beta cell proliferation, several genes required for glucose stimulated insulin secretion were also misregulated. In virgin mutants, *MafA, Foxa2,* and *Nkx2.2* mRNA levels were significantly repressed compared to virgin controls suggesting there may be defects in glucose stimulated insulin secretion in *Foxd3* mutant animals. Interestingly, in the pregnant mutants both *MafA* and *Foxa2* were upregulated while the mRNA encoding the SNARE protein Snap25 was significantly decreased. Both *Ins2* and *Vamp2* were

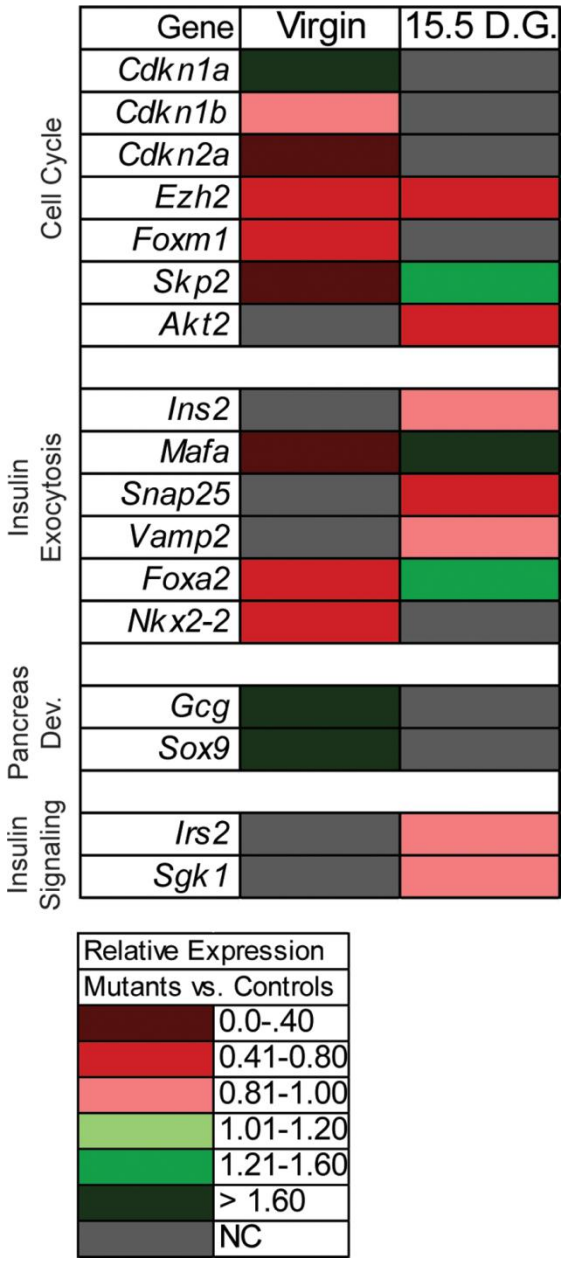

Figure 3.8: Gene expression profiling in *Foxd3* mutant and control pancreata. A. A TaqMan Low Density Array was used to analyze gene expression from mutant and control pancreata prior to and during pregnancy. The heat map illustrates relative changes in gene expression in mutant compared to controls at each stage ($p < 0.10$). Grey rectangles indicate no significant change in gene expression ($p > 0.10$). n=4 mice in each group. Abbreviations: D.G., days gestation; NC, no change.

slightly decreased in pregnant mutants compared to controls (less than 20 percent decrease in gene expression) but this change in expression is not likely to be biologically relevant. Lastly, a few genes required for pancreatic development were misregulated in the virgin *Foxd3* mutant animals. Both *Sox9* and *Gcg* were upregulated in the absence of Foxd3 although we did not detect changes in alpha cell mass (data not shown). An increase in these *Sox9* and *Gcg* genes may indicate the onset of an embryonic developmental program to compensate for defects in the adult mice. Although there was a slight reduction of *Irs2* and *Sgk1* (less than 20 percent change in gene expression) in pregnant mutant animals, the mRNA levels of these genes were very similar to those of controls suggesting there were no defects in insulin signaling in islets from mutant animals. Together these data suggest misregulation of genes known to control beta cell proliferation and beta cell function may account for glucose intolerance during pregnancy in *Foxd3* mutant animals.

Beta cell mass, proliferation, and size are decreased in mutant mice

Several of the misregulated genes (*Ezh2, Foxm1, Skp2,* and *Akt2*) are required for beta cell proliferation and beta cell mass expansion. Therefore, we quantified beta cell mass in 2 week and 8 week old virgin and 10 week old pregnant mice at 15.5 days gestation with and without the deletion of *Foxd3*. At 2 weeks of age, beta cell mass was similar in mutant and control mice. However, by 8 weeks of age beta cell mass in mutant mice was decreased 23 percent compared to controls (Figure 3.9A) although these mice were euglycemic (Figure 3.5A). Unsurprisingly, beta cell mass was decreased 30 percent

in pregnant mutant mice compared to control mice (Figure 3.9A). Predictably, beta cell mass was unchanged in heterozygous animals at 15.5 days gestation compared to controls (Figure 3.6C). These data demonstrate that, in agreement with previous studies, a 25 to 30 percent decrease in beta cell mass can be tolerated under basal physiological conditions in virgin mice (Ackermann-Misfeldt et al., 2008; Peshavaria et al., 2006). However, our data indicate that, during pregnancy a 30 percent decrease in beta cell mass may contribute to impaired glucose tolerance. Consistent with decreased beta cell mass, we detected an increase in alpha to beta cell area at 15.5 days gestation (Figure 3.9B). This change in proportion between alpha to beta cell area during pregnancy may also contribute to the defects in glucose tolerance.

Because we observed a defect in beta cell mass in 8 week old virgin and 10 week old pregnant mice, we assessed beta cell proliferation at these stages. Beta cells proliferate slowly in virgin mice at 8 weeks of age (reviewed in (Ackermann and Gannon, 2007)), therefore we measured BrdU incorporation for 1 week. The percent of beta cells that incorporated BrdU was similar between mutant and control mice (Figure 3.9D). This result was surprising, because beta cell mass was decreased by 23 percent in mutant mice at 8 weeks of age (Figure 3.9A). To determine if there was a defect in beta cell proliferation at earlier developmental stages, we assessed BrdU incorporation in younger mice (between 13 and 14 days) since beta cells proliferate more rapidly in neonatal rodents than adult rodents (Scaglia et al., 1997). At this time, BrdU incorporation in beta cells was similar between mutant and control animals (Figure 3.9C) supporting the notion that proliferation defects are not the fundamental cause of the slightly decreased beta cell mass in virgin mutants. During pregnancy, murine beta cells

Figure 3.9: Beta cell mass, beta cell proliferation, and beta cell size were decreased in mutant mice. A. The total beta cell mass was calculated and was similar between female mutant (white bars) and control (black bars) mice at 2 weeks of age. However, mutant mice had decreased beta cell mass compared to controls at both 8 weeks of age and 15.5 days gestation. B. The alpha to beta cell area was calculated by measuring the total glucagon-positive area divided by the total insulin-positive area. In virgin animals, the alpha to beta cell area ratio was similar between controls and mutants. However, the alpha to beta cell area was increased in pregnant mutants compared to pregnant control littermates suggesting a deficiency in the beta cell mass. C-E. BrdU incorporation between postnatal days 13 and 14 (C), 7 and 8 weeks of age (D) and 13.5 and 15.5 days gestation (E) was calculated by quantifying the number of BrdU/Insulin double-positive cells. BrdU incorporation between postnatal days 13 and 14 and 7 and 8 weeks of age was unchanged. In contrast, during pregnancy, BrdU incorporation between 13.5 and 15.5 days gestation was decreased approximately 2 fold in mutant mice compared to controls. n=3-4 animals per group. F. Beta cell size was calculated by measuring the insulin-positive area divided by the total number of beta cells from evenly spaced sections throughout the pancreas. In both virgin and pregnant females, beta cell size was decreased in mutant animals compared to control littermates. n=4-6 mice in each group. Error bars indicate SEM. * $p<0.05$. Abbreviations: D.G., days gestation.

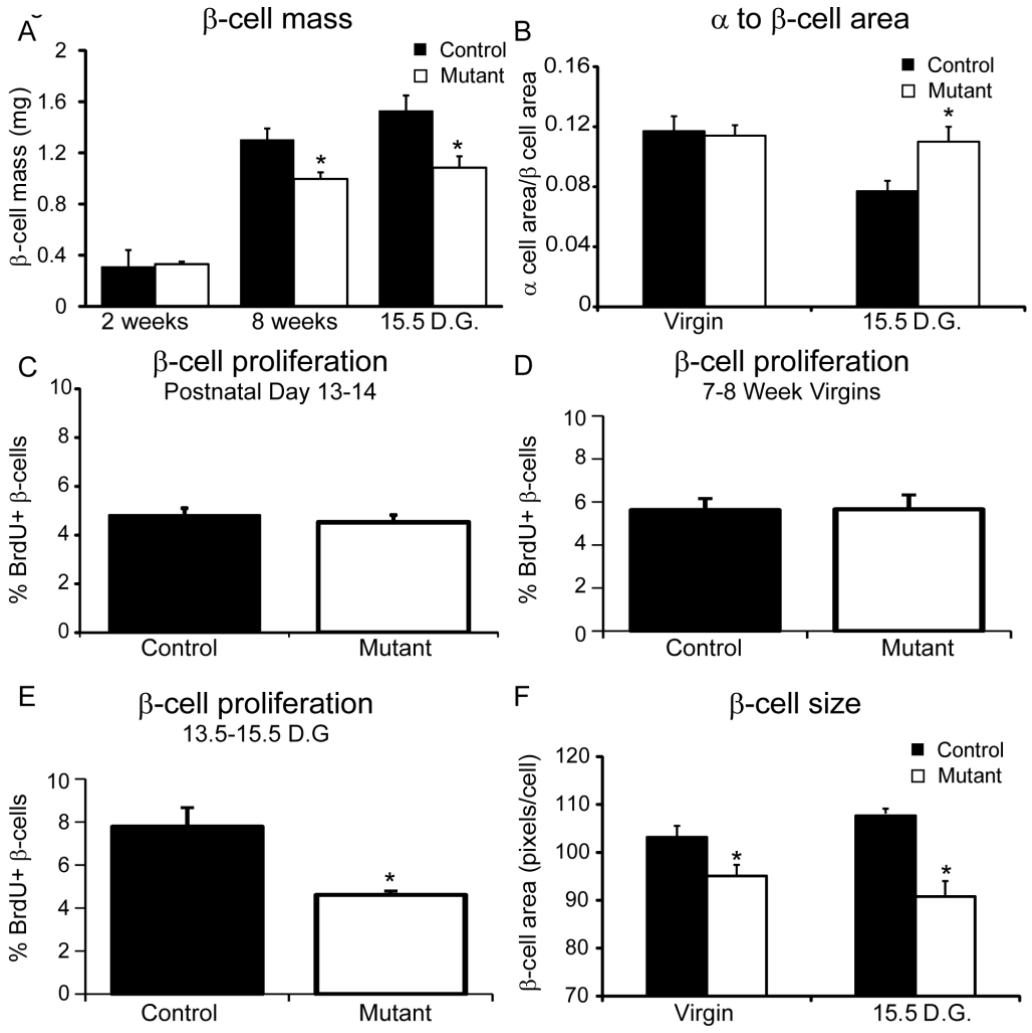
A
β-cell mass
β-cell mass (mg)
2
1.6
1.2
0.8
0.4
0
Control
Mutant
*
*
2 weeks
8 weeks
15.5 D.G.
B
α to β-cell area
α cell area/β cell area
0.16
0.12
0.08
0.04
0
Control
Mutant
*
Virgin
15.5 D.G.
C
β-cell proliferation
Postnatal Day 13-14
% BrdU+ β-cells
10
8
6
4
2
0
Control
Mutant
D
β-cell proliferation
7-8 Week Virgins
% BrdU+ β-cells
10
8
6
4
2
0
Control
Mutant
E
β-cell proliferation
13.5-15.5 D.G
% BrdU+ β-cells
10
8
6
4
2
0
*
Control
Mutant
F
β-cell size
β-cell area (pixels/cell)
120
110
100
90
80
70
Control
Mutant
*
*
Virgin
15.5 D.G.

proliferate to compensate for increased metabolic demand (Parsons et al., 1992; Sorenson and Brelje, 1997; Van Assche et al., 1978), and it is possible that different transcriptional networks and signals regulate this compensatory proliferation. Because beta cell proliferation during murine pregnancy peaks just prior to 15.5 days gestation (Karnik et al., 2007; Rieck and Kaestner, 2010; Zhang et al., 2010), we monitored BrdU incorporation between 13.5 and 15.5 days gestation. The percent of beta cells co-labeled with BrdU was approximately two-fold lower in mutants compared to controls (Figure 3.9E and Figure 3.10A-B) indicating that although Foxd3 was not absolutely required for beta cell proliferation, during pregnancy fewer *Foxd3* mutant beta cells proliferate compared with beta cells from control littermates. Another potential cause of decreased beta cell mass is increased beta cell apoptosis. To determine if Foxd3 is required for beta cell survival, we analyzed apoptosis at 15.5 days gestation, and in all samples analyzed we were unable to detect any TUNEL-positive beta cells (Figure 3.10C-D).

Another factor affecting beta cell mass is the size of individual cells. To determine if decreased hypertrophy contributes to decreased beta cell mass in both virgin and pregnant mutants, we analyzed beta cell size by measuring the total insulin-positive area divided by the total number of beta cells. We found that beta cell size was decreased in both virgin and pregnant mutants compared to control littermates (Figure 3.9F). This suggests that in virgin mutant mice, decreased hypertrophy contributed to decreased beta cell mass. However, in mutant mice, both decreased hypertrophy and proliferation combine to impact beta cell mass during pregnancy. Together with the results above, these data suggest that Foxd3 is required to maintain beta cell proliferation and size during pregnancy.

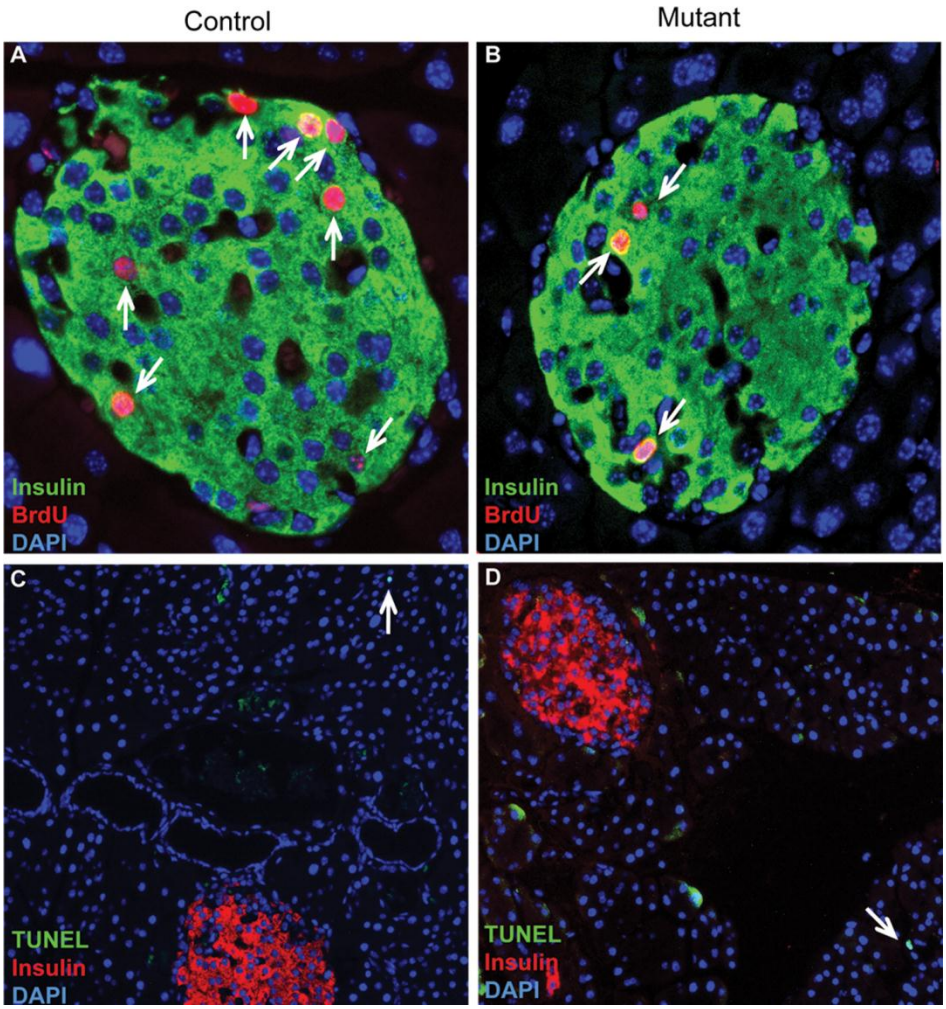

Figure 3.10: Foxd3 is required for beta cell proliferation but not beta cell survival. A-B. During pregnancy, fewer beta cells from mutant females (B) incorporate BrdU (red) compared to control littermates (A). Beta cells are indicated by insulin immunofluorescence (green). n = 4-6 mice in each group. Arrows indicate BrdU-positive β cells. Images were taken at 400x magnification. C-D. Using TUNEL assay together with insulin immunofluorescence, we were unable to detect TUNEL positive β cells in control (C) or mutant (D) mice. n= 4 animals in each group. Arrows indicate rare TUNEL-positive acinar cells. Images were taken at 200x magnification.

Foxd3 is not required to regulate glucose stimulated insulin secretion

Another physiological change caused by pregnancy is the response of beta cells to glucose. During pregnancy, beta cells become more sensitive to blood glucose levels and secrete more insulin when presented with lower glucose concentrations (Brelje et al., 1993; Parsons et al., 1992; Sorenson and Brelje, 1997). Because several genes required for beta cell function (*MafA, Snap25, Foxa2,* and *Nkx2.2*) were misregulated in the absence of Foxd3, we analyzed glucose stimulated insulin secretion using islet perfusion assays at 15.5 days gestation. The amount of secreted insulin was similar between mutant and control animals using both high glucose (16.7 mM) and KCl (20 mM in 5.6 mM glucose) to elicit a response (Figure 3.11). This suggests that although genes required for glucose stimulated insulin secretion were misregulated in the mutant animals, Foxd3 isnot required for enhanced glucose stimulated insulin secretion during pregnancy. These data further indicate that mutant beta cells function normally on a per cell basis and impaired glucose stimulated insulin secretion is not the underlying cause of glucose intolerance during pregnancy. Together, all of our data point to the conclusion that decreased beta cell mass in the absence of Foxd3 results in decreased serum insulin levels and glucose intolerance during pregnancy.

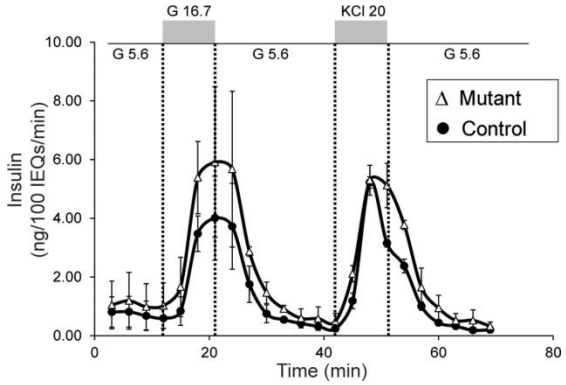

Figure 3.11: Foxd3 is not required for glucose stimulated insulin secretion during pregnancy**.** Islet perifusion assays were used to analyze insulin secretion in response to various stimuli (low glucose, high glucose, and KCl) and insulin levels from perifusates was normalized to 100 islet equivalents. The normalized amount of secreted insulin was similar between mutants (Δ) and controls (●). Note, all mice were at 15.5 D.G. Abbreviations: IEQs, islet equivalents; G 16.7, 16.7 mM glucose; G 5.6, 5.6 mM glucose; KCl 20, 20 mM KCl in 5.6 mM glucose. n= 2 animals per genotype.

Discussion

Foxd3 is dramatically downregulated during pregnancy in response to PL, and loss of Foxd3 results in impaired glucose tolerance during pregnancy, suggesting an important role for this protein during this metabolically challenging process. Here we characterized the role of Foxd3 in maintaining glucose homeostasis and beta cell mass expansion during pregnancy. Although beta cell mass was normal at postnatal day 14, and mutant mice were euglycemic under basal physiological conditions, pregnant mutant females were glucose intolerant during pregnancy, had decreased beta cell mass due to decreased beta cell proliferation and beta cell size, and several genes required to regulate cell proliferation were misregulated. These data clearly show that a pancreas-specific deletion of *Foxd3* is a novel mouse model of glucose intolerance during pregnancy.

The primary mechanism of beta cell mass expansion during normal homeostasis and pregnancy is beta cell proliferation, or self-renewal, of existing beta cells (Dor et al., 2004; Dor and Melton, 2008; Teta et al., 2007). Beta cells from *Foxd3* mutant mice showed decreased BrdU incorporation during pregnancy, indicating that loss of Foxd3 functionally impacts beta cell self-renewal at a time when beta cells must rapidly replicate to compensate for metabolic demand. Because Foxd3 is expressed in embryonic insulin-producing cells and the mutant pancreas develops normally, Foxd3 must not control the cell cycle directly and must not regulate embryonic beta cell proliferation. This finding is not surprising because postnatal and embryonic beta cells utilize different molecular pathways to regulate proliferation (Georgia and Bhushan, 2004, 2006; Kushner et al., 2005; Rane et al., 1999; Zhang et al., 2006). In addition, our data raise the possibility that Foxd3 regulates a "replication refractory period" that normally prevents serial beta cell proliferation (Salpeter et al., 2010; Teta et al., 2007), and Foxd3 may repress genes necessary to shorten the replication refractory period and therefore decrease the proportion of proliferating beta cells.

To identify the pathways through which Foxd3 function impacts beta cell proliferation, we analyzed gene expression differences between mutant and control pancreata and identified several misregulated genes required for cell proliferation. *Foxm1* transcription was decreased 2.3 fold in virgin *Foxd3* mutants; Foxm1 is required for beta cell proliferation following a 60 percent partial pancreatectomy and during pregnancy as a downstream mediator of PL signaling (Ackermann-Misfeldt et al., 2008; Ackermann and Gannon, 2007; Zhang et al., 2006). Additionally, there is a large variation in beta cell size in *Foxm1* mutant mice (Zhang et al., 2006), suggesting that decreased *Foxm1*

expression may be partially responsible for decreased beta cell size in *Foxd3* mutant animals. Another downregulated transcript, *Skp2*, is a target of Foxm1 (Wang et al., 2005), supporting the notion that the Foxm1 pathway was affected in *Foxd3* mutants. The cyclin dependent kinase inhibitor *Cdkn1a* was drastically upregulated in islets isolated from mutant animals. Cdkn1a inhibits CDK4 activity causing cell cycle arrest at G1 (Harper et al., 1993) and increased levels of *Cdkn1a* may restrict β cell proliferation in *Foxd3* mutants. The *enhancer of zeste homolog 2*, *Ezh2*, was also downregulated in islets from both virgin and, importantly, pregnant mutant mice. This protein is a histone methyltransferase required to repress the *Ink4a/Arf* locus that in turn regulates Foxm1 transcriptional activity and inhibits beta cell proliferation (Chen et al., 2009a; Kalinichenko et al., 2004). A beta cell-specific deletion of *Ezh2* resulted in decreased beta cell proliferation and hyperglycemia (Chen et al., 2009a). Although its role in regulating beta cell proliferation during pregnancy has not been analyzed, it is likely that pregnant *Ezh2* mutant mice will continue to have severe defects in glucose homeostasis. In addition to genes misregulated in virgin mutants, *Akt2* was downregulated in pregnant *Foxd3* mutants, and a compound mutation of *Akt2* and *Akt1* results in beta cell proliferation defects (Chen et al., 2009b). Because *Ezh2* and *Akt2* were downregulated in mutant mice during pregnancy, it is likely that they contribute to the proliferation defects observed during pregnancy. These data suggest that alteration of multiple parallel and interacting pathways in *Foxd3* mutants decreases proliferation, and Foxd3 impacts several factors that together control beta cell proliferation, beta cell size, and beta cell mass expansion during pregnancy (model, Figure 3.12).

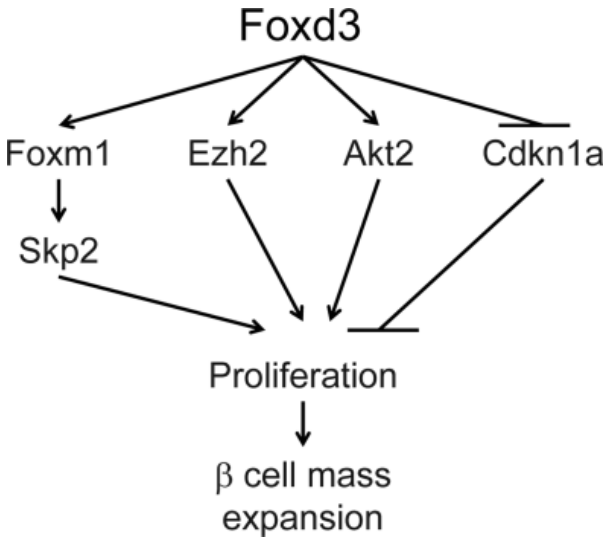

Figure 3.12: Model of Foxd3 function in the β cell. Foxd3 regulates several factors that control β cell proliferation including *Foxm1, Skp2, Ezh2, Akt2* and *Cdkn1a*. Arrows do not imply direct interactions.

Interestingly, *Foxd3* mutant mice exhibit a physiological defect during pregnancy despite the observation that Foxd3 is no longer expressed in maternal islets by 15.5 days gestation. This suggests that Foxd3 is required prior to pregnancy to permit beta cell proliferation during gestation and does not agree with models in which Foxd3 acts as a direct activator of genes required for beta cell proliferation. In ES cells, Foxd3 is required to maintain multipotency by inhibiting differentiation (Liu and Labosky, 2008). At a mechanistic level, Foxd3 "poises" the silent *Alb1* locus for transcription (Xu et al., 2009). Even though ES cells do not express *Alb1*, the locus is epigenetically modified in the pluripotent stem cells compared to primary fibroblasts that lack the potential to generate endoderm and express *Alb1* (Xu et al., 2009). Similarly, Foxd3 represses transcription of the B cell specific *Lambda5-PreB1* locus in ES cells, maintaining the locus in an inactive state despite active epigenetic marks. As cells differentiate toward a B cell fate, the Foxd3 mediated repression is relieved, concomitant with a different Forkhead protein

replacing Foxd3 at this binding site (Liber et al., 2010). A similar mechanism may occur in the pancreatic beta cell. Similar to the case of *Alb1*, Foxd3 may establish or maintain epigenetic mark(s) critical for upregulation of genes controlling beta cell proliferation when needed or, as in the *VpreB1* locus, remain as the last barrier to active transcription so that when needed, downstream genes can be activated quickly. When beta cells are stimulated to proliferate during pregnancy, Foxd3 may then be replaced by another Forkhead family member (perhaps Foxa1, Foxa2 or Foxm1) to activate expression of target genes regulating beta cell proliferation. Foxa1 and Foxa2 are required for activation of *Pdx1*, and through Pdx1, they regulate pancreatic differentiation and growth (Gao et al., 2008) while Foxm1 regulates beta cell proliferation (Ackermann-Misfeldt et al., 2008; Zhang et al., 2006; Zhang et al., 2010). Therefore, it is feasible that this mechanism is conserved in beta cells and Foxd3 is required to "poise" target genes while other Forkhead transcription factors are required for direct activation of gene expression. Because *Foxd3* was deleted from the pancreatic epithelium early in development prior to beta cell differentiation, target loci may never be "poised" and other Forkhead proteins may not have access to promote transcription of genes required for proliferation. Unfortunately, testing this model with the available reagents is not feasible. Ideally, to determine if Foxd3 is required to "poise" a locus for transcription, we would acutely ablate Foxd3 expression prior to pregnancy using a Tamoxifen-inducible Cre recombinase. However, we found that while both control and conditionally mutant female mice injected with Tamoxifen to activate Cre could mate, they were unable to become pregnant in a predictable manner (n = 9 females) even 6 weeks after the Tamoxifen injection. These findings are consistent with previously published data; rats

injected with Tamoxifen had smaller uteri and ovaries and their estrous cycles were arrested in diestrus (Kim et al., 2002; Orcheson et al., 1998; Tower et al., 2009). Therefore, this model awaits identification of direct targets of Foxd3, an active goal of our future work.

In summary, we have shown here that Foxd3 is required to regulate glucose homeostasis, beta cell proliferation, and beta cell mass during pregnancy. We have identified genes implicated in cell proliferation that are misregulated in the absence of Foxd3, and these data suggest that identification of molecules such as Foxd3 that control beta cell proliferation could be extended and co-opted for therapeutic applications requiring precise control of *in vivo* or *in vitro* expansion of existing beta cells.

CHAPTER IV

IDENTIFICATION OF FOXD3 TARGET GENES

Genes misregulated in the absence of Foxd3

Because Foxd3 is a critical regulator of stem cell properties in multiple lineages (Hanna et al., 2002; Liu and Labosky, 2008; Mundell et al., 2011; Mundell and Labosky, 2011; Teng et al., 2008; Tompers et al., 2005), Foxd3 target genes functioning directly downstream must regulate self-renewal, pluripotency, and/or survival of stem cells. I chose to attack this problem as a direct extension of my work in pancreatic beta cells because the discovery of genetic regulatory cascades controlling beta cell expansion is a key approach to unlocking this process for therapeutic applications. ES cells were used for initial identification of Foxd3 target genes because they are amenable to genetic manipulation and generating a large amount of biological material is relatively easy. Additionally, ES cells lacking Foxd3 have a distinct phenotype: 1) decreased capacity to self-renew, 2) decreased pluripotency, 3) increased apoptosis, and 4) maintained expression of stem cell proteins (Liu and Labosky, 2008). In order to assay gene expression in the absence of Foxd3, I used ES cells expressing the ubiquitous *CAAG-Cre*^{ER} transgene and carrying 2 *Foxd3*^{flox} alleles (*Foxd*$^{fl/fl}$*; CAAG-Cre*^{ER}). The entire Foxd3 coding sequence is excised when these ES cells are cultured with Tamoxifen (TM) added to the medium. In untreated ES cells (control), Foxd3 protein was readily detected (Figure 1.8). Following 12 hours of TM treatment (induced mutant), the level of Foxd3 protein expression was decreased but not abolished. However, after 24 hours of TM

treatment, Foxd3 protein was rarely detected (Figure 1.8). Therefore, my experiments assessing the effects of the loss of Foxd3 were completed at 24, 48, or 72 hours post TM treatment. As an initial characterization of genes misregulated in the absence of Foxd3, we performed a microarray pilot study (n=1 hybridization of samples) using the Affymetrix Gene/Exon microarray to determine which genes were misregulated in the absence of Foxd3 after 24 hours of TM treatment. We parsed the results obtained from the microarray and selected genes that encode proteins with functions related to the regulation of stem cell properties or genes that produce proteins with an unknown function. Genes that were misregulated in the absence of Foxd3 and were chosen for future analysis are illustrated in Table 4.1. Using quantitative reverse transcription PCR (qRT-PCR) to verify expression, I demonstrated that 12 of the 34 genes identified in the preliminary microarray were significantly misregulated ($p < 0.05$) in ES cells in the absence of Foxd3 (Figure 4.1).

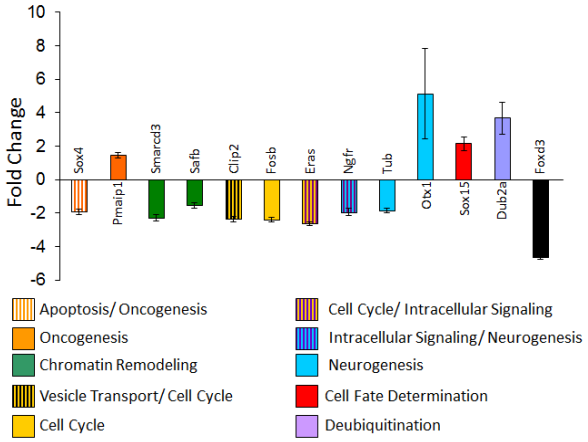

Figure 4.1: Genes that are misregulated in the absence of Foxd3 after 24 hours of culture with TM (induced mutant). The bars representing expression levels are color-coded based on biological function. The fold change in ES cells cultured for 24 hours without TM (control) is set to 1. Error bars indicate SEM.

Table 4.1: Genes misregulated in the absence of Foxd3 in ES cells (Fold change > 1.5). The gene names, fold change in the cells lacking Foxd3 compared to controls, and a brief statement of biological function are included.

Gene Name	Fold Change	Biological Information
Otx1	1.99	Regulates cell fate (Bicoid family member)
EG432649	1.9	Ubiquitin cycle/ligase activity
Ube1y1	1.81	Ubiquitin-activating enzyme E1
Tub	1.77	Tubby candidate gene
Grhl3	1.73	Developmental transcription factor
Hist1h2bb	1.68	Histone 2B gene
Socs2	1.63	Regulates cell growth
2410076i21Rik	1.62	Differentially expressed in ICM and ES cells
4930463MO5Rik	1.61	Suppresses p53 (ortholog of Klf4b)
5430411c19Rik	1.61	Expressed in obese and aged mice and human diabetic patients
Ngfr	1.61	Nerve growth factor (p75)- marker of NC stem cells
Clec2d	1.59	Natural killer cell receptor
LOC668686	1.58	Similar in sequence to apoptosis regulatory protein (Siva1)
E130309F12Rik	1.56	Regulates PRG3 (an apoptotic gene)
Eras	1.55	Promotes proliferation and self-renewal in mouse ES cells
Dub2a	1.54	Deubiquitinating enzyme 2a
Nrg3	1.53	Regulates proliferation and differentiation of satellite cells
Pmaip1	1.52	Promotes caspase expression and apoptosis
Sox15	1.51	Regulates myogenesis and CTCF expression
Fosb	-2.21	Required for osteoblast differentiation
Pi15	-2.13	Expressed in CNS
Safb	-1.89	Ubiquitously expressed nuclear matrix protein
Tac1	-1.87	Neurotransmitter
LOC345350	-1.84	Similar to Ubiquitin-conjugated enzyme, E2Q
LOC674405	-1.78	Binds DNA and heterochromatin
Evc2	-1.68	Unknown function
Sox4	-1.65	Cardiac outflow tract development
CDC2L1	-1.64	Regulates cell cycle
Fibin	-1.64	Secreted from lateral plate mesoderm
CLIP2	-1.62	Deleted in Williams Syndrome
Hirip3	-1.59	Associated with histones
Bnc1	-1.55	Zinc finger protein; associated with colony formation
Gap43	-1.52	Required for axonal regeneration
Smarcd3	-1.51	Plays a role in neural stem cells and myogenesis

Direct targets of Foxd3

Although the role of Foxd3 in regulating ES cell properties is well established, only a few Foxd3 target genes have been identified. To determine which of the misregulated genes are direct targets of Foxd3, we used a bioinformatics approach (rVista) to identify Foxd3 binding sites that are conserved between rodents and humans less than 20 kb upstream or downstream of the misregulated genes. Following the identification of putative Foxd3 binding sites, I used Chromatin Immunoprecipitation (ChIP) assays followed by quantitative PCR (qPCR) to amplify the putative binding sites and determine if Foxd3 occupied these regions in the genome. Using this assay, I determined that 6 of the 12 misregulated genes (*Sox4*, *Safb*, *Sox15*, *Fosb*, *Pmaip1* and *Smarcd3*) are direct targets of Foxd3 (Figure 4.2, left). Additionally, 3 of these targets are conserved in human ES cells (*SOX4*, *PMAIP1* and *SMARCD3*, Figure 4.2, right).

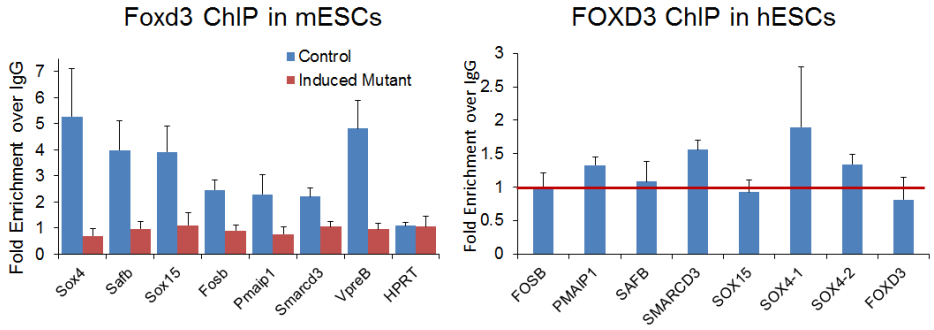

Figure 4.2: Direct targets of Foxd3. Left- using ChIP assays, we show here that 6 of the 12 misregulated genes are direct transcriptional targets of Foxd3 (*Sox4, Safb, Sox15, Fosb, Pmaip1, Smarcd3*). An intergenic enhancer at the *lambda5-VpreB (Vpreb)* locus serves as a positive control (Liber et al., 2010). Cells lacking Foxd3 (induced mutant, red bars) and the *HPRT* coding sequence were negative controls. Right- 3 of the 6 targets identified in mESCs (*PMAIP1, SMARCD3, SOX4*) are conserved in hESCs. Human chromatin from Steve Dalton, UGa, hESC Core Laboratory. The negative control for these experiments is the *FOXD3* coding region.

We hypothesize that all 6 identified targets of Foxd3 regulate ES cell properties, and a brief summary of the function of each protein is included below. The transcription factor Sox4 is required for cardiac outflow tract development, derived from the NC (Maschhoff et al., 2003; Schilham et al., 1996; Ya et al., 1998). Additionally, in developing B cells, Sox4 co-occupies a site in an intergenic enhancer of the *lambda5-preB* locus with Foxp1 and transcription of the surrounding genes (*Lambda5* and *PreB*) is required for B cell differentiation. Prior to occupancy of Foxp1 and Sox4, Foxd3 and Sox2 bind this region to "poise" the locus for transcription (Liber et al., 2010). The transcription factor FBJ osteosarcoma oncogene B (Fosb) promotes osteoblast differentiation while inhibiting adipogenesis (Sabatakos et al., 2000). The transcriptional modulator Sox15 regulates skeletal muscle differentiation in multiple progenitor cell lineages (Beranger et al., 2000; Lee et al., 2004; Savage et al., 2009). Smarcd3 (also called Baf60c), a member of the Swi/Snf chromatin remodeling complex, associates with MyoD to promote transcription of genes required for myogenesis (Forcales et al., 2011; Ochi et al., 2008). While all 4 factors have been implicated in regulating differentiation of disparate lineages, no one has carefully investigated the role of these proteins in maintaining ES cell properties, and I hypothesize that Sox4, Fosb, and Sox15 are critical regulators of pluripotency in ES cells.

In addition to genes that regulate pluripotency, two Foxd3 targets may regulate self-renewal of ES cells. The protein Smarcd3 is a component of a Swi/Snf complex in neural stem cells and is required to regulate self-renewal in this cell lineage (Lamba et al., 2008). While *Smarcd3* mRNA can be detected in ES cells (Figure 4.1), to date, no one has analyzed a role for this protein in regulating self-renewal of ES cells. In addition, the

nuclear scaffolding protein, Safb, is ubiquitously expressed, but a clear role for its function has yet to be determined. Some groups suggest that Safb may regulate the cell cycle consistent with the possibility that Safb may be required for ES cell proliferation and/or self-renewal (Debril et al., 2005; Huerta et al., 2007; Tapia et al., 2009). These findings suggest that these targets of Foxd3 may regulate self-renewal in ES cells.

Lastly, targets of Foxd3 are also required to prevent aberrant apoptosis. Safb indirectly represses apoptotic genes in breast cancer cells (Chan et al., 2007; Lee et al., 2007). Therefore, decreased *Safb* expression in ES cells (Figure 4.1) may lead to an increase in apoptosis. Finally, Pmaip1 is a direct target of Foxd3 and is a critical regulator of cell death. Pmaip1 (also called Noxa) is required for the activation of caspases and contributes to p53-dependent apoptosis (Li et al., 2006; Oda et al., 2000; Yakovlev et al., 2004). Altogether, these data from our laboratory and others suggests that Foxd3 functions upstream of critical regulators of stem cell property. Prior to this work, only a few direct targets of Foxd3 were identified. This work uncovered several factors that function downstream of Foxd3 and further characterization of these target genes will further elucidate gene regulatory networks controlling ES cell properties.

In addition to this candidate gene approach, members of the laboratory are taking an unbiased approach to determine all the loci occupied by Foxd3 in ES cells; we have generated an ES cell line carrying a Flag-tagged allele of *Foxd3* in the endogenous *Foxd3* locus (Michael Suflita, unpublished data). While the commercially available antibody works well for ChIP assays, ChIP-Seq applications required a robust signal. Therefore, these ES cells, and mice generated from these cell lines, will be used in ChIP-Seq experiments in collaboration with Dr. Klaus Kaestner at the University of Pennsylvania

to determine all Foxd3 target genes in ES cells, pancreatic beta cells, and NC progenitors allowing us to determine whether Foxd3 target genes are conserved among disparate cell lineages. Once additional targets are identified, their expression will be manipulated to further identify pathways and potential nodal points to manipulate cell fate specification and beta cell mass expansion.

The mechanism of action of Foxd3 is unresolved; there are several findings suggesting that Foxd3 functions as a transcription repressor, while others suggest that Foxd3 functions as an activator (Lee et al., 2006; Pan et al., 2006; Steiner et al., 2006; Thomas and Erickson, 2009). While it is possible that Foxd3 can function as either an activator or a repressor in different cellular contexts, the strongest evidence demonstrates that Foxd3 functions as a transcriptional repressor in mesoderm induction in *Xenopus* (Steiner et al., 2006; Yaklichkin et al., 2007), therefore, I chose to focus on analyzing Foxd3 targets that were upregulated in the absence of Foxd3, indicating that Foxd3 normally represses their transcription. Messenger RNA encoding the transcription factor *Sox15* is upregulated approximately 2 fold in the absence of Foxd3 (Figure 4.1). This increase in *Sox15* mRNA levels persists for at least 72 hours in culture with TM added (Figure 4.3, left).

Additionally, using an embryoid body (EB) assay to analyze gene expression in differentiated cells, I demonstrated that *Sox15* mRNA levels quickly decrease upon differentiation (Figure 4.3, right, red line). These data are in agreement with published work demonstrating that Sox15 is expressed in ES cells but not in differentiated cell lineages (Maruyama et al., 2005). Consistent with increased *Sox15* mRNA levels in the absence of Foxd3 in ES cells, *Sox15* mRNA levels persist in the EBs lacking Foxd3

(Figure 4.3B, blue line). Together, these data indicate that Sox15 expression decreases upon differentiation and is consistent with the hypothesis that Foxd3 represses Sox15 transcription directly.

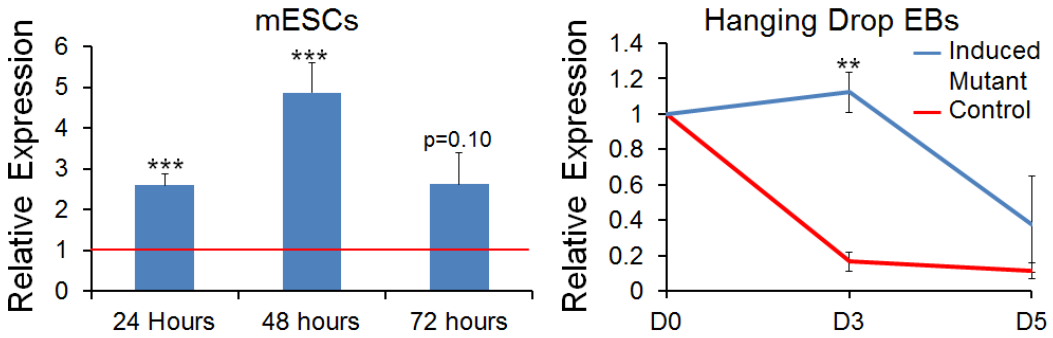

Figure 4.3: Left- qRT-PCR analysis of relative expression of *Sox15* in ES cells cultured with and without TM for the indicated amount of time. *Sox15* expression in induced mutant ES cells was increased at all 3 time points compared to untreated controls. The red line indicates relative expression in untreated (control) ES cells. Right- expression of *Sox15* in untreated (control) and TM treated (induced mutant) EBs determined by qRT-PCR compared to untreated ES cells at Day 0 (D0). In control EBs (red line), *Sox15* expression decreases upon differentiation and is barely detectable by 3 days in culture. Alternatively, *Sox15* expression persists in induced mutant EBs (blue line) and does not decrease until after 3 days in culture. Error bars indicate SEM. ** $p<0.01$, *** $p<0.001$.

To ensure that increased *Sox15* mRNA levels were due to an increase in transcription, I used ChIP to analyze phosphorylated-Ser5 RNA PolymeraseII (p5PolII) occupancy at the transcription start site of Foxd3 target genes. The Ser5 residue of PolII is only phosphorylated when transcription is initiated; therefore, an increase in p5PolII occupancy suggests an increase in transcription while a decrease in p5PolII occupancy suggests decreased transcription (Rahl et al., 2010). As expected, there was an increase of p5PolII at the proximal promoter of *Sox15* in mutant ES cells compared to controls.

Alternatively, there was a decrease of p5PolII at the proximal promoter of *Sox4*, a gene with decreased expression in the absence of Foxd3 (Figure 4.1). The distal promoter of *Albumin1* (*Alb1*) served as a negative control because this region of the genome is not transcribed and PolII is not recruited to that site (Figure 4.4). These data are consistent with the hypothesis that Foxd3 represses *Sox15* transcription in ES cells.

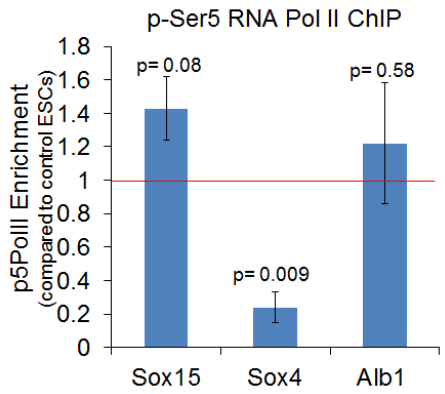

Figure 4.4: ChIP assays were used to determine p5PolII occupancy at the proximal promoter of genes misregulated induced mutant ES cells. The data represent the ratio of PolII occupancy in mutant ES cells compared to controls. The red line indicates PolII occupancy in controls. Error bars indicate SEM.

Manipulating expression of Foxd3 target genes

The significance of this work stems from the identification of novel regulators of self-renewal, pluripotency, and/or survival of ES cells. Because Sox15 is a direct target of Foxd3, and Sox15 is a critical regulator of skeletal muscle differentiation *in vitro* (Beranger et al., 2000; Lee et al., 2004; Savage et al., 2009), I sought to first characterize the effects of loss of Foxd3 on genes that function downstream of Sox15 and are required to regulate skeletal muscle development. Skeletal muscle is derived from paraxial

mesoderm and requires the myogenic bHLH transcription factors, MyoD and Myf5 (Figure 4.5). Following determination to the skeletal muscle lineage, myoblast progenitor cells divide, align, and fuse to generate multinucleated myotubes , resulting in mature muscle fibers that also contain muscle stem cells (Figure 4.5). A putative stem cell population, the satellite cells, is capable of proliferating to generate new myoblasts that fuse with mature muscle fibers, and production of myoblasts from satellite cells requires the function of Myf5 (Kuang et al., 2007).

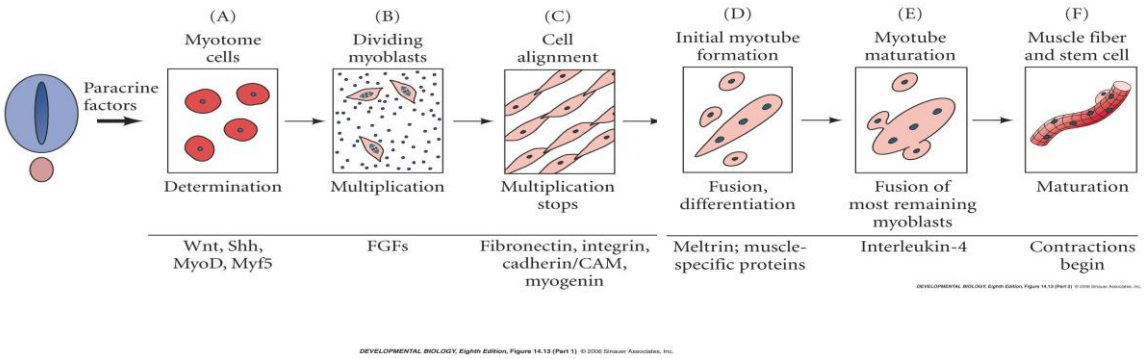

Figure 4.5: Schematic of myogenesis in culture. Image from "Developmental Biology" Ninth Edition by Scott Gilbert (Gilbert, 2010).

The transcription factors Pax3 and Sox15 function upstream of Myf5 and MyoD (Beranger et al., 2000; Lee et al., 2004; Savage et al., 2009). *Sox15* null animals cannot regenerate skeletal muscle following injury, while overexpression of Sox15 results in increased Pax3 expression, decreased Myf5 expression, and an expansion of immature myoblasts (Maruyama et al., 2005; Savage et al., 2009). Because Sox15 is upregulated in Foxd3 induced mutant ES cells and Sox15 inhibits myogenesis, I hypothesized that Foxd3 induced mutant ES cells cannot be directed to produce mature muscle. To

determine if genes functioning downstream of Sox15 are misregulated in the absence of Foxd3, I assayed mRNA levels of myogenic genes using qRT-PCR. As expected, *Myf5* expression decreased while *Pax3* expression increased (Figure 4.6), suggesting that Foxd3 functions upstream of Sox15 to regulate myogenesis. These data, together with previous work in the lab (Liu and Labosky, 2008), suggest that Foxd3 induced mutant ES cells precociously express genes required for mesoderm induction but cannot differentiate into skeletal muscle. This hypothesis will be directly tested using differentiation paradigms.

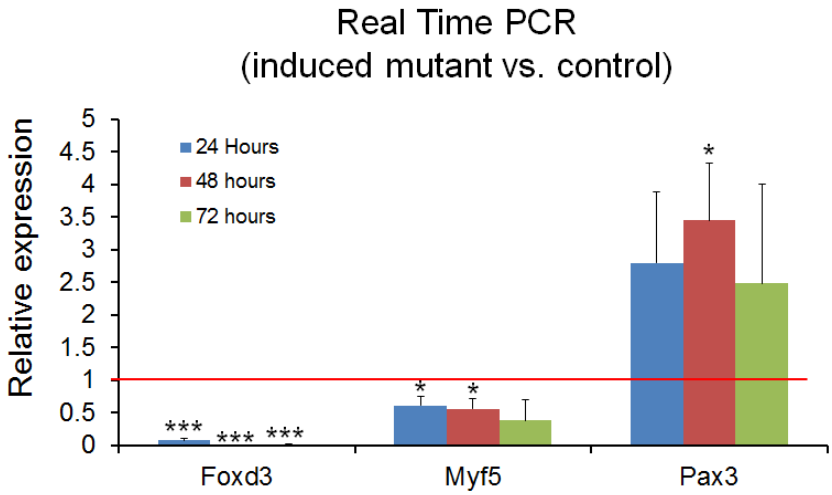

Figure 4.6: qRT-PCR data demonstrating the relative expression of *Foxd3*, *Myf5*, and *Pax3* mRNA in Foxd3 induced mutant ES cells cultured for 24, 48, and 72 hours. Myf5 expression is decreased while Pax3 expression is increased. Red line indicates expression of these mRNAs in control ESCs with no TM treatment. Error bars indicate SEM. * $p < 0.05$, *** $p < 0.001$

Together, these data are consistent with the model in Figure 4.7 in which Foxd3 represses *Sox15* transcription resulting in increased *Pax3* and decreased *Myf5*. An

increase in Pax3 expression in the skeletal muscle progenitors results in an increase self-renewal and decreased differentiation, limiting the number of mature skeletal muscle fibers (Epstein et al., 1995; Young and Wagers, 2010). Additionally, decreased *Myf5* results in decreased generation of skeletal muscle.

To determine if Foxd3 target genes regulate stem cell properties, induced cassette exchange (ICE) will be used to easily manipulate gene expression (Iacovino et al., 2011a; Iacovino et al., 2011b). Using ICE, Foxd3 target genes will be overexpressed in a Doxycycline inducible manner (Figure B.3). Using this method, I generated 12 ES cell lines to overexpress *Sox15* (6 lines contain *Sox15-Myc* and 6 lines contain *Sox15-HA*).

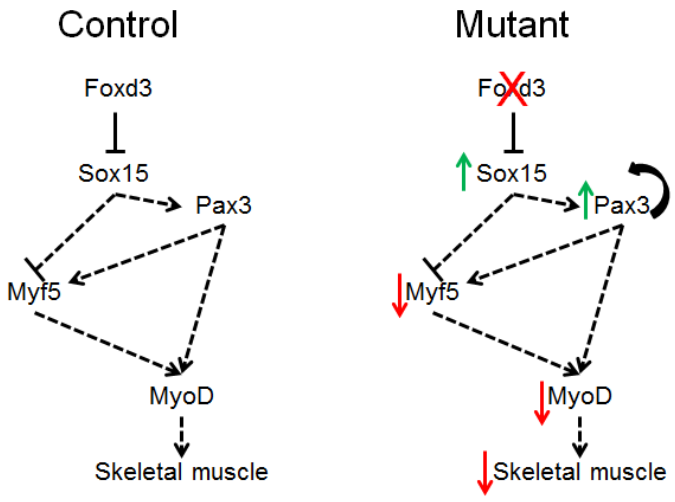

Figure 4.7: Model of Foxd3 and Sox15 in ES cells in the process of skeletal muscle differentiation. In a control progenitor cell (left), Foxd3 represses *Sox15* allowing precise regulation of *Pax3* and *Myf5* and proper skeletal muscle development. In the absence of Foxd3 (right), *Sox15* is upregulated resulting in an increase in *Pax3* and a decrease in *Myf5* expression. Based on data available in the literature, I hypothesize that these changes in gene expression will result in an increase in skeletal muscle progenitors but an inability to generate skeletal muscle from ES cells lacking Foxd3.

While the specific concentration of Doxycycline to induce overexpression of Sox15 has not been determined, I have confirmed that the cell lines do, in fact, express high levels of *Sox15* mRNA. Doxycycline will need to be titrated in order for the cells to express the appropriate amount of Sox15. Using these cells, we will determine if overexpression of Sox15 inhibits self-renewal, survival, and/or skeletal muscle differentiation *in vitro.* In an extension of this approach, expression levels of Foxd3 target genes can be reduced using this method with miR30 sequences flanking shRNAs to the genes of interest to ensure the shRNAs are transcribed with RNA Polymerase II (Wang et al., 2006). Using the newly generated ES cells lines, self-renewal, potency, and survival will be analyzed to determine how Foxd3 target genes regulate properties of ES cells. These data will further uncover components of gene regulatory networks required to maintain stem cell properties.

In summary, the future directions proposed here take advantage of manipulating Foxd3 expression to uncover components of gene regulatory networks controlling stem cell properties. Identification of factors that restrain self-renewal and/or factors that regulate differentiation to a desired cell lineage will be paramount in generating cell-based therapies from pluripotent stem cells or adult stem cells. Additionally, the experiments proposed here can be extended to beta cell biology. Targets of Foxd3 in the beta cell and the NC will be identified in Foxd3 ChIP-Seq experiments from isolated islets (proposed in Chapter 5). These targets can be manipulated in ES cells using ICE and then ES cells differentiated into the beta cell lineage to determine precisely how Foxd3 targets regulate beta cell development and/or beta cell mass expansion. The factors identified in these studies can be applied to the generation of beta cells to treat diabetic

patients. For example, identification of factors misregulated in the beta cell in the absence of NC may identify pathways that can be manipulated to facilitate beta cell maturation in directed differentiation protocols. Overall, the data presented and future experiments building off my thesis work can affect multiple aspects of stem cell biology and regenerative medicine.

CHAPTER V

FUTURE DIRECTIONS

Beta cell development in a model of reduced innervation

Using *Wnt1-Cre* to delete *Foxd3* results in a system where all NC derivatives are absent from the ENS providing an ideal model to study the requirement for NC derivatives on beta cell development. However, this genetic ablation model cannot be used to determine if a reduced number of NC derivatives also effects beta cell development, a much more likely *in vivo* scenario. Using the novel *Endothelin receptor type B (Ednrb)-iCre* transgenic line to delete Foxd3 results in a more restricted loss of Foxd3 limited to the vagal NC that gives rise to the ENS. These mutant mice are overtly normal but suffer from alteration in patterning the ENS with an overall reduction of enteric neurons (Figure 5.1 (Mundell et al., 2011)). To determine if this reduction of NC derivatives affects beta cell development, beta cell proliferation and maturation can be analyzed in control (*Foxd3*$^{fl/+}$*; Ednrb-iCre*) and mutant (*Foxd3*$^{fl/-}$*; Ednrb-iCre*) embryos.

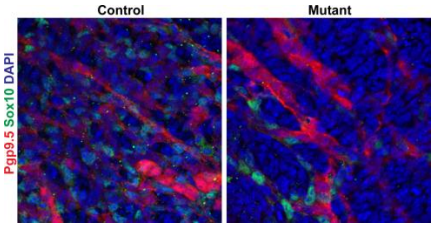

Figure 5.1: Ednrb-iCre induced Foxd3 mutation**.** Mutant (*Foxd3*$^{fl/-}$*; Ednrb-iCre*) embryos have fewer NC derivatives in the ENS than control (*Foxd3*$^{fl/+}$*; Ednrb-iCre*) embryos. Distal colons from mutant embryos at 15.5 dpc (right) have fewer neurons (Pgp9.5, red) and glia (Sox10, green) than control litter mates (left). Nuclei are highlighted with DAPI (blue).

If a critical mass of NC derivatives is required to restrain beta cell proliferation and promote beta cell maturation and this mass is not met in *Ednrb-iCre* induced mutants, these mice would likely have increased insulin-positive area and decreased beta cell maturation. If the results from mutant embryos are indistinguishable from controls, the amount of NC derivatives in pancreata from mutant embryos is sufficient for proper beta cell development. Additionally, these mutant mice are viable; therefore, if beta cell development is impaired, physiological experiments can be conducted on adult animals to determine if reduction in beta cell maturation is detrimental to normal glucose homeostasis.

Identification of pathways regulated by NC derivatives

To determine which beta cell genes are misregulated in the absence of NC derivatives, the mouse *Insulin-1* (*Ins1*) promoter driven GFP allele (*Tg(Ins1-EGFP)Hara1*, called MIP-EGFP (Hara et al., 2003)) can be bred with our mice to generate *Foxd3$^{fl/+}$; Wnt1-Cre, MIP-EGFP* (control) and *Foxd3$^{fl/-}$; Wnt1-Cre, MIP-EGFP* (mutant) embryos. The pancreata will be dissected and the EGFP-expressing beta cells isolated using flow cytometry (Hara et al., 2003). Once the control and mutant beta cells are isolated, RNA will be extracted and gene expression analyzed by high throughput analysis such as RNA Tag Profiling (Illumina). The results can be analyzed using DAVID Bioinformatics Database (david.abcc.ncifcrf.gov) to identify enriched biological themes (Gene Ontology terms) and pathways that are misregulated in the absence of NC derivatives (Huang da et al., 2009). Once misregulated pathways are identified, they can

be manipulated using pharmacological inhibitors to analyze functions of specific pathways in regulating beta cell proliferation and maturation during embryogenesis. These data could then be applied to improve cell culture paradigms for generating glucose responsive beta cells *in vitro*.

Pathways could also be queried using a candidate approach. One pathway of particular interest is extracellular regulated kinase (ERK) signaling. In beta cells, the ERK pathway is required for proliferation (Gupta et al., 2007). Additionally, hepatic activation of the ERK pathway results in increased beta cell proliferation through a neuronal relay suggesting a non-cell autonomous requirement for ERK in cells innervating the pancreas (Imai et al., 2008; Imai et al., 2009). To determine if ERK signaling is misregulated in the absence of NC derivatives, pancreata from various stages of development will be dissected and the beta cells isolated using flow cytometry (see above). Western blots can be used to assay the presence and relative concentration of phosphorylated ERK which is indicative of active ERK signaling. In the absence of NC and increased beta cell proliferation, ERK signaling should also be increased.

Our work has identified a novel role for NC in regulating beta cell mass expansion and maturation. The future directions proposed here will provide more detailed information about the requirement for NC derivatives on beta cell mass and function. Additionally, the proposed experiments provide an ideal system to identify novel factors controlling beta cell proliferation and/or beta cell maturation.

PDGF signaling

PDGF signaling is a critical regulator of beta cell proliferation in both humans and rodents (Chen et al., 2011). It is tempting to speculate that Foxd3 may also be altered in response to PDGF signaling. To test this hypothesis, the expression of Foxd3 can be analyzed in islets cultured with PDGF-AA ligand and in islets isolated from PDGFRalpha knockout mice. If PDGF signaling regulates Foxd3 expression, *Foxd3* mRNA levels should be altered when PDGF signaling is ablated (PDGFRalpha knockout mice compared to controls) or when PDGR signaling is activated (islets culture with or without PDGF-AA ligand). The results of these experiments may identify the PDGF pathway as a novel regulator of Foxd3 expression. Additionally, both PDGF signaling and Foxd3 are critical for maintenance of the NC lineage (Mundell and Labosky, 2011; Smith and Tallquist, 2010; Teng et al., 2008). These experiments may elucidate a genetic interaction between PDGF signaling and Foxd3 that is conserved in multiple cell lineages.

In both humans and rodents, PDGF is upstream of *Ezh2* transcription and *Ezh2* is misregulated in the absence of Foxd3 in the beta cell. Therefore, Foxd3 may also function to regulate transcriptional targets of PDGF signaling. It is important to note that PDGF signaling is not the sole regulator of Ezh2 expression within the beta cell and Foxd3 may be acting in a pathway independent of PDGF. To determine if Foxd3 is functioning independently of PDGF, islets isolated from pancreas-specific Foxd3 mutant animals and control littermates can be cultured with and without inhibitors of PDGF signaling such as Sunitinib or U0126 (Peppel et al., 2005; Roskoski, 2007). If Foxd3 functions downstream of PDGF signaling, the expression levels of *Ezh2* mRNA should be similar in the following groups: control treated, mutant untreated, and mutant treated. Additionally,

Ezh2 expression should be higher in islets isolated from control animals that were not treated with inhibitors. If Foxd3 functions independently of PDGF signaling, the expression levels of Ezh2 should be lower in islets isolated from Foxd3 mutant animals that were treated with inhibitors than untreated animals (Table 5.1). Together these data would allow us to conclude whether Foxd3 is a mediator of PDGF signaling.

Table 5.1: Predicted expression of Ezh2 in islets from Foxd3 mutant mice cultured with or without PDGF inhibitor. The color intensity indicates predicted *Ezh2* expression with dark blue indicating normal levels and lighter shades predicting lower levels of *Ezh2*.

	Foxd3 functions downstream of PDGF		Foxd3 does not function downstream of PDGF	
	Untreated	Treated	Untreated	Treated
Foxd3$^{fl/+}$ (control)	Normal Ezh2 expression	Decreased Ezh2 expression compared to untreated controls	Normal Ezh2 expression	Decreased Ezh2 expression compared to untreated controls
Foxd3$^{fl/-}$*; Pdx1-Cre* (mutant)	Decreased Ezh2 expression compared to untreated controls	Ezh2 expression that is similar to treated controls and untreated mutants	Decreased Ezh2 expression compared to untreated controls	Ezh2 expression that is less than treated controls and untreated mutants

Requirement for Foxd3 in obese animals

Beta cells in obese animals must expand to combat insulin resistance. Several factors required for beta cell mass expansion during pregnancy are also required for beta cell mass expansion in the obese state including, but not limited to, Foxm1, Skp2 and ERK signaling (Davis et al., 2010; Gupta et al., 2007; Imai et al., 2008; Imai et al., 2009; Zhong et al., 2007). Because Foxm1 and Skp2 function downstream of Foxd3, it is likely that Foxd3 will also play a role in beta cell mass expansion in rodents fed a high fat diet. My preliminary data indicate that Foxd3 is not required for glucose homeostasis in

animals fed a high fat diet for 8 weeks (Typical American Diet, TestDiet 5TLN). However, it must be noted that during 8 weeks of high fat diet feeding, there was only a modest increase in body mass compared to animals fed a normal chow (5.4 grams in females and 7.5 grams in males). Therefore, to fully understand the requirement for Foxd3 in regulating beta cell mass expansion and glucose homeostasis, physiological assays should be conducted when the animals are significantly obese. Additionally, using a pure genetic background may decrease variability in the amount of weight gain; the animals assayed were on a mixed genetic background consisting of C57BL/6, 129Sv6, and CD-1. If Foxd3 is required to maintain glucose homeostasis in obese animals, beta cell mass, size, proliferation, and function should be analyzed to determine the underlying cause for glucose intolerance. No defects in glucose homeostasis in obese Foxd3 mutant mice would suggest that Foxd3 is not required for beta cell mass expansion in this model.

Subcellular localization of Foxd3

In adult mice fed a normal chow (Laboratory Autoclavable Rodent Diet 5010, 5.1 percent fat), Foxd3 was detected in the nuclei of beta cells and a subset of PP cells (Figure 5.2A-C). Alternatively, in adult mice fed a higher fat, breeders chow (PicoLab Mouse Diet 20, 9.0 percent fat), Foxd3 was detected in the cytoplasm suggesting a change in subcellular localization of Foxd3 stimulated by obesity (Figure 5.2 D-F). Additionally, Foxd3 was detected in the cytoplasm of non-diabetic, obese Zucker fatty

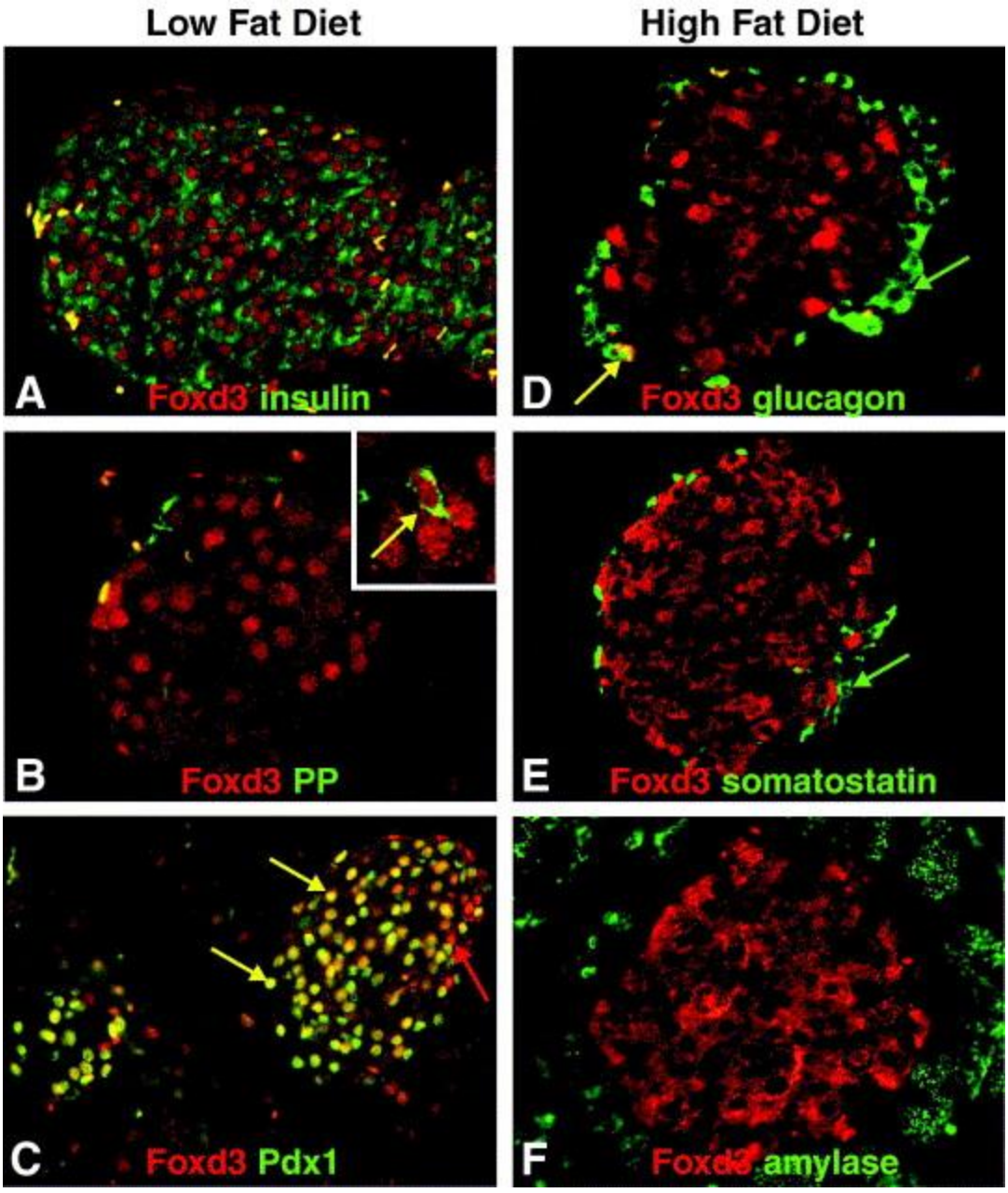

Figure 5.2: Subcellular localization of Foxd3 in mice fed a normal or higher fat chow. A-C. Foxd3 was detected in the nuclei of beta cells (A) and a subset of PP cells (B) and colocalized with Pdx1 (C) from mice fed a chow consisting of 5.1 percent fat. D-F. Alternatively, when animals were fed a diet consisting of 9.0 percent fat, Foxd3 was detected in the cytoplasm. Foxd3 was not detected in alpha (D), delta (E), or acinar cells (F). Yellow arrows, cells co-expressing Foxd3 and another protein. Red arrows, cells expressing Foxd3 only. Green arrows, cells not expressing Foxd3. Image taken from (Perera et al., 2006).

rats (ZF) while Foxd3 was detected in the nuclei of obese, diabetic rats (Zucker diabetic fatty rats, ZDF) suggesting that subcellular localization of Foxd3 may be required to prevent the onset of type 2 diabetes (Jetton et al., 2005; Perera et al., 2006; Tokuyama et al., 1995).

While Forkhead proteins are transcription factors and are predominantly localized to the nucleus, several Forkhead factors including Foxo4, Foxo6, and Foxm1 can be detected in the cytoplasm. Both Foxo4 and Foxo6 contain an atypical nuclear localization signal (NLS) required for nuclear import. In some instances, this NLS signal is phosphorylated by Akt, resulting in cytoplasmic localization and inhibited transcriptional activity of both proteins (Brownawell et al., 2001; Jacobs et al., 2003). Interestingly, Foxm1 is also subject to differential subcellular localization; during late G1 and S phase of the cell cycle, Foxm1 can be detected in the cytoplasm. However, at the transition from G2 to M phase, Foxm1 is phosphorylated in response to ERK signaling resulting in nuclear localization (Ma et al., 2005). Due to the requirement for Foxm1, ERK signaling, and Foxd3 in regulating beta cell proliferation (Ackermann-Misfeldt et al., 2008; Chen et al., 2011; Davis et al., 2010; Plank et al., 2011a; Zhang et al., 2006; Zhang et al., 2010), these data pose an interesting model in which subcellular localization of Foxm1 and Foxd3 may be regulated by ERK signaling and is critical for beta cell proliferation.

To determine how subcellular localization of Foxd3 is regulated, putative phosphorylation sites can be identified using KinasePhos (Huang et al., 2005). Once putative phosphorylation sites are identified, they can be mutated, constructs transiently transfected into beta cell lines, and subcellular localization characterized using immunocytochemistry to determine which phosphorylation sites are required for nuclear

and/or cytoplasmic localization of Foxd3 *in vitro*. Additionally, once potential phosphorylation sites and pathways are identified, cultured islets can be treated with pharmacological inhibitors of the appropriate pathway to determine if these pathways regulate Foxd3 subcellular localization *ex vivo*. Mouse models can be developed with point mutations of Foxd3 to determine the significance of phosphorylation sites *in vivo*. Data from these experiments will provide mechanistic details concerning Foxd3 function and localization in beta cells.

Mechanism of Foxd3 function in beta cells

Interestingly, mice with a *Pdx1-Cre* driven deletion of *Foxd3* exhibit glucose intolerance during pregnancy (Figure 3.5) although *Foxd3* expression normally decreases during pregnancy (Figure 3.1) suggesting that Foxd3 is required prior to pregnancy to establish a ground state in which beta cells will be capable of increased proliferation during pregnancy. A relay-model posed by a collaborating group suggests that Foxd3 binds to an intergenic enhancer at the *lambda5-VpreB* locus in ES cells. Upon differentiation to the B cell lineage, Foxd3 is replaced by Foxp1 and transcription of target genes ensues (Liber et al., 2010). Additionally, a complementary model suggests that Foxd3 functions as a "pioneer factor" and occupies the *Albumin1* locus in ES cells thereby maintaining the unmethylated state of a single CpG residue. Upon differentiation, Foxd3 is replaced by a Foxa family member resulting in activation of *Albumin1* expression (Xu et al., 2007). Both models suggest that Foxd3 is required prior to activation of target genes to maintain a binding site for other Forkhead proteins.

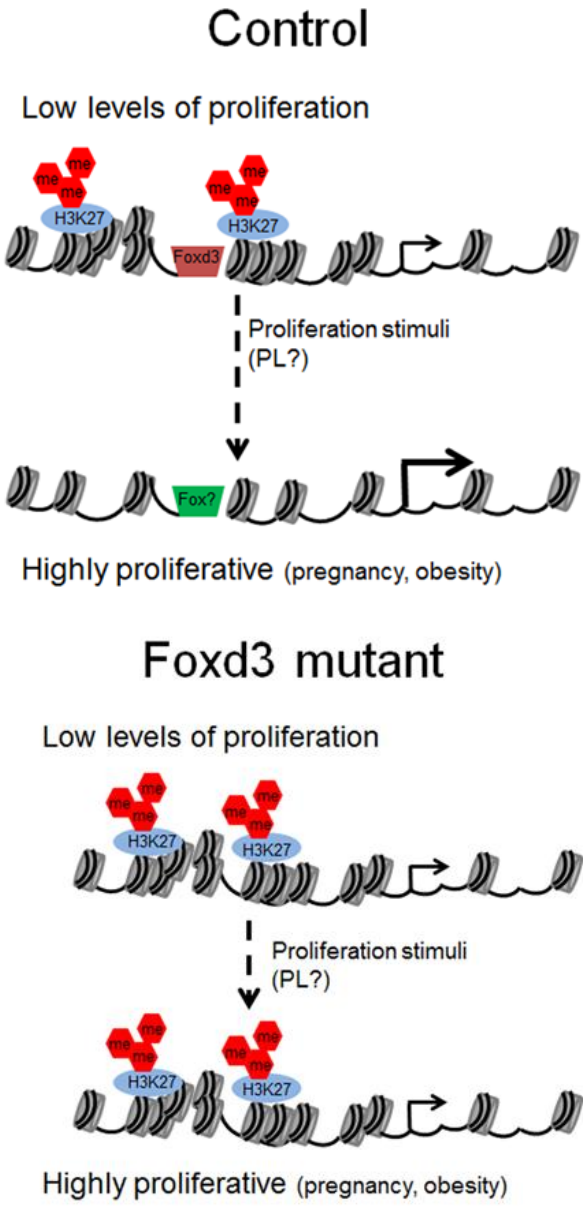

Figure 5.3: Model of Foxd3 mechanism in beta cells. Foxd3 is the initial factor in this a "relay model" required to increase the transcription of loci required for proliferation. Under basal physiological conditions when beta cell proliferation is rare, Foxd3 occupies its target loci and chromatin remains in a relatively "closed" conformation. Upon stimulation to proliferate, such as PL, Foxd3 is replaced by another Fox protein that promotes transcription. In the absence of Foxd3, no Fox proteins occupy target loci permitting only low levels of proliferation. Upon proliferation stimuli, other Forkhead factors are unable to bind the target loci resulting in low levels of proliferation.

Therefore, I propose the following model (Figure 5.3). In beta cells, Foxd3 occupies upstream regulatory elements of genes required for transcription. In the absence of a proliferation stimulus, Foxd3 continues to occupy these binding sites and allows low levels of proliferation. Upon a proliferation stimulus (such as PL), Foxd3 is displaced from the binding site and another Forkhead protein (potentially Foxa1, Foxa2, Foxm1, or Foxo1) occupies the site promoting an open chromatin confirmation, increased gene expression, and increased proliferation. In beta cells lacking Foxd3, key binding sites are not accessible for other Forkhead proteins resulting in low levels of transcription and basal levels of proliferation.

To test this model, it is crucial to identify the targets of Foxd3. Our lab has generated ES cells with one Flag-tagged allele of Foxd3. These targeted ES cells will be used to generate chimeric mice by blastocyst injection. Islets from these mice will be isolated and high throughput ChIP-Seq will be performed by Dr. Klaus Kaestner at the University of Pennsylvania to determine Foxd3 occupancy sites in the beta cell. Once the binding sites are identified, ChIP with antibodies against specific histones and histone modifications can be used to determine if there are changes in chromatin occupancy and therefore structure in the presence and absence of Foxd3 and during pregnancy. Additionally, bisulfite sequencing at Foxd3 occupancy sites will be used to determine if there are changes in DNA methylation status in the presence and absence of Foxd3. The impact of the forthcoming data from these experiments would be two-fold: 1) the ChIP-Seq experiments will identify downstream targets of Foxd3 and potentially identify novel regulators of beta cell proliferation and 2) the results from the epigenetic experiments

will provide information to support or contradict the existing models that Foxd3 functions as a “pioneer factor” to poise loci for transcription.

Conclusions

Our work identified a novel role for the transcription factor Foxd3 in regulating beta cell mass expansion during pregnancy. The future directions proposed here will determine if Foxd3 functions downstream of PDGF signaling to regulate expression of the polycomb protein Ezh2. Additionally, these experiments will determine if Foxd3 is required to regulate beta cell mass expansion in the obese state. Finally, the proposed genomic experiments will uncover mechanistic data regarding the subcellular localization and identification of Foxd3 target genes in the beta cell.

APPENDIX A

ECTOPIC EXPRESSION OF CRE RECOMBINASE IN THE CNS FROM PDX1-CRE MICE

The ability to conditionally ablate expression of specific genes in a temporal or spatial manner using Cre recombinase is critical for elucidating the tissue-specific function of genes of interest. However, this technology is limited by the expression pattern of Cre recombinase. Several Cre transgenic mouse lines have been generated to conditionally delete a particular gene of interest from the developing or adult pancreas. In the majority of these mouse lines, Cre-recombinase is expressed under control of the well characterized *Pdx1* or *Ins2* promoters. Here, we characterized Cre expression in the transgenic mouse line, *Tg(Ipf1-Cre)Tuv*, which was previously demonstrated to induce recombination throughout the entire Pdx1-expression domain (Hingorani et al., 2003). However, in addition to inducing expression in the endogenous Pdx1-expression domain, this mouse line also induced recombination in the hypothalamus and brain stem. We used the *Tg(Ipf1-Cre)Tuv* transgenic mouse line to delete Foxd3 in beta cells; therefore, we needed to rigorously validate Cre expression in this transgenic mouse. Therefore, genes that are expressed within the pancreas and hypothalamus are deleted from both regions using *Pdx1-Cre* or *Ins2-Cre* making physiological data analysis more difficult because the deletions are, therefore, not beta cell-specific. For example, using *Tg(Ins2-Cre)25Mgn*, also called *Rip-Cre*, to delete *Stat3* in beta cells also resulted in deletion of

Stat3 in the hypothalamus. These mutant mice were glucose intolerant, overweight, had increased fat mass, and increased Leptin levels. When wild type islets were transplanted into these animals the defects were not rescued, consistent with the hypothesis that reduced expression of *Stat3* in the hypothalamus rather than beta cells is responsible for the observed defects (Cui et al., 2004). Therefore, when using these transgenic mouse lines to delete a gene of interest, it is critical to know whether the gene is expressed in the hypothalamus.

To determine if recombination occurs in the central nervous system (CNS) of *Tg(Ipf1-Cre)Tuv* mice, we dissected brains from *Tg(Ipf1-Cre)Tuv; R26R*$^{LacZ/+}$ mice at postnatal day 14. The brains were sliced using a disposable razor blade and a mouse brain slicer (ASI Instruments, RBM-2000C) as illustrated in Figure A.1 and X-gal stained to detect beta-galactosidase activity. We found that *Tg(Ipf1-Cre)Tuv* mediates recombination in the hypothalamus (Figure A.1).

To determine if this recombination was specific to postnatal animals or if it occurs during embryogenesis, we analyzed Cre recombination in the CNS at 15.5 dpc. Beta galactosidase activity was detected in the CNS at 15.5 dpc suggesting that Cre recombinase is expressed in the hypothalamus and brain stem prior to 15.5 dpc (Figure A.2 A-D). Additionally, using the *R26R*^{YFP} reporter (Srinivas et al., 2001), we detected YFP expression in the CNS and pancreas at 15.5 dpc indicative of Cre recombination (Figure A.2 E-H). Together these data indicate that Cre-mediated recombination occurred prior to 15.5 dpc.

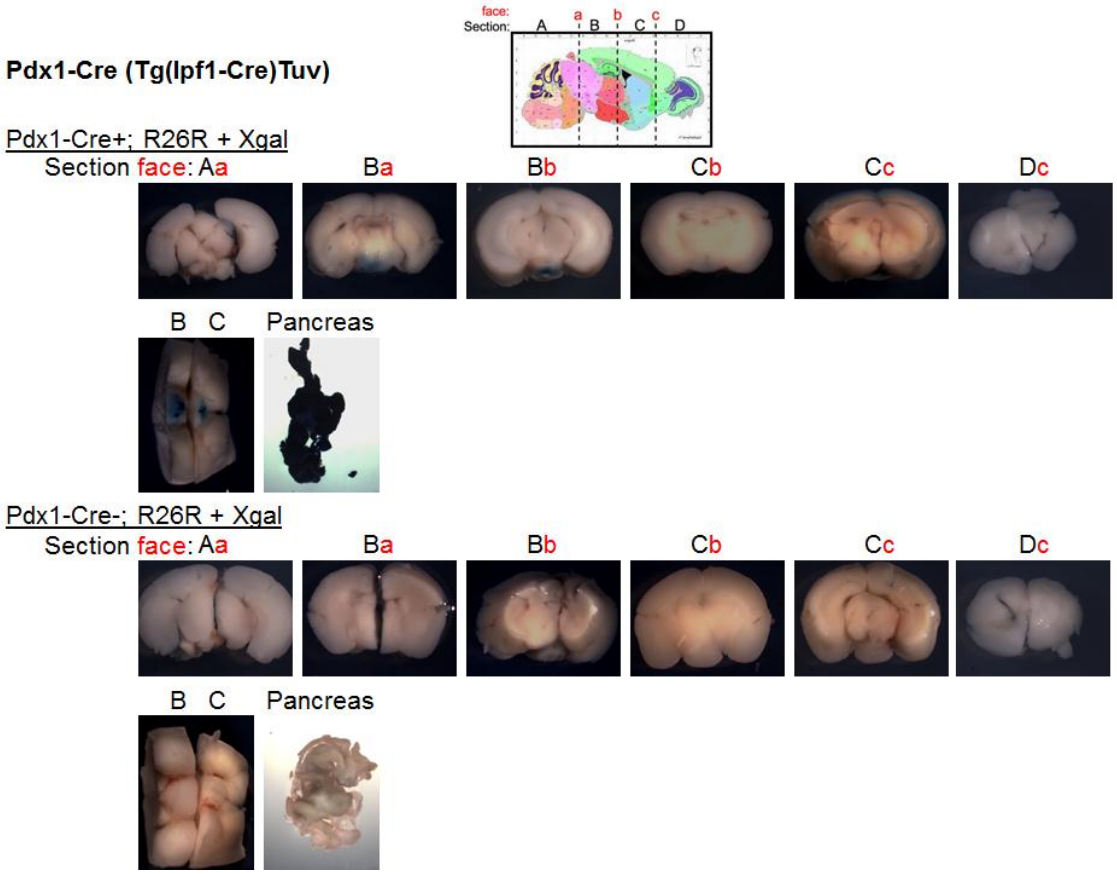

Figure A.1: The *Tg(Ipf1-Cre)Tuv* transgenic line showed localized Cre-mediated recombination within specific regions of the brain including the hypothalamus (region B). Postnatal day 14 brains were sliced, labeled, and imaged. Top panel: Schematic of brain sections used for analysis (http://www.brain-map.org). Middle panel: X-gal staining in *Tg(Ipf1-Cre)Tuv;R26R*$^{LacZ/+}$ brain (n = 4) was localized to the hypothalamus. Additionally, pancreata from these mice were X-gal positive. Bottom panel: X-gal positive cells were not detected in the hypothalamus or pancreas from *Tg(Ipf1-Cre)Tuv;R26R*$^{+/+}$ mice (n=4).

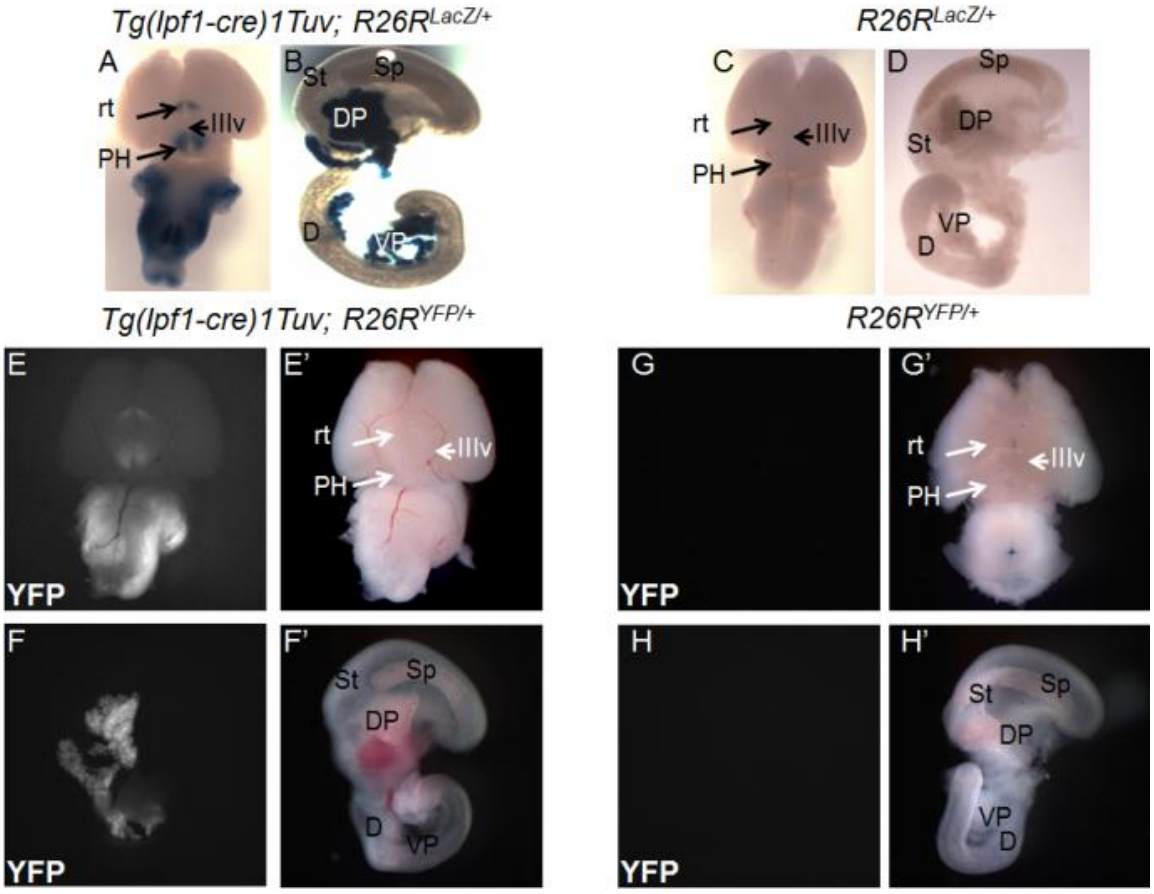

Figure A.2: A-D. The *Tg(Ipf1-Cre)Tuv* transgenic line showed localized Cre-mediated recombination within specific regions of the brain including the hypothalamus and brain stem at 15.5 dpc (A). The pancreas served as a control for Cre activity (B,D). Beta galactosidase activity was not detected in the brain or the pancreas in embryos lacking Cre-recombinase (C-D). E-H. Cre-mediated recombination was detected in the brain stem, hypothalamus, and pancreas in *Tg(Ipf1-Cre)Tuv* using the R26R^{YFP} reporter (E-F). YFP was not detected in the CNS of pancreas from embryos lacking the *Tg(Ipf1-Cre)Tuv* transgene (G-H). Rt, reticular thalamic nucleus; PH, posterior hypothalamus; IIIv, third ventricle; St, stomach; Sp, spleen; DP, dorsal pancreas; D, duodenum; VP, ventral pancreas.

To determine if *Cre* mRNA expression can be detected in the hypothalamus, this region of the CNS was dissected from adult *Tg(Pdx1-Cre)89.1Dam* mice. RNA was isolated and relative *Cre* expression was determined using qRT-PCR. Islets isolated from the same mice served as a positive control. While the level of *Cre* recombinase expression was higher in the pancreatic islets, *Cre* expression was detected in the hypothalamus (Figure A.3). To serve as a negative control, RNA was extracted from wild type hypothalamus and islets and *Cre* recombinase was not amplified using 40 qRT-PCR cycles suggesting that *Cre* recombinase was not expressed in these samples. The expression levels of Cre recombinase within the hypothalamus were indistinguishable between *Tg(Pdx1-Cre)89.1Dam* and *Tg(Ipf1-Cre)Tuv* transgenic mice.

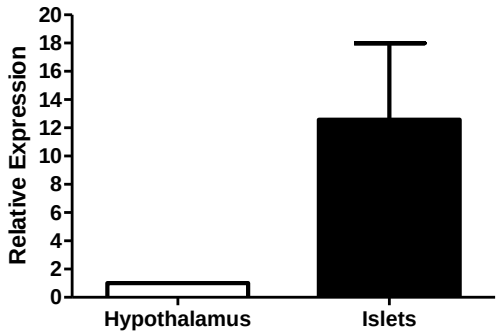

Figure A.3: Relative *Cre* mRNA expression in *Tg(Pdx1-Cre)89.1Dam* hypothalamus and islets (n=3). *Cre* mRNA was undetectable in hypothalamus and islets of wild type controls (not shown, n=2). Error bars indicate SEM.

Together, our data, along with the data of our collaborators (Wicksteed et al., 2010), indicated that both *Pdx1-Cre* and *Ins2-Cre* transgenic lines induce recombination within the CNS. Therefore, it is important for investigators using these transgenic lines to

ensure that their gene of interest is not expressed within the CNS resulting in non-specific effects of the mutation.

APPENDIX B

MATERIALS AND METHODS

Mouse lines and husbandry

The following mouse lines were maintained and interbred to generate mice and embryos of the appropriate genotype: *Foxd3*$^{tm3.Lby}$ (*Foxd3*^{flox}), *Foxd3*$^{tm1.Lby}$ (*Foxd3*$^{IRES\text{-}GFP}$), *Foxd3*$^{tm2.Lby}$ (*Foxd3*^{GFP}), *Tg(Ipf1-Cre)Tuv*, *Tg (Wnt1-Cre)11Rth*, *Gt(ROSA)26Sor*^{tm1Sor} (*R26R*^{LacZ}), *Gt(ROSA)26Sor*$^{tm1(EYFP)Cos}$ (*R26R*^{YFP}), and *Tg(Cag-cre/Esr1*)5Amc*. The mouse lines and genotyping were previously described (Danielian et al., 1998; Hanna et al., 2002; Hingorani et al., 2003; Soriano, 1999; Srinivas et al., 2001; Teng et al., 2008). The primer sequences used for genotyping are listed in Table B.1. For timed matings, females were checked daily for presence of a vaginal plug; noon on the day of an observed plug was considered 0.5 days post coitum (dpc). All mouse lines were maintained on a mixed genetic background consisting primarily of CD-1 and C57BL/6NHsd/129S6. Mice were housed on Bed ‘o Cobs corn cob bedding (The Andersons) unless they were being fasted; fasted mice were housed on Alpha-Dri bedding (Shepherd Specialty Papers) because mice would eat the corn cob bedding, therefore interfering with their fast. The mice on a normal chow were fed Laboratory Rodent Diet 5001 (Labdiets). All mice were handled in accordance with AAALAC standards and protocols with approval from the Vanderbilt University Institutional Animal Care and Use Committee (IACUC).

Table B.1: PCR Primer Sequences

Gene	Forward Primer Sequence (5'→3')	Reverse Primer Sequence (5'→3')	Application
Cre	ACCTGAAGATGTTCGCGATTATCT	ACCGTCAGTACGTGAGATATCTT	Genotyping
Foxd3^{fl}	CGGCTTTCTTTCGGGGGAC	ACATATCGCTGGCGCTGCCG	Genotyping
GFP	AAGGGCGAGGAGCTGTTCAC	TGCTGCTTCATGGGGTCGG	Genotyping
Wnt1-Cre	CTTCTATCGAACAAGCATGCG	GCCAATCTATCTGTGACGGC	Genotyping
PGK-neo	CTCCGGGCCTTTCGACCTG	CTGCGTGCAATCCATCTTGTTC	Genotyping
Clip2	GGAGCAGGGGTTGGTTGGTTGA	GCCAACTTGGTCCACAAAATGGCT	qPCR following ChIP
FosB	CCACCTCCCTCTGTTATGCCAGG	GACTCCTTCAGGCTGTGTTTGCAC	qPCR following ChIP
FosB	GCCTCGGGTTCTGCCTTCCA	ACACCCCTCTGTTCCTGTCCCA	qPCR following ChIP
hCLIP2	TTGAGGGAGTGGAGGTGTC	CAGAACCATGCCCTAGGAGT	qPCR following ChIP
hFOSB	GGGTTACTCTGCTTCCCTGA	GTGTGACTGGGTGGCTGA	qPCR following ChIP
hFOSB	TGGCCTCTCTCTCTCTCCTC	GAAGTTGGCGTCCTAGGCT	qPCR following ChIP
hNGFR	CAGGATTCAAACCCAAGACC	GGCCTTACTCCAGGTCCTTA	qPCR following ChIP
hPMAIP1	AACAAACACAATCGATCTACAGC	TGACAGTTAAACAAGAGGACATGA	qPCR following ChIP
hPMAIP1	TCCTACTGATTGCTCTCCCA	TAACCCAGCAGGTGCAATAA	qPCR following ChIP
hSAFB	GAGGCAAGTAAAGGTTAGCCA	GAGAGGTCCCAGAGTAGCCA	qPCR following ChIP
hSMARCD3	ACGAAGATTCCTGAGAGGGA	ACTGTTGTTTCAGGGAGCCT	qPCR following ChIP
hSMARCD3	TCATGCTGGACTACCAGGTC	CTCAAGATGCACCACTTTGG	qPCR following ChIP
hSOX15	AAAGGTGGAGCTGAGCTGTAG	AAGCAGCTGGTTTCCCTAAA	qPCR following ChIP
hSOX4	AAACGCTGGAAGCTGCTC	TCAGCCATGTGCTTGAGG	qPCR following ChIP
hSOX4	TTTGAATCGTGATAGCCAGATAA	TCCTGAAGCATGAAACTCCA	qPCR following ChIP
Ngfr	AAGGCCGGGGAGAGTCACCA	GCCTCCCAACTGCCCTGTGT	qPCR following ChIP
Pmaip1	CAGGGCCTGAGGTTTAAACTTTGGTT	CCTCAAAACCCTCCGGAAGCTCA	qPCR following ChIP
Pmaip1	TGGGCATAGGGTGTCAAGGATCG	ACGTTGTCAGCAGGGGCCAT	qPCR following ChIP
Safb	TGCAACACAGAAAAGCTAAAGTGAGCG	TGTGAGCCTAGTTCCCTGGTAGGT	qPCR following ChIP

Table B.1 Continued: PCR Primer Sequences

Gene	Forward Primer Sequence (5'→3')	Reverse Primer Sequence (5'→3')	Application
Smarcd3	GGAGGGATGGGATAGCACTCAGACA	GGCATGGTGATGAGCCACAGG	qPCR following ChIP
Smarcd3	CCCCAGCCCCTCCAGATTGC	GAGCCAGGGCTGGTGCAGAA	qPCR following ChIP
Sox15	AAGTGTGTGCAGCGGTGCCT	TCAGCAAAGCGCTAGCATGACCT	qPCR following ChIP
Sox4	CGACCCCAGCTGGTGCAAGA	CATGTCGGGCGACTGCTCCA	qPCR following ChIP
Sox4	TCCTGGGAAGTTGTGGGGCTG	TCACTGAGGAGGGGCTAGGTCA	qPCR following ChIP
λpreB	TCCCCATTGCCAGATAGAGACACA	TGGGCCCAACAGATTAACACAGAG	qPCR following ChIP
λpreB	TGACTTGCTTGTGCTTGCCTGGAC	ATAATAACAAAGTACTGAGAAAAC	qPCR following ChIP
2410076i21Rik	GGGAGTCTTGTCCTCACGAT	GTTCTTGCTGCCAATGAGTG	qRT-PCR
4930463M05Rik	TTTGACCCTTCCACTGAACA	GAACAGTGGCATTGTAACCG	qRT-PCR
5430411c19Rik	CACCAAATTTGTTCCTGTGG	GCAGGCTAACCGCTGTAGAT	qRT-PCR
Bnc1	GTCAGTGAAGACGAGCCAGA	TTCTCCTTGTGGAAGAGGCT	qRT-PCR
CDC2L1	CTCTGAGGAGGCCTCTGAAC	CTGGAACAACCAAGATGTGG	qRT-PCR
Clec2d	TAACAACACGATTCCCATCC	GCTACAGATCCACATCCGAA	qRT-PCR
CLIP2	AGGACCGACCCTACTCACAC	CACAGTCACATCTCCAAGGG	qRT-PCR
Cr	AAATGCTTCTGTCCGTTTGC	AATCGCGAACATCTTCAGGT	qRT-PCR
Cre	TGCAACGAGTGATGAGGTTC	GCAAACGGACAGAAGCATTT	qRT-PCR
Dub2a	ATGTGCAGCAGACTGACCTC	TTTCTCCGGGATTTCTTCAG	qRT-PCR
E130309F12Rik	CTCAACCGCGTCTCAGAGTA	GAACCACACACATTCCCAAA	qRT-PCR
EG432649	GCTCACCTCTCCTGATTCGT	TGATGTCTGGGATCCTTTGA	qRT-PCR
Eras	TACCCGAGTACAAGGCAGTG	CATGGTCTTTCACGAAGCAT	qRT-PCR
Evc2	CATCCTGAGAACAAGCTGGA	CTCAGAAGTCAGGATGGCAA	qRT-PCR
Fibin	ACAGAGGGAGAAGGTGCTGT	CAGGCTAGATCCCACTACCC	qRT-PCR
Fosb	GGCCTCTCCCTTTATCCTTT	CAGACCGGAGATCAGAGTCA	qRT-PCR
Foxd3	GTCCGCTGGGAATAACTTTCCGTA	ATGTACAAAGAATGTCCCTCCCACCC	qRT-PCR

Table B.1 Continued: PCR Primer Sequences

Gene	Forward Primer Sequence (5'→3')	Reverse Primer Sequence (5'→3')	Application
Gap43	CCGTGGACACATAACAAGGA	TTCTTCTCCACACCATCAGC	qRT-PCR
Glucagon	AGGAATTCATTGCGTGGCTG	CAATGGCGACTTCTTCTGGG	qRT-PCR
Grhl3	CGGTTCTGACGTTCACTGTT	CTCACAAAGGCATCTGCTGT	qRT-PCR
Hirip3	CAGGAAGCAGGTTAGGGAAG	CTCTCCTCCTGGCAGTTAGC	qRT-PCR
Hist1h2bb	ATGGGCATCATGAACTCGT	GTCGAGCGCTTGTTGTAATG	qRT-PCR
HPRT	TACGAGGAGTCCTGTTGAATGTTGC	GGGACGCAGCAACTGACATTTCTA	qRT-PCR
Insulin1	CAGCAAGCAGGTCATTGTTT	GGGACCACAAAGATGCTGTT	qRT-PCR
LOC668686	CCTGTGTGGGCAGTGTGTAT	TCAGGCTTCTCACCATCATC	qRT-PCR
LOC674405	AACTCACATGAGGCTGGCTT	CCAAGTGAACCTCTCCTCGT	qRT-PCR
Mafa	TCGACCTGATGAAGTTCGAG	CAGAAGCTGGGCGAAGAG	qRT-PCR
Mafb	CCCACACATTGGCAACTAAC	AACGGAAGGGACTTGAACAC	qRT-PCR
Myf5	ATGTAACAGCCCTGTCTGG	CAGCACATGCATTTGATACA	qRT-PCR
Myf6	GTAAGGGAGTGCAGATTGTG	TGCGTTCCTCTGAAGAAATA	qRT-PCR
MyoD1	CTGATGGCATGATGGATTAC	CTCACTGTAGTAGGCGGTGT	qRT-PCR
Myogenin	CAACCCAGGAGATCATTTG	GTAAGGGAGTGCAGATTGTG	qRT-PCR
Neurogenin3	ATCCATCACTTTTTCCAGGGTG	TCATCTATGGGCCAAGAGCTG	qRT-PCR
Ngfr	CTGCCTTCCTCTGTCTGTCA	CACTGTTGGCTTCAGGCTTA	qRT-PCR
Nkx2.2	GCAGCGACAACCCCTACA	ATTTGGAGCTCGAGTCTTGG	qRT-PCR
Nrg3	TTATCGGATCCAACAGACCA	CCACGATGACAATTCCAAAG	qRT-PCR
Otx1	TGTTCGCAAAGACTCGCTAC	ACCAAACCTGGACTCTGGAC	qRT-PCR
Pdx1	CTGAGGGACAAAGATGCAGA	TTCTAATTCAGGGCGTTGTG	qRT-PCR
Pi15	CTGCAGTCAGCCTTGTGATT	TATTGGCTGGCAGAGATGAG	qRT-PCR
Pmaip1	GAGTGCACCGGACATAACTG	CTCGTCCTTCAAGTCTGCTG	qRT-PCR
Safb	AAGGCCATTGAAGATGAAGG	CCTCGTCTTCTGGTTTCCTC	qRT-PCR
Skp2	AGCCGAGGTGAATGAGAGTT	AGCATGAATGCTCCACAAAG	qRT-PCR

Table B.1 Continued: PCR Primer Sequences

Gene	Forward Primer Sequence (5'→3')	Reverse Primer Sequence (5'→3')	Application
Smarcd3	AGATGTGGAGGTGGAGGAAC	TCCAGAGCACTGATCTCCTG	qRT-PCR
Socs2	CCGAATGCAGCTATGTGAAA	AGACTGAGCCCAACTGTCCT	qRT-PCR
Sox15	AACTACCCAAGGGAGCAGAG	CTGCAGTGGGAAGAGGTGTA	qRT-PCR
Sox4	ACTGCAATCGACTGCTTCAG	ACGTTGGTAGCCGGAGTATC	qRT-PCR
Tac1	TGATGAAGGAGCTGTCCAAG	CACAGGAGTCTCTGCTTCCA	qRT-PCR
Tub	CTAGATGATGAGGGCAGCAA	CATTGGCCTGTACCATCAAG	qRT-PCR
Ube1y1	GAGGATGCTGAGGAATTGGT	ACTTCCGGATAAGGTCGATG	qRT-PCR
Sox15 Insertion	ATAGTCGACGCCAACCAGCTCCTCAC	ATAGAATTCAAGGGGTTACTGGCATG	Subcloning & Sequencing
Myc	AATTCTATCCTTAGAGGACCTTAGGC	GGCCGCCTAAGGTGTCATAAGGATAG	Subcloning
HA	AATTCATATCCGAACCTGACCTAGGC	GGCCGCCTAGGTCCTCCTCGGATAGG	Subcloning
Sox15 Seq	GACAGCCTACCTGCCTGGC		Sequencing

To assay BrdU incorporation, 5-bromo-2-deoxyuridine (BrdU, Sigma B5002) was dissolved in sterile PBS and postnatal pups or pregnant dams were intraperitoneally injected with 50 mg BrdU per kg body weight 24 and/or 48 hours prior to sacrifice. In contrast, to assess BrdU incorporation in adult mice for 1 week continuously, BrdU was placed in the drinking water (0.8 mg/mL) and treated water replaced after 4 days to ensure BrdU activity. To induce Cre-mediated recombination and acutely delete the *Foxd3* coding sequence in *Tg(Cag-cre/Esr1)5Amc; Foxd3*$^{flox/flox}$ mice, 20 mg Tamoxifen (Sigma T5648) was dissolved in 100 μL of 100 % ethanol. The Tamoxifen/ethanol solution was then diluted in 900 μL of corn oil (Sigma C8267) and vortexed for 5 to 10 minutes. Adult mice were intraperitoneally injected with 100 μL (2 mg) of the corn oil and Tamoxifen solution one week prior to mating or sacrifice.

Histology and immunohistochemistry

Beta galactosidase staining: Tissues and embryos were dissected in cold PBS and then fixed overnight at 4°C in 1 percent formaldehyde (Sigma F1635), 0.2% glutaraldehyde (Sigma G6257), 2 mM magnesium chloride, 5 mM EGTA, and 0.02% Nonidet P40 (NP40, Roche 11 332 473 001). The following day, the samples were washed 3 times for 30 minutes each in PBS at room temperature. Tissues were permeabilized with 2 mM magnesium chloride, 0.01% sodium deoxycholate, and 0.02% NP40 in PBS 3 times for 2 hours each at room temperature. A 20 mg/mL stock solution of 5-Bromo-4-chloro-indolyl-beta-D-galactosidase (X-gal, RPI B71800) was prepared by adding 1 g of X-gal to 50 mL of N,N-dimethylformamide (DMF, Sigma D4551). This stock solution should

be stored at -20°C long term. Immediately following permeabilization, the samples were stained overnight at room temperature with freshly prepared 5 mM potassium hexacyanoferrate (II) trihydrate (Ferro, Sigma P3289), 5 mM potassium ferricyanide (III, Ferri, Sigma 455946), 2 mM magnesium chloride, 0.02% NP40, and 1 mg/mL X-gal in PBS. Following staining, tissues were washed 3 times for 30 minutes in PBS and were imaged or prepared for immunohistochemistry.

Paraffin embedded sections: Embryos and tissues were dissected in cold PBS and fixed overnight in filter sterilized 4% paraformaldehyde (PFA) in PBS. Following fixation, embryos were washed 3 times for 30 minutes in PBS and dehydrated using a series of ethanol washes. Each ethanol wash was performed at room temperature for 30 minutes and the following concentrations of ethanol were used: 1 wash in 30% ethanol and 2 washes in each of 70, 95, and 100% ethanol. Following the ethanol washes, samples were placed in 2 xylenes washes for 30 minutes each. If samples were previously stained for beta galactosidase activity, Histoclear™ was used instead of xylenes because xylenes will cause the blue signal to fade. Samples were placed in 50% xylenes (or Histoclear™) and 50% paraffin (Paraplast Plus) followed by 2 washes in molten paraffin at 60°C for 30 minutes. Following the paraffin washes, samples were embedded in Histoplex cassettes (Starplex Scientific). Samples were then cut into 7 micron sections using Accu-Edge low profile blades (Sakura) and sections were placed on to positively charged slides under water at 45°C.

Appropriate slides were chosen for staining after screening the slides on a stereoscope, looking for morphological landmarks. Slides were incubated in xylenes twice for 5 minutes to dissolve paraffin surrounding the tissue and then sections were rehydrated in a

series of ethanol washes: 2 washes of 100% and 95% ethanol and 1 wash of 70% followed by a 50% ethanol wash. Slides were then placed in distilled water. If necessary following rehydration, slides were placed in 3% hydrogen peroxide for 10 minutes if biotin-avidin amplification (TSA or DAB) and/or antigen retrieval was performed (see Table B.2). Next, tissue sections were outlined using a Pap pen and blocking solution (5% normal donkey serum, 0.1% Triton X-100, and 1% bovine serum albumin in PBS) was pipetted on top of each section and the slides incubated at room temperature for at least one hour. After this blocking step, the blocking solution was removed and primary antibody diluted in blocking solution was added to the sections and the slides were incubated overnight at 4°C. See Table B.2 for appropriate dilutions of primary antibody. The following day, slides were washed 3 times in PBS for 3 minutes. Secondary antibody was diluted in 0.1% Triton X-100 in PBS. All secondary antibodies were used at a 1:500 dilution with the exception of Cy3 conjugates which were used at 1:800. Secondary antibody solution was added to the tissue as above for the primary antibody and incubated for 1 hour at room temperature. When fluorescently conjugated secondary antibodies were used, this incubation was performed in the dark (under aluminum foil). Following the incubation, slides were washed 3 times for 3 minutes in PBS. To detect nuclei, the slides were incubated for 5 minutes in 4’,6-diamidino-2-phenylindole (DAPI) in distilled water (1:2000) and washed again. For colorimetric analyses, either Hematoxylin (Richard Allen Scientific) or Eosin Y (Thermo Scientific) was used as a counterstain. For samples requiring TSA or DAB amplification, protocols from the TSA Kit (#22, Invitrogen) or ABC Kit (Vector Labs), respectively, were followed. Samples that were fluorescently labeled were mounted with Aqua Polymount (Polysciences, Inc)

Table B.2- Antibodies used for immunohistochemistry or immunofluorescent analyses

Antigen	Species	Source	Conc.	Application	Special Directions
β III Tubulin	Mouse	Covance (Tuj1)	1:500	PE	
BrdU	Mouse	Beckton Dickinson	1:100	ICC, PE	Unmask with 0.25% Trypsin at 37 C for 5 minutes
CD31	Mouse	Pharmigen	1:100	PE	Unmask in 0.1 mg/mL proteinase K at 37C and TSA
FABP7	Rabbit	Dr. Thomas Muller	1:1000	PE	
Foxd3	Rabbit	Labosky Lab	1:1000	FS, ICC, PE	Unmask in citrate buffer at 95C for 1 hour
GFP	Chicken	Abcam	1:500	PE, ICC, WM	
Ghrelin	Rabbit	Phoenix Pharmaceuticals	1:100	PE	Add primary antibodies sequentially
Glucagon	Rabbit	Millipore	1:500	FS, PE	
Glut2	Rabbit	Millipore	1:1000	PE	
Insulin	Guinea Pig	Millipore	1:500	FS, PE	
Neurog3	Mouse	DSHB	1:1000	FS, PE	Unmask in citrate buffer at 95C for 1 hour and TSA
p75	Rabbit	Promega	1:200	WM	
Pancreatic Polypeptide	Rabbit	Millipore	1:100	FS, PE	
Pdx1	Guinea Pig	Dr. Christopher Wright	1:2500	PE, WM	Unmask in citrate buffer at 95C for 1 hour
Pdx1	Goat	Dr. Christopher Wright	1:10000	PE	Unmask in citrate buffer at 95C for 1 hour
Pdx1	Rabbit	Dr. Christopher Wright	1:1000	PE	Unmask in citrate buffer at 95C for 1 hour
Pgp9.5	Rabbit	AbD Serotec	1:1000	PE	
Phospho-Histone3	Rabbit	Upstate	1:250	WM	
Somatostatin	Rat	Millipore	1:100	FS, PE	
Sox10	Goat	Santa Cruz	1:15	WM	Use only Cy5 conjugated secondary antibody- No BSA
Sox15	Rabbit	Dr. Ibrahim Adham	1:50	ICC	
Sox9	Rabbit	Millipore	1:1000	FS, PE	Unmask in citrate buffer at 95C for 1 hour

Abbreviations: FS: frozen section, ICC: immunocytochemistry, PE: paraffin embedded, WM: whole mount

while colorimetrically labeled slides were dehydrated in ethanol and xylenes (or Histoclear™) and mounted with Cytoseal 60 (Richard Allen Scientific). TUNEL analysis was completed with the In Situ Cell Death Kit (Roche).

Frozen sections: Embryos and tissues were dissected in cold PBS and fixed overnight in 4% paraformaldehyde (PFA). Following fixation, the embryos were washed 3 times for 30 minutes in PBS and equilibrated in 30% sucrose until the tissue sank. The tissue was then placed in Optimal Cutting Temperature (OCT, Tissue Tek) in cryomolds (Tissue Tek) and then frozen on dry ice. Blocks were stored long term at -80°C. Seven micron sections were cut in a Leica CM3050 S using cryocut low profile blades (Leica) and the sections were placed on positively-charged slides (Mercedes Medical 7255/90°). The slides were stored at -20°C until they were processed for immunohistochemistry.

Slides were washed in PBS for 30 minutes to remove the OCT, permeabilized in 0.2% Triton-X 100 in PBS for 30 minutes, and sections were circled using a Pap pen. Blocking solution (5% normal donkey serum, 0.1% Triton X-100, and 1% bovine serum albumin in PBS) was added to the section and the slides were incubated at room temperature for at least one hour. After the incubation, the blocking solution was removed, primary antibody diluted in blocking solution was added to the sections, and slides were incubated overnight at 4°C. See Table B.2 for appropriate dilutions of primary antibody. The following day, the slides were washed 3 times in PBS for 3 minutes. Secondary antibody was diluted in 0.1% Triton X-100 in PBS. All secondary antibodies were used at 1:500 with the exception of Cy3 conjugates which were used at 1:800. The secondary antibody was added to the tissue and incubated for 1 hour at room

temperature in the dark. Following the incubation, slides were washed 3 times for 3 minutes in PBS. To detect nuclei, slides were incubated for 5 minutes in 4',6-diamidino-2-phenylindole (DAPI) in distilled water (1:2000). Samples were mounted with Aqua Polymount (Polysciences, Inc).

Immunocytochemistry: Cell culture medium was removed and the cells were washed with PBS. Four percent PFA in PBS was added to the cells for 30 minutes at room temperature. The cells were washed 3 times for 3 minutes at room temperature with PBS. Blocking solution (1% normal donkey serum and 0.1% Triton X-100 in PBS) was added to the samples for 30 minutes at room temperature. Following the incubation, the blocking solution was removed and primary antibody (see Table B.2) diluted in blocking solution was added to the samples prior to an overnight incubation at 4°C. The next day, the primary antibody was removed and samples were washed 3 times for 3 minutes in PBS. Secondary antibodies (Cy2 conjugates 1:500, Cy3 conjugates 1:800, and Cy5 conjugates 1:500) were diluted in 0.1% Triton X-100 in PBS and added to the samples for 1 hour at room temperature in the dark. The samples were then washed 3 times for 3 minutes. DAPI, diluted in distilled water (1:2000), was added to the samples for 5 minutes. Samples were then mounted with Aqua Polymount (Polysciences, Inc) or visualized on an inverted microscope.

Whole mount immunofluorescence: Embryos and tissues were dissected in cold PBS and fixed overnight in 4% paraformaldehyde (PFA). Following fixation, samples were washed 3 times for 30 minutes in PBS and then permeabilized for 30 minutes at room temperature in 0.5% Triton X-100 in PBS. Following permeabilization samples were incubated in blocking solution (10% normal donkey serum and 0.1% Triton X-100 in

PBS) overnight at 4°C. The next day, blocking solution was removed, primary antibody (see Table B.2) diluted in blocking solution was added to the samples and the samples were incubated overnight at 4°C. The primary antibody was then removed and samples washed 4 times for 1 hour each in 0.1% Triton X-100 in PBS. Samples were incubated overnight in secondary antibodies (Cy2 conjugates 1:500, Cy3 conjugates 1:800, and Cy5 conjugates 1:500) diluted in 0.1% Triton X-100 in PBS. The samples were washed 4 times for 1 hour in 0.1% Triton X-100 in PBS. Nuclei were detected by incubating the samples in DAPI (1:2000) diluted in distilled water for 15 minutes at room temperature. The samples were mounted on positively charged slides with Aqua Polymount (Polysciences, Inc).

Quantitative analyses and imaging

Paraffin and frozen sections were imaged using a Zeiss AxioSkop2 Plus fluorescent microscope equipped with a Q Imaging Retiga 2000R camera or a Zeiss Axio Observer A1 fluorescent microscope and an AxioCam MRc5 camera. Images from whole mount samples were taken using an Olympus FV1000 scanning laser confocal microscope.

For BrdU incorporation, islets from 5 sections evenly spaced throughout the pancreas ensuring equal representation of the dorsal and ventral pancreas (accounting for approximately 5 to 8% of total pancreatic mass) were imaged using a Zeiss AxioSkop2 Plus equipped with a Q Imaging Retiga 2000R camera. The total number of BrdU-positive beta cells was divided by the total number of insulin-positive beta cells. For beta

cell mass, the pancreas was embedded in a manner to ensure equal representation of the dorsal and ventral pancreas. Five evenly spaced pancreatic sections (accounting for 5 to 8% of the total pancreatic mass) were imaged using an Ariol SL-50 imaging system. Insulin-positive area and total pancreatic area were determined using ImageJ software (National Institutes of Health) and beta cell mass determined by dividing total beta cell-positive area by total pancreatic area multiplied by pancreatic wet weight. To determine individual beta cell size, every islet from 4 evenly spaced sections (accounting for approximately 4 to 6% of total pancreatic mass) was imaged as above. The total insulin-positive area from each section was calculated using Adobe Photoshop. The area was then divided by the total number of beta cells per section. At least 5,000 beta cells per animal were counted.

Physiology assays

Intraperitoneal glucose tolerance tests: Mice were transferred to cages containing Alpha Dri bedding (Shepherd Specialty Papers) and fasted for precisely 16 hours. Twenty milligrams of dextrose was dissolved in 1 mL of water and then filter-sterilized. Following the fast, the tail vein was punctured and a glucose measurement obtained using a glucometer (FreeStyle). The mice were then subjected to an intraperitoneal injection of 2 mg dextrose per gram body weight. Glucose measurements were obtained with blood samples from the tail vein using a glucometer at 15, 30, 60, 90, and 120 minutes post injection. In some instances, when mice were extremely glucose intolerant, glucose measurements were obtained every 30 minutes until the mouse returned to baseline

glucose levels. Following the glucose tolerance test, mice were fed and returned to the mouse facility or sacrificed and the pancreas dissected for future analysis.

Serum insulin levels: Mice were transferred to cages containing Alpha Dri bedding (Shepherd Specialty Papers) and fasted for precisely 16 hours. Twenty milligrams of dextrose was dissolved in 1 mL of water and then filter sterilized. The mice were restrained in a 50 mL conical tube (Falcon) with a large hole at the tip to allow breathing. The fur on the upper outer thigh over the saphenous vein was shaved with a disposable razor and the area sterilized with isopropanol. The saphenous vein was punctured with a 19 gauge needle and at least 25 μL of blood was collected with Microvette CB 300 capillary tube (Fisher Scientific). Light pressure was applied to the wound to stop bleeding. The mice were then intraperitoneally injected with 2 mg dextrose per gram body weight. Blood samples were collected as above at 15 and 30 minutes post glucose injection. The samples were then centrifuged at maximum speed for 10 minutes in an Eppendorf 5417C centrifuge. The serum was collected and stored at -80°C until further analysis. Serum insulin content was measured using Insulin Ultra-Sensitive ELISA (Alpco Diagnostics) as directed. All samples were run in duplicate.

Islet perifusion: Islet perifusions were performed by the Vanderbilt Islet Procurement and Analysis core as described using 16.7 mM glucose and 20 mM KCl in 5.6 mM glucose as stimuli (Brissova et al., 2004). Insulin was extracted from perifusates in acid alcohol for 48 hours and insulin levels measured using radioimmunoassays performed by the Vanderbilt Hormone Assay and Analytical Services Core. The total amount of insulin was normalized to 100 islet equivalents (IEQ) to standardize the data for comparison.

Embryonic stem cell techniques

Generating feeders: All manipulations need to be performed with sterile technique, tools, and supplies. The heads and all internal organs were removed from 13.5 dpc embryos in sterile PBS using sterile dissection tools. The carcasses were transferred to a new dish of clean PBS to minimize contamination probability. Following dissection, carcasses were loaded into a sterile 3 mL syringe with a 21 gauge needle. The carcasses were passed through the needle 5 times resulting in small evenly sized pieces of tissue. The resulting pieces were then plated on a 150 mm tissue culture plate coated with gelatin (0.1%) in 25 mLs mouse embryonic fibroblast (MEF) medium (10% FBS, 1% penicillin/streptomycin, 1% L-glutamine in DMEM 11965). Approximately 3 carcasses equivalents are sufficient for each 150 mm dish.

The cells were grown to confluence and then split 1:3 after approximately 5 days. To split MEFs, the medium was aspirated into a vacuum flask and the cells were washed with 10 mL PBS to remove residual serum. The cells were trypsinized using 5mL 0.25% Trypsin (Gibco) at 37°C for 5 minutes. Following trypsinization, 16 mL of MEF medium was added to each plate to stop the reaction. The whole volume (21 mL) was divided among 3 new gelatinized plates (7mL each) and 13 mL of MEF medium was added to each new dish. The cells were passaged 3 or 4 times to produce a sufficient number of MEFs. Once a sufficient number was obtained, the cells were harvested and irradiated in 50 mL of MEF medium in 50 mL conical tubes (Falcon) by the Vanderbilt Transgenic Mouse/ESC Shared Resource core using a cesium source. It is extremely important to keep the cells on ice during this time as it may take several hours. Only 6.0×10^7 cells should be irradiated in each conical tube. Following irradiation, the cells were centrifuged

for 3 minutes at 1,000 rpm in an IEC Centra CL2 centrifuge. Following centrifugation, the cells are resuspended in MEF freezing medium (20% FBS, 10% DMSO in MEF medium) to give a final concentration of 2.5 x 10^6 cells/mL. Cells were then aliquoted in 1 mL aliquots in Cryogenic vials (Nalgene) and the vials were placed in Cryo 1C freezing containers (Nalgene) filled with 250 mL isopropyl alcohol and then placed at -80°C overnight. The following day, the cells were transferred to a liquid nitrogen tank. Before use, one vial irradiated MEFs should be plated on gelatinized plates and maintained and observed for 5 days to ensure cells are recovered at the appropriate density and there is no proliferation in the cultures.

Isolating Leukemia Inhibitory Factor (LIF): Chinese hamster ovary (CHO) cells carrying the expression plasmid 8/242 720 LIFD (Genetics Institute, Cambridge) were grown to confluence in CHO medium (10% FBS, 1% L-glutamine, 1% penicillin/streptomycin in alpha medium 12561) in a 10 cm tissue culture dish. Once cells reached confluence they were split 1:10 using 0.25% Trypsin. Once 100 plates of CHO cells were obtained (2 passages) the cells were grown to confluence and the medium containing secreted LIF was collected, pipetted into 500 μL aliquots, and stored at -20°C. LIF (1:1000) was tested in ESC culture to ensure there was no differentiation of ES cells. If a 1:1000 dilution of LIF is not sufficient, different dilutions may be tested. These cells were a generous gift from Dr. Klaus Kaestner, University of Pennsylvania.

Culture: Embryonic stem (ES) cells were grown on irradiated MEFs in ES cell medium (15% FBS, 1% L-glutamine, 1% non-essential amino acids, 0.1% gentamicin, 0.1% CHO-LIF, and 3 μL beta mercaptoethanol in DMEM 11965) at 37°C with 5% carbon dioxide. Once ES cells were approximately 80% confluent, they were passaged at 1:3.

The medium was aspirated, the plate was rinsed with PBS, 1 mL of 0.25% trypsin was added to the plate, and the plate was then incubated for 5 minutes at 37°C. Following the incubation, 5 mL of ES cell medium was added to the plate and the cells were dissociated into a single cell suspension by pipetting. The appropriate amount of cells was then transferred to a new feeder dish containing ES cell medium. In order to delete *Foxd3* from *Foxd3*$^{fl/fl}$*; CAAG-Cre*^{ER} ES cells, 2 μm 4-Hydroxytamoxifen (TM) was added to culture (Sigma H7904). Stock solutions of TM were prepared in advance (1 mM in 95% ethanol) and stored at -20°C.

When ES cells needed to be frozen for future use, the cells were trypsinized as above and 5 mL of ES cell medium was added to stop the reaction. A small amount (usually 10 μL) of the cells was diluted 1 to 5 in ES cell medium. The cells were counted using a hemacytometer (5 of the 9 squares were counted, see Figure B.1) and the total number of cells was calculated using the following calculation:

in 5 squares ÷ 5 (# of squares) x (2000) x 5 (dilution factor) x 6 (total volume) = total cells.

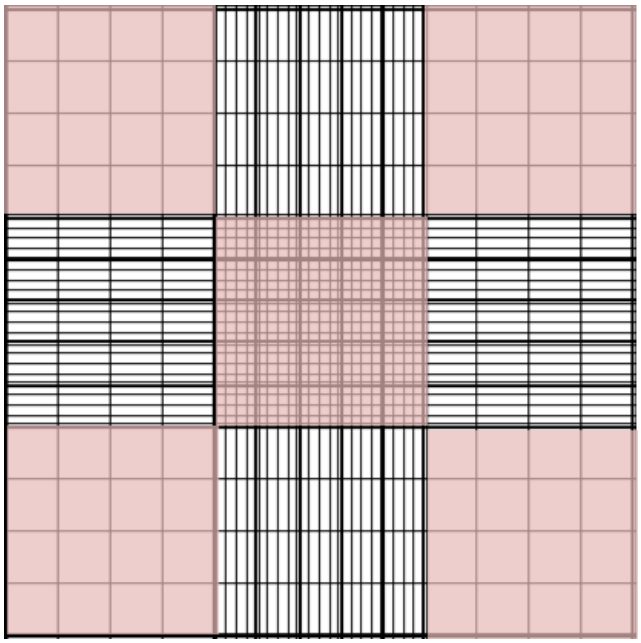

Figure B.1: Schematic of a grid from a hemacytometer. Cells in the red shaded squares are counted (5 squares total). Image modified from hausserscientific.com.

The total number of vials needed was calculated by dividing the total number of cells by $3x10^7$. The cells were centrifuged for 3 minutes at 1000 rpm. The medium was aspirated and cells resuspended in the appropriate amount of freezing medium (30% FBS and 10% DMSO in ES cell medium). The cells were frozen overnight at -80°C in Cryo 1C freezing containers (Nalgene) filled with 250 mL isopropyl alcohol. The following day the cells were transferred to a liquid nitrogen tank.

Generation of Doxycycline-inducible ES cell lines: Ten micrograms of the p2loxP vector (Iacovino et al., 2011b) was digested with EcoRI and SalI (50 μL reaction, 2 μL each enzyme) for 3 hours at 37°C. Samples were run on an agarose gel; the band containing the 3.5 kb DNA fragment was extracted and purified using the Wizard SV Gel and PCR Purification kit (Promega), and was eluted in a final volume of 30 μL . Following

purification, the samples were treated with 3.5 μL Antarctic Phosphatase buffer (NEB) and 1 μL Antarctic Phosphatase. Samples were incubated for 15 minutes at 37°C and 15 minutes at 56°C. Another microliter of Antarctic Phosphatase was added and the 37°C and 56°C incubations were repeated. The samples were purified using the Wizard SV Gel and PCR Purification kit.

Sox15 cDNA was amplified from the pMXs-Sox15vector (Addgene 13359) using PCR with *Sox15* insertion primers (see Table B.1) and AmpliTaq Gold DNA polymerase (Applied Biosystems N8080247). The PCR product was purified with the Wizard SV Gel and PCR Purification kit. The purified PCR product was digested with 1uL EcoRI and SalI in a total volume of 50 μL. DNA samples were purified with the Wizard SV Gel and PCR Purification kit.

The purified vector and PCR products were ligated using T4 DNA Ligase (NEB M0202) for 15 minutes at room temperature in a total reaction volume of 10 μL using molar ratios of 1:1, 1:3, 3:1, and 1:0 (vector: insert). One microliter of the ligation was added to 80 μL of competent DH5alpha cells. The cells were incubated on ice for 10 minutes followed by a heat shock at 42°C for 90 seconds. The samples were then placed on ice for 1 minute, 1 mL of LB was added, the samples were incubated at 37°C for 1 hour, and 100 μL was plated on LB amp plates. The plates were incubated at 37°C overnight. The following day, 24 colonies were picked into 5 mL LB with 5 μL 50 mg/mL ampicillin. The cultures were grown in a shaking incubator overnight at 37°C and 200 rpm.

DNA was purified from the bacterial pellets with the Wizard Plus SV Minipreps DNA Purification System (Promega). Two microliters from each miniprep were digested with EcoRI and SalI in a 50 μL reaction and then 10 μL of the digest was run on a 1% agarose gel. The presence of a 700 base pair band indicated insertion of the Sox15 cDNA into the vector. Four samples with the band corresponding to Sox15 cDNA were sequenced by the Vanderbilt University DNA Sequencing Core using both Sox15 insertion primers (See Table B.1) to ensure the correct sequence.

The p2lox-Sox15 vector (10 μg) was digested with EcoRI and NotI (50 μL reaction, 2 μL each enzyme) for 3 hours at 37°C. The vector backbone was purified using the Wizard SV Gel and PCR Purification kit (Promega) and was eluted in a final volume of 30 μL . Following purification, the samples were treated with 3.5 μL Antarctic Phosphatase buffer (NEB) and 1 μL Antarctic Phosphatase. The samples were incubated for 15 minutes at 37°C and 15 minutes at 56°C. Another microliter of Antarctic Phosphatase was added and the 37°C and 56°C incubations were repeated. The samples were purified using the Wizard SV Gel and PCR Purification kit.

Oligos were generated with the HA and Myc tag sequenced flanked by EcoRI (5') and NotI (3') restriction enzyme sequences (See Table B.1). Seven hundred nanomoles of oligo was kinased using the following reaction: 1 μL T4 Polynucleotide Kinase (PNK) buffer, 1 μL T4 PNK, 1 μL 100 mM ATP. The samples were incubated for 1 hour at 37°C. The forward and reverse oligos were combined and then annealed by heating to 95°C for 5 minutes and then slowly cooling to room temperature. Once oligos were cool, they were purified using a phenol: chloroform extraction.

The purified vector and annealed oligos were ligated using T4 DNA Ligase (NEB M0202) for 15 minutes at room temperature in a total reaction volume of 10 μL . Molar ratios of 1:1, 1:3, 3:1, and 1:0 (vector: insert) were used. One microliter of the ligation was added to 80 μL of competent DH5alpha cells. The cells were incubated on ice for 10 minutes followed by a heat shock at 42°C for 90 seconds. The samples were then placed on ice for 1 minute, 1 mL of LB was added, the samples were incubated at 37°C for 1 hour, and 100 μL was plated on LB amp plates. The plates were incubated at 37°C overnight. The following day, 24 colonies were picked into 5 mL LB with 5 μL 50 mg/mL ampicillin. The cultures were grown in a shaking incubator overnight at 37°C and 200 rpm.

DNA was purified with the Wizard Plus SV Minipreps DNA Purification System (Promega). Two microliters from each miniprep were digested with EcoRI and NotI in a 50 μL reaction and then 10 μL of the digest was run on a 2% agarose gel. The presence of a faint 70 base pair band indicates insertion of the HA or Myc oligo into the vector. Three samples with the band corresponding to oligo sequence were sequenced by the Vanderbilt University DNA Sequencing Core using the forward the Sox15 insertion and the Sox15 Seq primer (See Table B.1) to ensure the correct sequence.

Once the sequences were verified, a culture carrying p2lox-Sox15-HA and 1 p2lox-Sox15-Myc DNA was grown in 200 mL LB and 200 μL 50 mg/mL Ampicillin overnight. The DNA was isolated using the Plasmid Maxi Kit (Qiagen 12162) following the standard protocol. The DNA was resuspended in 200 μL sterile TE. The amount of

DNA was quantified using a NanoDrop Spectrophotometer (ND-1000). A schematic of the completed vector is illustrated in Figure B.2.

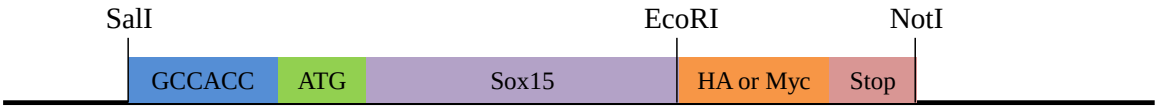

Figure B.2: DNA sequences inserted into the p2LoxP vector. A Kozak sequence and the *Sox15* cDNA were added between SalI and EcoRI restriction enzyme sites. An HA or Myc tag and a stop codon was inserted between EcoRI and NotI restriction enzyme sites. Diagram is not drawn to scale.

AINV ES cells were cultured as described above for 2 passages (Iacovino et al., 2011b). Once the cells were 60% confluent following the second passage, 1 μg/mL Doxycycline (1 mg/mL stock solution is stored at -20°C) was added to the culture medium to induce expression of Cre recombinase. The following day, the ES cells were fed normally and 1 hour later the ES cell medium was aspirated, cells were rinsed with PBS, 1 mL 0.25% Trypsin was added to the dish, and the dish was incubated at 37°C for 5 minutes. Following the incubation, 4 mL medium was added, and the cells were dissociated into a single cell suspension. The cells were counted (see above) and 5 x 10^7 cells were transferred to each of 2- 15 mL conical tubes. The cells were centrifuged at 1,000 rpm for 3 minutes. The medium was aspirated, the cells were resuspended in 800 μL sterile PBS, and the resuspended cells were transferred to a Gene Pulser Cuvette (BioRad 165-2088). Ten micrograms of p2lox-Sox15-HA or p2lox-Sox15-Myc were added to the appropriate cuvette. The cells were electroporated in a Gene Pulser II (BioRad) at 500 μF and 0.25 mV. The electroporated cells were plated on 10 cm plates

with irradiated MEFs in ES cell medium. Recombination was mediated using "induced cassette exchange" (Iacovino et al., 2011b) as diagrammed in Figure B.3. In correctly targeted ES cells, *Sox15* was inserted downstream of a tetracycline response element in the *HPRT* locus and the tetracycline reverse transcriptional activator was located in the *ROSA26* locus. Therefore, in the presence of Doxycycline, expression of *Sox15* was induced from the *HPRT* locus.

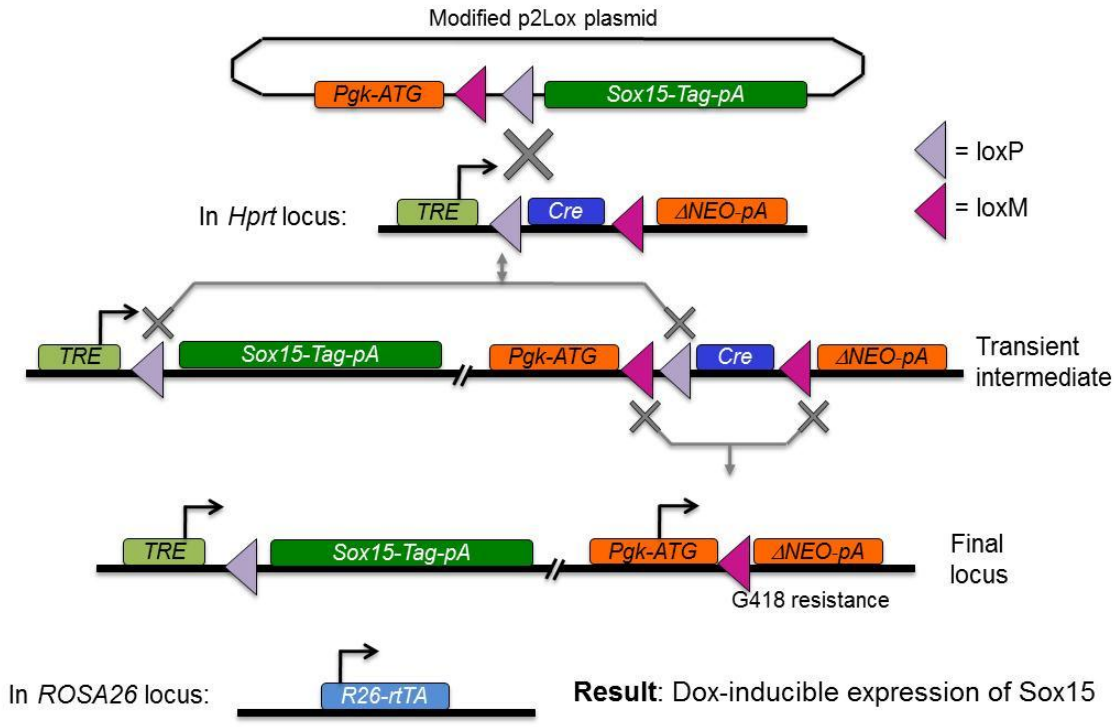

Figure B.3: Induced cassette exchange**.** Culturing ES cells with Doxycycline 24 hours prior to electroporation induces the reverse Tetracycline transactivator causing expression of Cre recombinase. Cre mediates recombination placing *Sox15* downstream of the tetracycline response element (TRE). Additionally, Cre autoexcises its coding sequence allowing expression of Neomycin (for positive selection) from the PGK promoter. rtTA is expressed from the *ROSA26* locus. Schematic is modified from an illustration designed by PAL.

After 1 day in culture, 30 μg/mL Geneticin was added to the medium for positive selection. The ES cell medium with Geneticin was refreshed daily. After 8 days in culture with Geneticin, ES cell medium was aspirated, and 10 mL PBS was added to each dish. ES cell colonies were picked (48 HA and 48 Myc) with a P20 pipette and transferred to a 96 well dish. Once 96 colonies were picked, 50 μL 0.25% Trypsin was added to each well. The plate was incubated at 37°C for 5 minutes. Following the incubation 100 μL ES cell medium was added to each well, the cells were dissociated into a single cell suspension, and the cells were transferred to a new 96 well plate containing feeders.

The cells were grown until confluence in the 96 well dish and 6 wells containing p2lox-Sox15-HA and 6 wells containing p2lox-Sox15-Myc were split and transferred into the top 6 wells of 2-24 well plates containing feeders (1 plate for p2lox-Sox15-Myc and 1 plate for p2lox-Sox15-HA). The cells were grown to confluence and then split 1:3. Again, the cells were grown to confluence. One of the 3 wells was harvested for genotyping and the other 2 were split to 60 mm dishes and cultured normally as above. Once an adequate number of plates were obtained, cells were frozen (see technique above) at a concentration of 3×10^6 cells/mL in freezing medium (10% DMSO and 20% FBS in complete ES cell medium). To genotype ES cells, cells were centrifuged at 1,000 rpm for 3 minutes. The medium was aspirated and cells were washed with 5 mL PBS. The cells were centrifuged at 1,000 rpm for 3 minutes. The wash was repeated twice. Once the cells were adequately washed, they were lysed overnight at 55°C in lysis buffer with Proteinase K (100 mM NaCl, 50 mM Tris-HCl pH 7.5, 10 mM EDTA, 0.5% SDS, and 1 mg/mL Proteinase K in sterile water), and DNA was isolated using phenol: chloroform extraction. Insertion of the construct was verified using PCR with PGK-Neo

primers (see Table B.1). To verify overexpression of Sox15, ES cells were cultured in 100 ng/mL Doxycycline and the cells were prepared for immunocytochemistry (see above) and real time PCR (see below).

Hanging drop embryoid bodies (EBs): ES cells were grown on a 60 mm dish until they were approximately 80% confluent. The ES cells were fed ES cell medium and then incubated at 37°C for at least 1 hour. The plate of cells was washed with 5 mL PBS, 1 mL of 0.25% trypsin was added, and the plate was placed in the tissue culture incubator for 5 minutes. In order to deplete the feeder cells, dissociated cells were "preplated" as follows: cells were dissociated into a single cell suspension, transferred to a gelatinized 100 mm plate, and incubated for 45 minutes at 37°C. During this time, the MEFs adhered to the plate while ES cells remained in the medium. The medium was removed and the cells were diluted to a final concentration of 2×10^4 cells/mL. A multichannel pipette was used to place 96- 20 μL drops of medium containing ES cells on the underside of the lid from a 150 mm dish. The total number of drops plated depended on the type of assay used. To collect EBs for RNA isolation at 3, 5, 7, 9, and 11 days, 3 dishes were used. The 150 mm dishes were filled with PBS and the lid containing hanging drops was carefully placed on the dish. The remaining cells were harvested for RNA isolation at day 0 (see RNA isolation section).

After 3 days in culture, hanging drops from one dish were harvested by pipetting excess medium on the lid to dissociate the drops from the lid. The samples were centrifuged at 1000 rpm for 3 minutes, washed 3 times with PBS, and EBs collected for future RNA isolation. EBs from the remaining dishes were collected and transferred to non-adherent 96 well plates (Corning Costar 3474). One-hundred microliters of medium

was added to each well. After 2 more days in culture, the EBs from 48 wells were collected to harvest for RNA. The remaining EBs were transferred to adherent 96 well dishes (Corning Costar 3595). After an additional 2 days in culture, the medium from 48 wells was aspirated, the wells were rinsed with PBS and 25 μL of 0.25% Trypsin added and the plate was incubated at 37C for 5 minutes. Following the incubation, 100 μL of medium was added and the cells harvested. The remaining wells were fed by aspirating the ES cell medium and replacing it with 100 μL fresh medium. On days 9 and 11 in culture, EBs were harvested in a manner identical to that at day 7.

TUNEL assay: ES cells were grown to approximately 80% confluence, the medium was aspirated, the cells were rinsed once with PBS, 1 mL of 0.25% Trypsin was added, and they were placed in the incubator for 5 minutes. Following the incubation 4 mL of ES cell medium was added, the cells were dissociated into a single cell suspension, and a 1:10 dilution was plated on 4 well chamber slides (Lab-TekII 154917) with and without 100 ng/mL Doxycycline. ES cell medium was replenished daily. After 2 days in culture, ES cell medium was aspirated, and the cells were rinsed with PBS and fixed with 4% PFA in PBS for 1 hour at room temperature. Following fixation, the cells were washed twice with PBS, permeabilized on ice for 2 minutes in 0.1% Triton-X 100 and 0.1% sodium citrate, and washed twice again in PBS. Fifty microliters of Enzyme solution was added to 450 μL Label solution (proprietary solutions, Fluorescein in situ Cell Death Detection Kit, Roche 11684795001) and 150 μL of the solution was added to each chamber. The slides were incubated in the dark for 1 hour at 37°C. Following the incubation, cells were washed twice with PBS. To label nuclei, a 1:5000 dilution of DAPI in water was added to each well, incubated 3 minutes and then the samples were washed

once with PBS. The slides were mounted with Aqua Polymount (Polysciences, Inc). To calculate the percentage of cell death, the total number of TUNEL positive cells was divided by the total number of nuclei (DAPI) and multiplied by 100%.

RNA isolation and quantification

Sample preparation/harvest: Whole pancreata and hypothalamus were harvested by dissecting in cold, RNase free PBS (Gibco 14040), immediately placed in RNA Later (Ambion AM7020) and stored at -20°C until RNA isolation. Islets were isolated from the Islet Procurement and Isolation Core (Brissova et al., 2004), washed 3 times in RNase free PBS and frozen at -80°C until RNA isolation. Cell culture samples were fed with complete medium 1 hour prior to harvesting. To harvest, medium was aspirated, the dishes were washed with PBS, and 0.25% Trypsin was added to the dish. The cells were placed at 37°C for 5 minutes. Following the incubation, complete medium was added to quench the Trypsin reaction. The cells were centrifuged for 3 minutes at 1000 rpm. The medium was aspirated and cell pellets washed three times with PBS. Cells were then frozen in liquid nitrogen and placed at -80°C until isolation.

Isolation of RNA: RNA was isolated using the RNeasy Mini Kit (Qiagen 74104) with minor modifications. The samples were resuspended in 350 μL of buffer RLT. Larger tissues (pancreas and hypothalamus) were dissociated using a 19 gauge syringe. The samples were then added to a QIAShredder column (Qiagen 79654) and centrifuged at maximum speed for 2 minutes. The column was removed and 350 μL RNase free 70% ethanol was added to the flow-through. This solution was added to an RNeasy Mini column and centrifuged for 20 seconds at maximum speed. The flow-through was

discarded, 700 μL buffer RW1 was added to the column and the samples were centrifuged at maximum speed for 20 seconds. The flow-through was discarded, 500 μL buffer RPE (with ethanol added) was added to the column, and the samples were centrifuged at maximum speed for 20 seconds. Following the wash, the flow-through was discarded, 500 μL buffer RPE was added to the column and the samples were centrifuged for 2 minutes at maximum speed. Prewarmed, nuclease-free water (40 μL) was added to the column and incubated for 1 minute at room temperature. The columns were then transferred to nuclease free Eppendorf tubes and centrifuged for 1 minute at maximum speed. The flow-through was added to the column (for a second elution) and the samples were centrifuged at maximum speed for 1 minute.

To remove genomic DNA, the TURBO DNA-free kit (Ambion Am1907) was used. Four microliters (0.1X volume) of TURBO DNase buffer and 1 μL TURBO DNase were added to the samples and the samples were incubated at 37°C for 25 minutes. Following incubation, 4.5 μL (0.1X volume) TURBO DNase inactivation reagent was added to the samples. The samples were incubated at room temperature for 3 minutes and then centrifuged for 2 minutes at maximum speed. The supernatant was transferred to a clean, nuclease-free Eppendorf tube. The concentration of the samples was determined using a NanoDrop Spectrophotometer (ND-1000).

Reverse transcription: The GoScript Reverse Transcription System (Promega A5001) was used to generate cDNA. Using the concentrations obtained from the NanoDrop Spectrophotometer (ND-1000), an equal amount of RNA (50ng- 1μg) was used for each reaction (up to 4 μL). RNA was added to nuclease free PCR tubes and nuclease-free

water was added to give a total volume of 4 μL. One microliter of random primers was added to the tubes, and the samples were mixed well, briefly centrifuged, incubated for 5 minutes at 70°C, and then incubated 1 minute on ice. Once the incubation was complete, the following kit components were added to each sample: 4 μL buffer, 4 μL $MgCl_2$, 1 μL dNTPs, 1 μL RNasin, 1 μL reverse transcriptase, and 4 μL nuclease free water. The samples were then mixed, briefly centrifuged, and placed in a thermocycler with the following program: 5 minutes at 25°C, 1 hour at 42°C, 15 minutes at 72°C, and held at 4°C. For non-quantitative analyses, 1 μL RNaseH was added to each sample and the samples incubated at 37°C for 20 minutes.

Quantitative PCR: The GoTaq qPCR Master Mix (Promega A6001) was used for qPCR analyses. For each 10 μL reaction, the following components were used: 5 μL master mix, 0.1 μL CXR, 1.5 μL 2.5 mM oligos (Table B.1), template DNA, and sterile water. All samples were run in duplicate or triplicate. The samples were run in a MicroAmp plate (Applied Biosystems 4346906) in an Applied Biosystems 7900HT Fast Real-Time PCR System. The "standard" real time protocol was used with a TM of 56°C and an additional dissociation step.

The delta-delta Ct (Critical Threshold) method was used to determine relative expression in the case of qRT-PCR and fold enrichment in the case of qPCR following ChIP experiments. The Ct values were obtained from the real time machine and the calculation was performed as follows:

Primer Specific Ct – Loading Control Ct = Delta Ct

Delta Ct Mutant – Delta Ct Control = Delta Delta Ct

$2^{-\text{Delta Delta Ct}}$ = Relative Expression or Fold Enrichment

In the case of qRT-PCR, the Loading Control Ct was HPRT or 18S rRNA. In the case of qPCR following ChIP the Loading Control Ct was amplification of the Input sample and the Delta Ct Control was the Delta Ct of the IgG sample.

Taq-Man low density arrays: RNA was isolated using the RNeasy Mini Kit (see above), genomic DNA was removed using TURBO DNA-free (Ambion), and cDNA was generated using the High Capacity cDNA Reverse Transcription Kit (Applied Biosystems 4374966). Four hundred nanograms of total RNA was diluted in 10 μL nuclease-free water. The following kit components were added to each sample: 2 μL buffer, 0.8 μL dNTPs, 2 μL random primers, 1 μL MultiScribe reverse transcriptase, 1 μL RNase Inhibitor, and 3.2 μL nuclease free water. The samples were transferred to a thermocycler and the following reaction was used: 10 minutes at 25°C, 2 hours at 37°C, 5 minutes at 85°C and hold at 4°C.

Following reverse transcription, the samples were prepared for amplification in the Taq-Man low density array using the Taq-Man Universal PCR Master Mix (Applied Biosystems 4304437). cDNA (5 μL of the above reaction, 100 ng) was added to 45 μL nuclease free water and 50 μL of the Taq-Man Universal PCR Master Mix. The entire sample was loaded into a Taq-Man Low Density array card (TaqMan Probes are listed in Table B.3), centrifuged at 3000 rpm for 2 minutes, and sealed. The CD that was provided

Table B.3: TaqMan probes used for Low Density Arrays

Gene Name	ABI ID Number	Gene Name	ABI ID Number
18S	Hs99999901_s1	Irs2	Mm03038438_m1
4921505C17Rik (Rictor)	Mm01307318_m1	Isl1	Mm00517585_m1
Akt1	Mm01331624_m1	Mafa	Mm00845209_s1
Akt2	Mm00545827_m1	Mafb	Mm00627481_s1
Arx	Mm00545903_m1	Men1	Mm00484963_m1
Bmi1	Mm03053308_g1	Neurog3	Mm00437606_s1
Ccnd2	Mm00438072_m1	Nkx2-2	Mm00839794_m1
Cdc25a	Mm00483162_m1	Nkx6-1	Mm00454962_m1
Cdk4	Mm00726334_s1	Onecut1	Mm00839394_m1
Cdkn1a	Mm00432448_m1	Pax4	Mm01159036_m1
Cdkn1b	Mm00438168_m1	Pax6	Mm00443081_m1
Cdkn2a	Mm01257348_m1	Pdx1	Mm00435565_m1
Cdkn2c	Mm00483243_m1	Prdm16	Mm00712556_m1
Cdkn2d	Mm00486943_m1	Prkca	Mm00440858_m1
Ezh2	Mm00468449_m1	Pten	Mm00477210_m1
Foxa2	Mm00839704_mH	Ptf1a	Mm00479622_m1
Foxd3	Mm02384867_s1	Sgk1	Mm00441380_m1
Foxm1	Mm00514924_m1	Skp2	Mm00449925_m1
Foxo1	Mm00490672_m1	Slc2a2	Mm00446224_m1
Gcg	Mm00801712_m1	Snap25	Mm00456921_m1
Gjd2	Mm00439121_m1	Sox9	Mm00448840_m1
Hnf4a	Mm00433964_m1	Stx1a	Mm00444008_m1
Ins1	Mm01950294_s1	Stxbp1	Mm00436837_m1
Ins2	Mm00731595_gH	Vamp2	Mm00494118_g1

with the low density arrays containing the real time PCR program (Applied Biosystems) was loaded into the computer and the reaction was completed. All samples were run in duplicate and data analyzed using the delta delta Ct method.

Chromatin immunoprecipitation

ES cells were grown to 80% confluence. The ES cell medium was aspirated, replaced with fresh ES cell medium, and placed in the tissue culture incubator for at least 1 hour. Following the incubation, the plates were rinsed with PBS, 1 mL 0.25% Trypsin was added and the plates were placed in the incubator for 5 minutes. Following the incubation, 4 mL of ES cell medium was added and the cells were dissociated into a single cell suspension by pipetting. The cells were then transferred to a 15 mL conical tube and 135 μL 37% Formaldehyde was added (1% final concentration of Formaldehyde). The samples were incubated at 37°C for 10 minutes. Next, 625 μL 1M glycine (final concentration 0.125 M glycine) was added and samples incubated at room temperature for 5 minutes to stop the crosslinking reaction. The samples were centrifuged at 1000 rpm for 3 minutes and the supernatant aspirated. Five milliliters of PBS was added to wash the cell pellet, the samples were spun at 1000 rpm for 3 minutes, and the supernatant aspirated. This PBS wash was repeated twice. Following the third wash, the samples were either used immediately or flash frozen in liquid nitrogen and stored at -80°C.

The cross-linked cells were resuspended in 7 mL swelling buffer (25 mM Hepes pH 7.9, 1.5 mM $MgCl_2$, 10mM KCl, 0.1% NP-40) and incubated on ice for 10 minutes.

The cells were centrifuged at 3,500 rpm for 10 minutes at 4°C and the supernatant aspirated. The cell pellets were resuspended in 1 mL sonication buffer (50 mM Hepes pH 7.9, 140 mM NaCl, 1mM EDTA, 1% Triton X-100, 0.1% Sodium deoxycholate, 0.1% SDS) and 10 μL protease inhibitors (Sigma P8340) and transferred to a 1.5 mL Eppendorf tube. The samples were sonicated for 5 minutes and the sonication was repeated twice. Following sonication, the samples were centrifuged for 15 minutes at maximum speed. The supernatant was collected and centrifuged again as above. The remaining supernatant was precleared by adding 75 μL of the appropriate agarose beads (See Table B.4) and 10 μL IgG antibody (Santa Cruz Biotechnology sc-2027) and incubated for at least 4 hours at 4°C. The samples were then centrifuged at 1200 rpm for 15 minutes. The supernatant was collected and the amount of chromatin was quantified by making a 1:10 dilution of chromatin (2 μL) in 0.1M NaOH (18 μL). The amount of chromatin lysate was quantified using a NanoDrop Spectrophotometer (ND-1000) measuring the nucleic acid concentration at 260 nm. The appropriate amount of chromatin (see Table B.4) was transferred to a clean Eppendorf tube and the appropriate amount of primary antibody was added (see Table B.4). The samples were incubated overnight at 4°C. The remaining chromatin was saved as an input.

Table B.4: Antibodies used for chromatin immunoprecipitation assays

Antigen	Source	Concentration	Agarose Beads
Foxd3	Millipore	7 μg antibody/100 μg chromatin	Protein A
H3K14ac	Millipore	5 μL antibody/25 μg chromatin	Protein A
H3K27me3	Millipore	5 μg antibody/25 μg chromatin	Protein A
H3K4me2	Millipore	5 μL antibody/25 μg chromatin	Protein A
H4ac	Millipore	5 μL antibody/25 μg chromatin	Protein A
IgG	Santa Cruz	5 μL antibody/25 μg chromatin	Protein A or G
RNA Pol II pSer5	Abcam	2 μL antibody/25 μg chromatin	Protein A
Sox2	Santa Cruz	7 μL antibody/100 μg chromatin	Protein G

The next morning, 60 μL of the appropriate agarose beads (see Table B.4) were added to the samples and then the samples were incubated on a nutator at 4°C for 4 hours. Following the incubation, samples were centrifuged at 1200 rpm for 5 minutes. The supernatant was removed by aspiration into a vacuum flask with a gel-loading tip (Fisherbrand 02707181). At this time, it was crucial to remove all of the supernatant from the agarose beads but not remove the agarose beads. The beads were washed by adding 1 mL of sonication buffer, incubating the samples at 4°C on the nutator for 5 minutes, centrifuging as above for 5 minutes, and removing the supernatant. This step was repeated for the following wash buffers Buffer A (50 mM Hepes pH 7.9, 500 mM NaCl, 1mM EDTA, 1% Triton X-100, 0.1% Sodium deoxycholate, 0.1% SDS), Buffer B (20 mM Tris pH 8.0, 1 mM EDTA, 250 mM LiCl, 0.5% NP-40, 0.5% Sodium deoxycholate), and TE (10 mM Tris pH 8.0, 1mM EDTA) twice. Elution buffer (50 mM Tris pH 8.0, 1 mM EDTA, 1% SDS) was made fresh and 250 μL elution buffer was added to each sample. The samples were incubated 5 minutes at 65°C, 15 minutes on a nutator at room temperature, and then the samples were centrifuged at 1200 rpm for 5 minutes. The eluates were collected in a fresh Eppendorf tube and the elution was repeated. TE was

added to the input samples to give at total volume of 500 μL. Following elution, 20 μL of 4M NaCl and 1 μL of 10 mg/mL RNaseA (Clonetech Labs, Inc 740505) were added to each sample and the samples were incubated overnight at 65°C.

The following morning, 4 μL of 0.5 M EDTA pH 8.0 and 5 μL 20 mg/mL Proteinase K (Research Products Incorporated 39450-01-6) were added to the samples and the samples incubated at 45°C for 2 hours. After the incubation, 500 μL of Phenol: Chloroform: Isoamyl Alcohol (Sigma P3808) was added to each sample. Samples were rocked on a nutator for 20 minutes at room temperature, then centrifuged for 10 minutes at maximum speed and 450 μL of the aqueous (top) layer was collected. To precipitate the immunoprecipitated DNA, 900 μL 100% ethanol, 45 μL 3.5mM sodium acetate, and 1 μL Pellet Paint (Novagen 69049) were added and the samples were incubated at -20°C for at least 1 hour. The samples were then centrifuged for 10 minutes at maximum speed and the supernatant was carefully removed. The pellet was washed with 100 μL 70% ethanol and allowed to dry. The DNA was resuspended in 35 μL TE. Following resuspension, the samples were prepared for qPCR. This protocol was provided by Niall Dillon, Imperial College London.

Animal cap assays

Bacteria from the following glycerol stocks were grown overnight at 37°C at 200 rpm in 10 mL LB with 10 μL Ampicillin: pCS2-mFoxd3, pCS2-Eng-mFoxd3, and pCS2-VP16-mFoxd3. DNA was purified using the Wizard Plus SV Minipreps DNA

Purification System (Promega). Fifteen micrograms of DNA from each sample was digested with NsiI (NEB) in a total volume of 100 μL for 3 hours at 37°C. Two microliters of the sample were run on a 1% agarose gel to ensure proper digestion. DNA was purified from the remaining sample using phenol-chloroform extraction. One microgram of DNA was transcribed as directed using the mMessage mMachine Sp6 kit (Ambion AM1340). Following transcription, the RNA was isolated using the NucAway Spin Columns (Ambion AM10070). One microliter of the RNA was run on a 2% phosphate gel to ensure a minimal amount of degradation. The RNA samples were diluted to 25 ng/uL (VP16-mFoxd3) or 10 ng/uL (Eng-mFoxd3 and mFoxd3).

Xenopus laevis injections were performed by Justin Wells in Dr. Christopher Wright's laboratory (Cha et al., 2006). A sperm solution was prepared by dissecting testes from male *Xenopus* and then mincing the testes into small pieces to extract the sperm. The sperm solution was added to freshly isolated *Xenopus* eggs and incubated at room temperature for 45 minutes. Following the incubation, the embryos were dejellied and injected at the 1 cell stage with 10 nL of each RNA (0.25 ng of VP16-mFoxd3 and 0.10 ng of Eng-mFoxd3 and mFoxd3 (Steiner et al., 2006). The embryos were incubated overnight at 17°C. The following morning, a small cube was removed from the animal pole of the embryo and the animal caps were transferred to a new dish and allowed to develop for 6 hours. After 6 hours, the animal caps were imaged and analyzed for convergent extension.

Statistical analyses

For all quantitative assays, the mean and standard error of the mean (SEM) were calculated. One common computer program used to calculate these values is Microsoft Excel. The following prompts within Excel were used: (Mean: =avg (enter data points)) and (SEM: =stdev (enter data points)/sqrt (count (enter data points))). Additionally, for most statistical analyses here, a two-tailed Student's t-test was used to determine significance. Again, Microsoft Excel can be used to determine p-values using a Student's t-test. The following Excel prompt was used to determine p-values: (=ttest(enter data points group 1, enter data points group 2, 2,2)). This calculation assumed that variances among both groups were equal. In the case of glucose tolerance tests, a Student's t-test is inappropriate because repeated measures are taken from the same animal. In this instance, a "repeated measures ANOVA with Bonferoni post-tests" was used to determine statistical significance with Graph Pad Prism software.

BIBLIOGRAPHY

Abdou, A.G., Asaad, N.Y., Elkased, A., Said, H., and Dawoud, M. (2011). Adult Pancreatic Neuroblastoma, an Unusual Site and Fatal Outcome. Pathol Oncol Res.

Ackermann-Misfeldt, A., Costa, R.H., and Gannon, M. (2008). Beta-cell proliferation, but not neogenesis, following 60% partial pancreatectomy is impaired in the absence of FoxM1. Diabetes *57*, 3069-3077.

Ackermann, A.M., and Gannon, M. (2007). Molecular regulation of pancreatic beta-cell mass development, maintenance, and expansion. J Mol Endocrinol *38*, 193-206.

ACS (2005). Cancer Facts and Figures.

ADA (2011). National Diabetes Fact Sheet (American Diabetes association).

Adams, M.S., and Bronner-Fraser, M. (2009). Review: the role of neural crest cells in the endocrine system. Endocr Pathol *20*, 92-100.

Ahlgren, U., Jonsson, J., Jonsson, L., Simu, K., and Edlund, H. (1998). beta-cell-specific inactivation of the mouse Ipf1/Pdx1 gene results in loss of the beta-cell phenotype and maturity onset diabetes. Genes & development *12*, 1763-1768.

Ahlgren, U., Pfaff, S.L., Jessell, T.M., Edlund, T., and Edlund, H. (1997). Independent requirement for ISL1 in formation of pancreatic mesenchyme and islet cells. Nature *385*, 257-260.

Ahnfelt-Ronne, J., Ravassard, P., Pardanaud-Glavieux, C., Scharfmann, R., and Serup, P. (2010). Mesenchymal bone morphogenetic protein signaling is required for normal pancreas development. Diabetes *59*, 1948-1956.

Alipio, Z., Liao, W., Roemer, E.J., Waner, M., Fink, L.M., Ward, D.C., and Ma, Y. (2010). Reversal of hyperglycemia in diabetic mouse models using induced-pluripotent stem (iPS)-derived pancreatic beta-like cells. Proc Natl Acad Sci U S A *107*, 13426-13431.

Aramata, S., Han, S.I., Yasuda, K., and Kataoka, K. (2005). Synergistic activation of the insulin gene promoter by the beta-cell enriched transcription factors MafA, Beta2, and Pdx1. Biochim Biophys Acta *1730*, 41-46.

Artner, I., Blanchi, B., Raum, J.C., Guo, M., Kaneko, T., Cordes, S., Sieweke, M., and Stein, R. (2007). MafB is required for islet beta cell maturation. Proc Natl Acad Sci U S A *104*, 3853-3858.

Artner, I., Hang, Y., Mazur, M., Yamamoto, T., Guo, M., Lindner, J., Magnuson, M.A., and Stein, R. (2010). MafA and MafB regulate genes critical to beta-cells in a unique temporal manner. Diabetes *59*, 2530-2539.

Artner, I., Le Lay, J., Hang, Y., Elghazi, L., Schisler, J.C., Henderson, E., Sosa-Pineda, B., and Stein, R. (2006). MafB: an activator of the glucagon gene expressed in developing islet alpha- and beta-cells. Diabetes *55*, 297-304.

Bellamy, L., Casas, J.P., Hingorani, A.D., and Williams, D. (2009). Type 2 diabetes mellitus after gestational diabetes: a systematic review and meta-analysis. Lancet *373*, 1773-1779.

Beranger, F., Mejean, C., Moniot, B., Berta, P., and Vandromme, M. (2000). Muscle differentiation is antagonized by SOX15, a new member of the SOX protein family. The Journal of biological chemistry *275*, 16103-16109.

Berne, R.M. (1993). Physiology (St. Louis, Mosby Year Book).

Bhushan, A., Itoh, N., Kato, S., Thiery, J.P., Czernichow, P., Bellusci, S., and Scharfmann, R. (2001). Fgf10 is essential for maintaining the proliferative capacity of epithelial progenitor cells during early pancreatic organogenesis. Development (Cambridge, England) *128*, 5109-5117.

Bonner-Weir, S. (2000). Perspective: Postnatal pancreatic beta cell growth. Endocrinology *141*, 1926-1929.

Bonner-Weir, S., Li, W.C., Ouziel-Yahalom, L., Guo, L., Weir, G.C., and Sharma, A. (2010). Beta-cell growth and regeneration: replication is only part of the story. Diabetes *59*, 2340-2348.

Bouwens, L., and Rooman, I. (2005). Regulation of pancreatic beta-cell mass. Physiol Rev *85*, 1255-1270.

Boyer, D.F., Fujitani, Y., Gannon, M., Powers, A.C., Stein, R.W., and Wright, C.V. (2006). Complementation rescue of Pdx1 null phenotype demonstrates distinct roles of proximal and distal cis-regulatory sequences in pancreatic and duodenal expression. Developmental biology *298*, 616-631.

Brelje, T.C., Scharp, D.W., Lacy, P.E., Ogren, L., Talamantes, F., Robertson, M., Friesen, H.G., and Sorenson, R.L. (1993). Effect of homologous placental lactogens, prolactins, and growth hormones on islet B-cell division and insulin secretion in rat, mouse, and human islets: implication for placental lactogen regulation of islet function during pregnancy. Endocrinology *132*, 879-887.

Brissova, M., Fowler, M., Wiebe, P., Shostak, A., Shiota, M., Radhika, A., Lin, P.C., Gannon, M., and Powers, A.C. (2004). Intraislet endothelial cells contribute to revascularization of transplanted pancreatic islets. Diabetes *53*, 1318-1325.

Brownawell, A.M., Kops, G.J., Macara, I.G., and Burgering, B.M. (2001). Inhibition of nuclear import by protein kinase B (Akt) regulates the subcellular distribution and activity of the forkhead transcription factor AFX. Mol Cell Biol *21*, 3534-3546.

Bruno, M.J. (1995). Maldigestion associated with exocrine pancreatic insufficiency: implications of gastrointestinal physiology and properties of enzyme preparations for a cause-related and patient-tailored treatment. Am J Gastroenterol *90*, 1383-1393.

Buchanan, T.A., Xiang, A.H., Peters, R.K., Kjos, S.L., Marroquin, A., Goico, J., Ochoa, C., Tan, S., Berkowitz, K., Hodis, H.N., *et al.* (2002). Preservation of pancreatic beta-cell function and prevention of type 2 diabetes by pharmacological treatment of insulin resistance in high-risk hispanic women. Diabetes *51*, 2796-2803.

Butler, A.E., Cao-Minh, L., Galasso, R., Rizza, R.A., Corradin, A., Cobelli, C., and Butler, P.C. (2010). Adaptive changes in pancreatic beta cell fractional area and beta cell turnover in human pregnancy. Diabetologia *53*, 2167-2176.

Butler, A.E., Janson, J., Bonner-Weir, S., Ritzel, R., Rizza, R.A., and Butler, P.C. (2003). Beta-cell deficit and increased beta-cell apoptosis in humans with type 2 diabetes. Diabetes *52*, 102-110.

Butler, P.C., Meier, J.J., Butler, A.E., and Bhushan, A. (2007). The replication of beta cells in normal physiology, in disease and for therapy. Nat Clin Pract Endocrinol Metab *3*, 758-768.

Cao, R., Wang, L., Wang, H., Xia, L., Erdjument-Bromage, H., Tempst, P., Jones, R.S., and Zhang, Y. (2002). Role of histone H3 lysine 27 methylation in Polycomb-group silencing. Science (New York, NY *298*, 1039-1043.

Cha, Y.R., Takahashi, S., and Wright, C.V. (2006). Cooperative non-cell and cell autonomous regulation of Nodal gene expression and signaling by Lefty/Antivin and Brachyury in Xenopus. Developmental biology *290*, 246-264.

Chan, C.W., Lee, Y.B., Uney, J., Flynn, A., Tobias, J.H., and Norman, M. (2007). A novel member of the SAF (scaffold attachment factor)-box protein family inhibits gene expression and induces apoptosis. Biochem J *407*, 355-362.

Chandak, G.R., Janipalli, C.S., Bhaskar, S., Kulkarni, S.R., Mohankrishna, P., Hattersley, A.T., Frayling, T.M., and Yajnik, C.S. (2007). Common variants in the TCF7L2 gene are strongly associated with type 2 diabetes mellitus in the Indian population. Diabetologia *50*, 63-67.

Chen, H., Gu, X., Liu, Y., Wang, J., Wirt, S.E., Bottino, R., Schorle, H., Sage, J., and Kim, S.K. (2011). PDGF signalling controls age-dependent proliferation in pancreatic beta-cells. Nature.

Chen, H., Gu, X., Su, I.H., Bottino, R., Contreras, J.L., Tarakhovsky, A., and Kim, S.K. (2009a). Polycomb protein Ezh2 regulates pancreatic beta-cell Ink4a/Arf expression and regeneration in diabetes mellitus. Genes & development *23*, 975-985.

Chen, W.S., Peng, X.D., Wang, Y., Xu, P.Z., Chen, M.L., Luo, Y., Jeon, S.M., Coleman, K., Haschek, W.M., Bass, J., *et al.* (2009b). Leptin deficiency and beta-cell dysfunction underlie type 2 diabetes in compound Akt knockout mice. Mol Cell Biol *29*, 3151-3162.

Choi, J.B., Uchino, H., Azuma, K., Iwashita, N., Tanaka, Y., Mochizuki, H., Migita, M., Shimada, T., Kawamori, R., and Watada, H. (2003). Little evidence of transdifferentiation of bone marrow-derived cells into pancreatic beta cells. Diabetologia *46*, 1366-1374.

Claiborn, K.C., and Stoffers, D.A. (2008). Toward a cell-based cure for diabetes: advances in production and transplant of beta cells. Mt Sinai J Med *75*, 362-371.

Collombat, P., Hecksher-Sorensen, J., Broccoli, V., Krull, J., Ponte, I., Mundiger, T., Smith, J., Gruss, P., Serup, P., and Mansouri, A. (2005). The simultaneous loss of Arx and Pax4 genes promotes a somatostatin-producing cell fate specification at the expense of the alpha- and beta-cell lineages in the mouse endocrine pancreas. Development (Cambridge, England) *132*, 2969-2980.

Collombat, P., Mansouri, A., Hecksher-Sorensen, J., Serup, P., Krull, J., Gradwohl, G., and Gruss, P. (2003). Opposing actions of Arx and Pax4 in endocrine pancreas development. Genes & development *17*, 2591-2603.

Cozar-Castellano, I., Weinstock, M., Haught, M., Velazquez-Garcia, S., Sipula, D., and Stewart, A.F. (2006). Evaluation of beta-cell replication in mice transgenic for hepatocyte growth factor and placental lactogen: comprehensive characterization of the G1/S regulatory proteins reveals unique involvement of p21cip. Diabetes *55*, 70-77.

Crabtree, J.S., Scacheri, P.C., Ward, J.M., McNally, S.R., Swain, G.P., Montagna, C., Hager, J.H., Hanahan, D., Edlund, H., Magnuson, M.A., *et al.* (2003). Of mice and MEN1: Insulinomas in a conditional mouse knockout. Mol Cell Biol *23*, 6075-6085.

Crawford, L.A., Guney, M.A., Oh, Y.A., Deyoung, R.A., Valenzuela, D.M., Murphy, A.J., Yancopoulos, G.D., Lyons, K.M., Brigstock, D.R., Economides, A., *et al.* (2009). Connective tissue growth factor (CTGF) inactivation leads to defects in islet cell lineage allocation and beta-cell proliferation during embryogenesis. Molecular endocrinology (Baltimore, Md *23*, 324-336.

Cui, Y., Huang, L., Elefteriou, F., Yang, G., Shelton, J.M., Giles, J.E., Oz, O.K., Pourbahrami, T., Lu, C.Y., Richardson, J.A., *et al.* (2004). Essential role of STAT3 in body weight and glucose homeostasis. Mol Cell Biol *24*, 258-269.

D'Amour, K.A., Bang, A.G., Eliazer, S., Kelly, O.G., Agulnick, A.D., Smart, N.G., Moorman, M.A., Kroon, E., Carpenter, M.K., and Baetge, E.E. (2006). Production of pancreatic hormone-expressing endocrine cells from human embryonic stem cells. Nat Biotechnol *24*, 1392-1401.

Dahlgren, A., Zethelius, B., Jensevik, K., Syvanen, A.C., and Berne, C. (2007). Variants of the TCF7L2 gene are associated with beta cell dysfunction and confer an increased risk of type 2 diabetes mellitus in the ULSAM cohort of Swedish elderly men. Diabetologia *50*, 1852-1857.

Danielian, P.S., Muccino, D., Rowitch, D.H., Michael, S.K., and McMahon, A.P. (1998). Modification of gene activity in mouse embryos in utero by a tamoxifen-inducible form of Cre recombinase. Curr Biol *8*, 1323-1326.

Davis, D.B., Lavine, J.A., Suhonen, J.I., Krautkramer, K.A., Rabaglia, M.E., Sperger, J.M., Fernandez, L.A., Yandell, B.S., Keller, M.P., Wang, I.M., *et al.* (2010). FoxM1 is up-regulated by obesity and stimulates beta-cell proliferation. Molecular endocrinology (Baltimore, Md *24*, 1822-1834.

Debril, M.B., Dubuquoy, L., Feige, J.N., Wahli, W., Desvergne, B., Auwerx, J., and Gelman, L. (2005). Scaffold attachment factor B1 directly interacts with nuclear receptors in living cells and represses transcriptional activity. J Mol Endocrinol *35*, 503-517.

Desgraz, R., and Herrera, P.L. (2009). Pancreatic neurogenin 3-expressing cells are unipotent islet precursors. Development (Cambridge, England) *136*, 3567-3574.

Devendra, D., Liu, E., and Eisenbarth, G.S. (2004). Type 1 diabetes: recent developments. Bmj *328*, 750-754.

Dhawan, S., Tschen, S.I., and Bhushan, A. (2009). Bmi-1 regulates the Ink4a/Arf locus to control pancreatic beta-cell proliferation. Genes & development *23*, 906-911.

Dor, Y., Brown, J., Martinez, O.I., and Melton, D.A. (2004). Adult pancreatic beta-cells are formed by self-duplication rather than stem-cell differentiation. Nature *429*, 41-46.

Dor, Y., and Melton, D.A. (2008). Facultative endocrine progenitor cells in the adult pancreas. Cell *132*, 183-184.

Edlund, H. (2002). Pancreatic Organogenesis--developmental mechanisms and implications for therapy. Nat Rev Genet *3*, 524-532.

Edvell, A., and Lindstrom, P. (1998). Vagotomy in young obese hyperglycemic mice: effects on syndrome development and islet proliferation. Am J Physiol *274*, E1034-1039.

Ekeblad, S., Skogseid, B., Dunder, K., Oberg, K., and Eriksson, B. (2008). Prognostic factors and survival in 324 patients with pancreatic endocrine tumor treated at a single institution. Clin Cancer Res *14*, 7798-7803.

Epstein, J.A., Lam, P., Jepeal, L., Maas, R.L., and Shapiro, D.N. (1995). Pax3 inhibits myogenic differentiation of cultured myoblast cells. The Journal of biological chemistry *270*, 11719-11722.

Esni, F., Johansson, B.R., Radice, G.L., and Semb, H. (2001). Dorsal pancreas agenesis in N-cadherin- deficient mice. Developmental biology *238*, 202-212.

Feig, D.S., Zinman, B., Wang, X., and Hux, J.E. (2008). Risk of development of diabetes mellitus after diagnosis of gestational diabetes. Cmaj *179*, 229-234.

Finegood, D.T., Scaglia, L., and Bonner-Weir, S. (1995). Dynamics of beta-cell mass in the growing rat pancreas. Estimation with a simple mathematical model. Diabetes *44*, 249-256.

Forcales, S.V., Albini, S., Giordani, L., Malecova, B., Cignolo, L., Chernov, A., Coutinho, P., Saccone, V., Consalvi, S., Williams, R., *et al.* (2011). Signal-dependent incorporation of MyoD-BAF60c into Brg1-based SWI/SNF chromatin-remodelling complex. EMBO J.

Freemark, M., Avril, I., Fleenor, D., Driscoll, P., Petro, A., Opara, E., Kendall, W., Oden, J., Bridges, S., Binart, N., *et al.* (2002). Targeted deletion of the PRL receptor: effects on islet development, insulin production, and glucose tolerance. Endocrinology *143*, 1378-1385.

Gannon, M., Ables, E.T., Crawford, L., Lowe, D., Offield, M.F., Magnuson, M.A., and Wright, C.V. (2008). pdx-1 function is specifically required in embryonic beta cells to generate appropriate numbers of endocrine cell types and maintain glucose homeostasis. Developmental biology *314*, 406-417.

Gao, N., LeLay, J., Vatamaniuk, M.Z., Rieck, S., Friedman, J.R., and Kaestner, K.H. (2008). Dynamic regulation of Pdx1 enhancers by Foxa1 and Foxa2 is essential for pancreas development. Genes & development *22*, 3435-3448.

Genevay, M., Pontes, H., and Meda, P. (2010). Beta cell adaptation in pregnancy: a major difference between humans and rodents? Diabetologia *53*, 2089-2092.

Genuth, S. (2006). Insights from the diabetes control and complications trial/epidemiology of diabetes interventions and complications study on the use of intensive glycemic treatment to reduce the risk of complications of type 1 diabetes. Endocr Pract *12 Suppl 1*, 34-41.

Georgia, S., and Bhushan, A. (2004). Beta cell replication is the primary mechanism for maintaining postnatal beta cell mass. J Clin Invest *114*, 963-968.

Georgia, S., and Bhushan, A. (2006). p27 Regulates the transition of beta-cells from quiescence to proliferation. Diabetes *55*, 2950-2956.

Gilbert, S.F. (2010). Developmental Biology, Ninth Edition (Sinaur Associates).

Gittes, G.K., Galante, P.E., Hanahan, D., Rutter, W.J., and Debase, H.T. (1996). Lineage-specific morphogenesis in the developing pancreas: role of mesenchymal factors. Development (Cambridge, England) *122*, 439-447.

Golosow, N., and Grobstein, C. (1962). Epitheliomesenchymal interaction in pancreatic morphogenesis. Developmental biology *4*, 242-255.

Grapin-Botton, A. (2005). Ductal cells of the pancreas. Int J Biochem Cell Biol *37*, 504-510.

Gu, G., Dubauskaite, J., and Melton, D.A. (2002). Direct evidence for the pancreatic lineage: NGN3+ cells are islet progenitors and are distinct from duct progenitors. Development (Cambridge, England) *129*, 2447-2457.

Gu, Y., Lindner, J., Kumar, A., Yuan, W., and Magnuson, M.A. (2011). Rictor/mTORC2 is essential for maintaining a balance between beta-cell proliferation and cell size. Diabetes *60*, 827-837.

Guillam, M.T., Hummler, E., Schaerer, E., Yeh, J.I., Birnbaum, M.J., Beermann, F., Schmidt, A., Deriaz, N., and Thorens, B. (1997). Early diabetes and abnormal postnatal pancreatic islet development in mice lacking Glut-2. Nature genetics *17*, 327-330.

Guney, M.A., Petersen, C.P., Boustani, A., Duncan, M.R., Gunasekaran, U., Menon, R., Warfield, C., Grotendorst, G.R., Means, A.L., Economides, A.N., *et al.* (2011). Connective tissue growth factor acts within both endothelial cells and {beta} cells to promote proliferation of developing {beta} cells. Proc Natl Acad Sci U S A *108*, 15242-15247.

Gupta, R.K., Gao, N., Gorski, R.K., White, P., Hardy, O.T., Rafiq, K., Brestelli, J.E., Chen, G., Stoeckert, C.J., Jr., and Kaestner, K.H. (2007). Expansion of adult beta-cell mass in response to increased metabolic demand is dependent on HNF-4alpha. Genes & development *21*, 756-769.

Hanna, L.A., Foreman, R.K., Tarasenko, I.A., Kessler, D.S., and Labosky, P.A. (2002). Requirement for Foxd3 in maintaining pluripotent cells of the early mouse embryo. Genes & development *16*, 2650-2661.

Hara, M., Wang, X., Kawamura, T., Bindokas, V.P., Dizon, R.F., Alcoser, S.Y., Magnuson, M.A., and Bell, G.I. (2003). Transgenic mice with green fluorescent protein-labeled pancreatic beta -cells. Am J Physiol Endocrinol Metab *284*, E177-183.

Hariharan, D., Saied, A., and Kocher, H.M. (2008). Analysis of mortality rates for pancreatic cancer across the world. HPB (Oxford) *10*, 58-62.

Harper, J.W., Adami, G.R., Wei, N., Keyomarsi, K., and Elledge, S.J. (1993). The p21 Cdk-interacting protein Cip1 is a potent inhibitor of G1 cyclin-dependent kinases. Cell *75*, 805-816.

Harrison, K.A., Thaler, J., Pfaff, S.L., Gu, H., and Kehrl, J.H. (1999). Pancreas dorsal lobe agenesis and abnormal islets of Langerhans in Hlxb9-deficient mice. Nature genetics *23*, 71-75.

Hart, A., Papadopoulou, S., and Edlund, H. (2003). Fgf10 maintains notch activation, stimulates proliferation, and blocks differentiation of pancreatic epithelial cells. Dev Dyn *228*, 185-193.

Hasegawa, Y., Ogihara, T., Yamada, T., Ishigaki, Y., Imai, J., Uno, K., Gao, J., Kaneko, K., Ishihara, H., Sasano, H., *et al.* (2007). Bone marrow (BM) transplantation promotes beta-cell regeneration after acute injury through BM cell mobilization. Endocrinology *148*, 2006-2015.

Haumaitre, C., Barbacci, E., Jenny, M., Ott, M.O., Gradwohl, G., and Cereghini, S. (2005). Lack of TCF2/vHNF1 in mice leads to pancreas agenesis. Proc Natl Acad Sci U S A *102*, 1490-1495.

Herbarth, B., Pingault, V., Bondurand, N., Kuhlbrodt, K., Hermans-Borgmeyer, I., Puliti, A., Lemort, N., Goossens, M., and Wegner, M. (1998). Mutation of the Sry-related Sox10 gene in Dominant megacolon, a mouse model for human Hirschsprung disease. Proc Natl Acad Sci U S A *95*, 5161-5165.

Herrera, P.L. (2000). Adult insulin- and glucagon-producing cells differentiate from two independent cell lineages. Development (Cambridge, England) *127*, 2317-2322.

Hess, D., Li, L., Martin, M., Sakano, S., Hill, D., Strutt, B., Thyssen, S., Gray, D.A., and Bhatia, M. (2003). Bone marrow-derived stem cells initiate pancreatic regeneration. Nat Biotechnol *21*, 763-770.

Hingorani, S.R., Petricoin, E.F., Maitra, A., Rajapakse, V., King, C., Jacobetz, M.A., Ross, S., Conrads, T.P., Veenstra, T.D., Hitt, B.A., *et al.* (2003). Preinvasive and invasive ductal pancreatic cancer and its early detection in the mouse. Cancer Cell *4*, 437-450.

Honig, G., Liou, A., Berger, M., German, M.S., and Tecott, L.H. (2010). Precise pattern of recombination in serotonergic and hypothalamic neurons in a Pdx1-cre transgenic mouse line. J Biomed Sci *17*, 82.

Horb, L.D., and Slack, J.M. (2000). Role of cell division in branching morphogenesis and differentiation of the embryonic pancreas. Int J Dev Biol *44*, 791-796.

Hromas, R., Ye, H., Spinella, M., Dmitrovsky, E., Xu, D., and Costa, R.H. (1999). Genesis, a Winged Helix transcriptional repressor, has embryonic expression limited to the neural crest, and stimulates proliferation in vitro in a neural development model. Cell Tissue Res *297*, 371-382.

Huang da, W., Sherman, B.T., and Lempicki, R.A. (2009). Systematic and integrative analysis of large gene lists using DAVID bioinformatics resources. Nat Protoc *4*, 44-57.

Huang, H.D., Lee, T.Y., Tzeng, S.W., and Horng, J.T. (2005). KinasePhos: a web tool for identifying protein kinase-specific phosphorylation sites. Nucleic Acids Res *33*, W226-229.

Huerta, M., Munoz, R., Tapia, R., Soto-Reyes, E., Ramirez, L., Recillas-Targa, F., Gonzalez-Mariscal, L., and Lopez-Bayghen, E. (2007). Cyclin D1 is transcriptionally down-regulated by ZO-2 via an E box and the transcription factor c-Myc. Mol Biol Cell *18*, 4826-4836.

Iacovino, M., Bosnakovski, D., Fey, H., Rux, D., Bajwa, G., Mahen, E., Mitanoska, A., Xu, Z., and Kyba, M. (2011a). Inducible cassette exchange: a rapid and efficient system enabling conditional gene expression in embryonic stem and primary cells. Stem cells (Dayton, Ohio) *29*, 1580-1588.

Iacovino, M., Chong, D., Szatmari, I., Hartweck, L., Rux, D., Caprioli, A., Cleaver, O., and Kyba, M. (2011b). HoxA3 is an apical regulator of haemogenic endothelium. Nat Cell Biol *13*, 72-78.

Ianus, A., Holz, G.G., Theise, N.D., and Hussain, M.A. (2003). In vivo derivation of glucose-competent pancreatic endocrine cells from bone marrow without evidence of cell fusion. J Clin Invest *111*, 843-850.

Iguchi, H., Ikeda, Y., Okamura, M., Tanaka, T., Urashima, Y., Ohguchi, H., Takayasu, S., Kojima, N., Iwasaki, S., Ohashi, R., *et al.* (2005). SOX6 attenuates glucose-stimulated insulin secretion by repressing PDX1 transcriptional activity and is down-regulated in hyperinsulinemic obese mice. The Journal of biological chemistry *280*, 37669-37680.

Iguchi, H., Urashima, Y., Inagaki, Y., Ikeda, Y., Okamura, M., Tanaka, T., Uchida, A., Yamamoto, T.T., Kodama, T., and Sakai, J. (2007). SOX6 suppresses cyclin D1 promoter activity by interacting with beta-catenin and histone deacetylase 1, and its down-regulation induces pancreatic beta-cell proliferation. The Journal of biological chemistry *282*, 19052-19061.

Imai, J., Katagiri, H., Yamada, T., Ishigaki, Y., Suzuki, T., Kudo, H., Uno, K., Hasegawa, Y., Gao, J., Kaneko, K., *et al.* (2008). Regulation of pancreatic beta cell mass by neuronal signals from the liver. Science (New York, NY *322*, 1250-1254.

Imai, J., Oka, Y., and Katagiri, H. (2009). Identification of a novel mechanism regulating beta-cell mass: neuronal relay from the liver to pancreatic beta-cells. Islets *1*, 75-77.

Jacobs, F.M., van der Heide, L.P., Wijchers, P.J., Burbach, J.P., Hoekman, M.F., and Smidt, M.P. (2003). FoxO6, a novel member of the FoxO class of transcription factors with distinct shuttling dynamics. The Journal of biological chemistry *278*, 35959-35967.

Jacquemin, P., Yoshitomi, H., Kashima, Y., Rousseau, G.G., Lemaigre, F.P., and Zaret, K.S. (2006). An endothelial-mesenchymal relay pathway regulates early phases of pancreas development. Developmental biology *290*, 189-199.

Jetton, T.L., Lausier, J., LaRock, K., Trotman, W.E., Larmie, B., Habibovic, A., Peshavaria, M., and Leahy, J.L. (2005). Mechanisms of compensatory beta-cell growth in insulin-resistant rats: roles of Akt kinase. Diabetes *54*, 2294-2304.

Johnson, J.D., Ahmed, N.T., Luciani, D.S., Han, Z., Tran, H., Fujita, J., Misler, S., Edlund, H., and Polonsky, K.S. (2003). Increased islet apoptosis in Pdx1+/- mice. J Clin Invest *111*, 1147-1160.

Jonsson, J., Carlsson, L., Edlund, T., and Edlund, H. (1994). Insulin-promoter-factor 1 is required for pancreas development in mice. Nature *371*, 606-609.

Jorgensen, M.C., Ahnfelt-Ronne, J., Hald, J., Madsen, O.D., Serup, P., and Hecksher-Sorensen, J. (2007). An illustrated review of early pancreas development in the mouse. Endocrine reviews *28*, 685-705.

Jung, J., Zheng, M., Goldfarb, M., and Zaret, K.S. (1999). Initiation of mammalian liver development from endoderm by fibroblast growth factors. Science (New York, NY *284*, 1998-2003.

Kalinichenko, V.V., Major, M.L., Wang, X., Petrovic, V., Kuechle, J., Yoder, H.M., Dennewitz, M.B., Shin, B., Datta, A., Raychaudhuri, P., *et al.* (2004). Foxm1b transcription factor is essential for development of hepatocellular carcinomas and is negatively regulated by the p19ARF tumor suppressor. Genes & development *18*, 830-850.

Karnik, S.K., Chen, H., McLean, G.W., Heit, J.J., Gu, X., Zhang, A.Y., Fontaine, M., Yen, M.H., and Kim, S.K. (2007). Menin controls growth of pancreatic beta-cells in pregnant mice and promotes gestational diabetes mellitus. Science (New York, NY *318*, 806-809.

Karnik, S.K., Hughes, C.M., Gu, X., Rozenblatt-Rosen, O., McLean, G.W., Xiong, Y., Meyerson, M., and Kim, S.K. (2005). Menin regulates pancreatic islet growth by promoting histone methylation and expression of genes encoding p27Kip1 and p18INK4c. Proc Natl Acad Sci U S A *102*, 14659-14664.

Kassem, S.A., Ariel, I., Thornton, P.S., Scheimberg, I., and Glaser, B. (2000). Beta-cell proliferation and apoptosis in the developing normal human pancreas and in hyperinsulinism of infancy. Diabetes *49*, 1325-1333.

Kawaguchi, Y., Cooper, B., Gannon, M., Ray, M., MacDonald, R.J., and Wright, C.V. (2002). The role of the transcriptional regulator Ptf1a in converting intestinal to pancreatic progenitors. Nature genetics *32*, 128-134.

Kim, H., Toyofuku, Y., Lynn, F.C., Chak, E., Uchida, T., Mizukami, H., Fujitani, Y., Kawamori, R., Miyatsuka, T., Kosaka, Y., *et al.* (2010). Serotonin regulates pancreatic beta cell mass during pregnancy. Nat Med *16*, 804-808.

Kim, H.S., Shin, J.H., Moon, H.J., Kim, T.S., Kang, I.H., Seok, J.H., Kim, I.Y., Park, K.L., and Han, S.Y. (2002). Evaluation of the 20-day pubertal female assay in Sprague-Dawley rats treated with DES, tamoxifen, testosterone, and flutamide. Toxicol Sci *67*, 52-62.

Kim, S.K., Hebrok, M., and Melton, D.A. (1997). Notochord to endoderm signaling is required for pancreas development. Development (Cambridge, England) *124*, 4243-4252.

Kojima, H., Fujimiya, M., Matsumura, K., Younan, P., Imaeda, H., Maeda, M., and Chan, L. (2003). NeuroD-betacellulin gene therapy induces islet neogenesis in the liver and reverses diabetes in mice. Nat Med *9*, 596-603.

Krapp, A., Knofler, M., Ledermann, B., Burki, K., Berney, C., Zoerkler, N., Hagenbuchle, O., and Wellauer, P.K. (1998). The bHLH protein PTF1-p48 is essential for the formation of the exocrine and the correct spatial organization of the endocrine pancreas. Genes & development *12*, 3752-3763.

Krishnamurthy, J., Ramsey, M.R., Ligon, K.L., Torrice, C., Koh, A., Bonner-Weir, S., and Sharpless, N.E. (2006). p16INK4a induces an age-dependent decline in islet regenerative potential. Nature *443*, 453-457.

Kroon, E., Martinson, L.A., Kadoya, K., Bang, A.G., Kelly, O.G., Eliazer, S., Young, H., Richardson, M., Smart, N.G., Cunningham, J., *et al.* (2008). Pancreatic endoderm derived from human embryonic stem cells generates glucose-responsive insulin-secreting cells in vivo. Nat Biotechnol *26*, 443-452.

Kuang, S., Kuroda, K., Le Grand, F., and Rudnicki, M.A. (2007). Asymmetric self-renewal and commitment of satellite stem cells in muscle. Cell *129*, 999-1010.

Kumar, M., Jordan, N., Melton, D., and Grapin-Botton, A. (2003). Signals from lateral plate mesoderm instruct endoderm toward a pancreatic fate. Developmental biology *259*, 109-122.

Kurtz, A., Zimmer, A., Schnutgen, F., Bruning, G., Spener, F., and Muller, T. (1994). The expression pattern of a novel gene encoding brain-fatty acid binding protein correlates with neuronal and glial cell development. Development (Cambridge, England) *120*, 2637-2649.

Kushner, J.A., Ciemerych, M.A., Sicinska, E., Wartschow, L.M., Teta, M., Long, S.Y., Sicinski, P., and White, M.F. (2005). Cyclins D2 and D1 are essential for postnatal pancreatic beta-cell growth. Mol Cell Biol *25*, 3752-3762.

Labosky, P.A., and Kaestner, K.H. (1998). The winged helix transcription factor Hfh2 is expressed in neural crest and spinal cord during mouse development. Mechanisms of development *76*, 185-190.

Lamba, D.A., Hayes, S., Karl, M.O., and Reh, T. (2008). Baf60c is a component of the neural progenitor-specific BAF complex in developing retina. Dev Dyn *237*, 3016-3023.

Lammert, E., Cleaver, O., and Melton, D. (2001). Induction of pancreatic differentiation by signals from blood vessels. Science (New York, NY *294*, 564-567.

Lammert, E., Cleaver, O., and Melton, D. (2003). Role of endothelial cells in early pancreas and liver development. Mechanisms of development *120*, 59-64.

Laybutt, D.R., Preston, A.M., Akerfeldt, M.C., Kench, J.G., Busch, A.K., Biankin, A.V., and Biden, T.J. (2007). Endoplasmic reticulum stress contributes to beta cell apoptosis in type 2 diabetes. Diabetologia *50*, 752-763.

Laybutt, D.R., Weir, G.C., Kaneto, H., Lebet, J., Palmiter, R.D., Sharma, A., and Bonner-Weir, S. (2002). Overexpression of c-Myc in beta-cells of transgenic mice causes proliferation and apoptosis, downregulation of insulin gene expression, and diabetes. Diabetes *51*, 1793-1804.

Le Douarin, N.M.a.K., C. (1999). The Neural Crest (Cambridge, Cambridge University Press).

Lee, H.C., Huang, H.Y., Lin, C.Y., Chen, Y.H., and Tsai, H.J. (2006). Foxd3 mediates zebrafish myf5 expression during early somitogenesis. Developmental biology *290*, 359-372.

Lee, H.J., Goring, W., Ochs, M., Muhlfeld, C., Steding, G., Paprotta, I., Engel, W., and Adham, I.M. (2004). Sox15 is required for skeletal muscle regeneration. Mol Cell Biol *24*, 8428-8436.

Lee, Y.B., Colley, S., Norman, M., Biamonti, G., and Uney, J.B. (2007). SAFB re-distribution marks steps of the apoptotic process. Exp Cell Res *313*, 3914-3923.

Li, J., Lee, B., and Lee, A.S. (2006). Endoplasmic reticulum stress-induced apoptosis: multiple pathways and activation of p53-up-regulated modulator of apoptosis (PUMA) and NOXA by p53. The Journal of biological chemistry *281*, 7260-7270.

Liber, D., Domaschenz, R., Holmqvist, P.H., Mazzarella, L., Georgiou, A., Leleu, M., Fisher, A.G., Labosky, P.A., and Dillon, N. (2010). Epigenetic priming of a pre-B cell-

specific enhancer through binding of Sox2 and Foxd3 at the ESC stage. Cell Stem Cell *7*, 114-126.

Lifson, N., Lassa, C.V., and Dixit, P.K. (1985). Relation between blood flow and morphology in islet organ of rat pancreas. Am J Physiol *249*, E43-48.

Lin, C.Y., Gurlo, T., Haataja, L., Hsueh, W.A., and Butler, P.C. (2005). Activation of peroxisome proliferator-activated receptor-gamma by rosiglitazone protects human islet cells against human islet amyloid polypeptide toxicity by a phosphatidylinositol 3'-kinase-dependent pathway. The Journal of clinical endocrinology and metabolism *90*, 6678-6686.

Lindsay, R.S. (2008). Commentary: Type 2 diabetes and birth weight--genetic and environmental effects. Int J Epidemiol *37*, 192-193.

Liu, Y., and Labosky, P.A. (2008). Regulation of embryonic stem cell self-renewal and pluripotency by Foxd3. Stem cells (Dayton, Ohio) *26*, 2475-2484.

Liu, Z., and Habener, J.F. (2008). Glucagon-like peptide-1 activation of TCF7L2-dependent Wnt signaling enhances pancreatic beta cell proliferation. The Journal of biological chemistry *283*, 8723-8735.

Lonovics, J., Guzman, S., Devitt, P.G., Hejtmancik, K.E., Suddith, R.L., Rayford, P.L., and Thompson, J.C. (1981). Action of pancreatic polypeptide on exocrine pancreas and on release of cholecystokinin and secretin. Endocrinology *108*, 1925-1930.

Lyssenko, V., Lupi, R., Marchetti, P., Del Guerra, S., Orho-Melander, M., Almgren, P., Sjogren, M., Ling, C., Eriksson, K.F., Lethagen, A.L., *et al.* (2007). Mechanisms by which common variants in the TCF7L2 gene increase risk of type 2 diabetes. J Clin Invest *117*, 2155-2163.

Ma, R.Y., Tong, T.H., Cheung, A.M., Tsang, A.C., Leung, W.Y., and Yao, K.M. (2005). Raf/MEK/MAPK signaling stimulates the nuclear translocation and transactivating activity of FOXM1c. J Cell Sci *118*, 795-806.

Maedler, K., Carr, R.D., Bosco, D., Zuellig, R.A., Berney, T., and Donath, M.Y. (2005). Sulfonylurea induced beta-cell apoptosis in cultured human islets. The Journal of clinical endocrinology and metabolism *90*, 501-506.

Maehr, R., Chen, S., Snitow, M., Ludwig, T., Yagasaki, L., Goland, R., Leibel, R.L., and Melton, D.A. (2009). Generation of pluripotent stem cells from patients with type 1 diabetes. Proc Natl Acad Sci U S A *106*, 15768-15773.

Martin, M., Gallego-Llamas, J., Ribes, V., Kedinger, M., Niederreither, K., Chambon, P., Dolle, P., and Gradwohl, G. (2005). Dorsal pancreas agenesis in retinoic acid-deficient Raldh2 mutant mice. Developmental biology *284*, 399-411.

Maruyama, M., Ichisaka, T., Nakagawa, M., and Yamanaka, S. (2005). Differential roles for Sox15 and Sox2 in transcriptional control in mouse embryonic stem cells. The Journal of biological chemistry *280*, 24371-24379.

Maschhoff, K.L., Anziano, P.Q., Ward, P., and Baldwin, H.S. (2003). Conservation of Sox4 gene structure and expression during chicken embryogenesis. Gene *320*, 23-30.

Mathews, V., Hanson, P.T., Ford, E., Fujita, J., Polonsky, K.S., and Graubert, T.A. (2004). Recruitment of bone marrow-derived endothelial cells to sites of pancreatic beta-cell injury. Diabetes *53*, 91-98.

Mathiesen, E.R., and Vaz, J.A. (2008). Insulin treatment in diabetic pregnancy. Diabetes/metabolism research and reviews *24 Suppl 2*, S3-20.

Matsuoka, T.A., Zhao, L., Artner, I., Jarrett, H.W., Friedman, D., Means, A., and Stein, R. (2003). Members of the large Maf transcription family regulate insulin gene transcription in islet beta cells. Mol Cell Biol *23*, 6049-6062.

Matthews, D.R., Cull, C.A., Stratton, I.M., Holman, R.R., and Turner, R.C. (1998). UKPDS 26: Sulphonylurea failure in non-insulin-dependent diabetic patients over six years. UK Prospective Diabetes Study (UKPDS) Group. Diabet Med *15*, 297-303.

Meier, J.J., Bhushan, A., Butler, A.E., Rizza, R.A., and Butler, P.C. (2005). Sustained beta cell apoptosis in patients with long-standing type 1 diabetes: indirect evidence for islet regeneration? Diabetologia *48*, 2221-2228.

Milne, T.A., Hughes, C.M., Lloyd, R., Yang, Z., Rozenblatt-Rosen, O., Dou, Y., Schnepp, R.W., Krankel, C., Livolsi, V.A., Gibbs, D., *et al.* (2005). Menin and MLL cooperatively regulate expression of cyclin-dependent kinase inhibitors. Proc Natl Acad Sci U S A *102*, 749-754.

Miralles, F., Czernichow, P., Ozaki, K., Itoh, N., and Scharfmann, R. (1999). Signaling through fibroblast growth factor receptor 2b plays a key role in the development of the exocrine pancreas. Proc Natl Acad Sci U S A *96*, 6267-6272.

Molotkov, A., Molotkova, N., and Duester, G. (2005). Retinoic acid generated by Raldh2 in mesoderm is required for mouse dorsal endodermal pancreas development. Dev Dyn *232*, 950-957.

Montanya, E., Nacher, V., Biarnes, M., and Soler, J. (2000). Linear correlation between beta-cell mass and body weight throughout the lifespan in Lewis rats: role of beta-cell hyperplasia and hypertrophy. Diabetes *49*, 1341-1346.

Morioka, T., Asilmaz, E., Hu, J., Dishinger, J.F., Kurpad, A.J., Elias, C.F., Li, H., Elmquist, J.K., Kennedy, R.T., and Kulkarni, R.N. (2007). Disruption of leptin receptor expression in the pancreas directly affects beta cell growth and function in mice. J Clin Invest *117*, 2860-2868.

Mundell, N., Plank, J., Frist, A., Zhu, L., Shin, M., Southard-Smith, M., and Labosky, P. (2011). Enteric nervous system specific deletion of Foxd3 disrupts glial cell differentiation and activates compensatory enteric progenitors. Developmental biology *Manuscript resubmitted*.

Mundell, N.A., and Labosky, P.A. (2011). Neural crest stem cell multipotency requires Foxd3 to maintain neural potential and repress mesenchymal fates. Development (Cambridge, England) *138*, 641-652.

Murtaugh, L.C., and Melton, D.A. (2003). Genes, signals, and lineages in pancreas development. Annual review of cell and developmental biology *19*, 71-89.

Navarro-Tableros, V., Sanchez-Soto, M.C., Garcia, S., and Hiriart, M. (2004). Autocrine regulation of single pancreatic beta-cell survival. Diabetes *53*, 2018-2023.

Nekrep, N., Wang, J., Miyatsuka, T., and German, M.S. (2008). Signals from the neural crest regulate beta-cell mass in the pancreas. Development (Cambridge, England) *135*, 2151-2160.

Nelms, B.L., Labosky P.A. (2010). Transcriptional Control of Neural Crest Development (Morgan and Claypool Life Sciences).

Nelms, B.L., Pfaltzgraff, E.R., and Labosky, P.A. (2011). Functional interaction between Foxd3 and Pax3 in cardiac neural crest development. Genesis *49*, 10-23.

Nielsen, J.H., Galsgaard, E.D., Moldrup, A., Friedrichsen, B.N., Billestrup, N., Hansen, J.A., Lee, Y.C., and Carlsson, C. (2001). Regulation of beta-cell mass by hormones and growth factors. Diabetes *50 Suppl 1*, S25-29.

Nir, T., Melton, D.A., and Dor, Y. (2007). Recovery from diabetes in mice by beta cell regeneration. J Clin Invest *117*, 2553-2561.

Ochi, H., Hans, S., and Westerfield, M. (2008). Smarcd3 regulates the timing of zebrafish myogenesis onset. The Journal of biological chemistry *283*, 3529-3536.

Oda, E., Ohki, R., Murasawa, H., Nemoto, J., Shibue, T., Yamashita, T., Tokino, T., Taniguchi, T., and Tanaka, N. (2000). Noxa, a BH3-only member of the Bcl-2 family and candidate mediator of p53-induced apoptosis. Science (New York, NY *288*, 1053-1058.

Offield, M.F., Jetton, T.L., Labosky, P.A., Ray, M., Stein, R.W., Magnuson, M.A., Hogan, B.L., and Wright, C.V. (1996). PDX-1 is required for pancreatic outgrowth and differentiation of the rostral duodenum. Development (Cambridge, England) *122*, 983-995.

Ohlsson, H., Karlsson, K., and Edlund, T. (1993). IPF1, a homeodomain-containing transactivator of the insulin gene. Embo J *12*, 4251-4259.

Olerud, J., Kanaykina, N., Vasylovska, S., King, D., Sandberg, M., Jansson, L., and Kozlova, E.N. (2009). Neural crest stem cells increase beta cell proliferation and improve islet function in co-transplanted murine pancreatic islets. Diabetologia *52*, 2594-2601.

Orcheson, L.J., Rickard, S.E., Seidl, M.M., and Thompson, L.U. (1998). Flaxseed and its mammalian lignan precursor cause a lengthening or cessation of estrous cycling in rats. Cancer Lett *125*, 69-76.

Pan, F.C., and Wright, C. (2011). Pancreas organogenesis: from bud to plexus to gland. Dev Dyn *240*, 530-565.

Pan, G., Li, J., Zhou, Y., Zheng, H., and Pei, D. (2006). A negative feedback loop of transcription factors that controls stem cell pluripotency and self-renewal. FASEB J *20*, 1730-1732.

Papizan, J.B., Singer, R.A., Tschen, S.I., Dhawan, S., Friel, J.M., Hipkens, S.B., Magnuson, M.A., Bhushan, A., and Sussel, L. (2011). Nkx2.2 repressor complex regulates islet beta-cell specification and prevents beta-to-alpha-cell reprogramming. Genes & development *25*, 2291-2305.

Park, S., Hong, S.M., Sung, S.R., and Jung, H.K. (2008). Long-term effects of central leptin and resistin on body weight, insulin resistance, and beta-cell function and mass by the modulation of hypothalamic leptin and insulin signaling. Endocrinology *149*, 445-454.

Parsons, J.A., Brelje, T.C., and Sorenson, R.L. (1992). Adaptation of islets of Langerhans to pregnancy: increased islet cell proliferation and insulin secretion correlates with the onset of placental lactogen secretion. Endocrinology *130*, 1459-1466.

Pattyn, A., Morin, X., Cremer, H., Goridis, C., and Brunet, J.F. (1999). The homeobox gene Phox2b is essential for the development of autonomic neural crest derivatives. Nature *399*, 366-370.

Pei, X.H., Bai, F., Tsutsui, T., Kiyokawa, H., and Xiong, Y. (2004). Genetic evidence for functional dependency of p18Ink4c on Cdk4. Mol Cell Biol *24*, 6653-6664.

Peppel, K., Zhang, L., Orman, E.S., Hagen, P.O., Amalfitano, A., Brian, L., and Freedman, N.J. (2005). Activation of vascular smooth muscle cells by TNF and PDGF: overlapping and complementary signal transduction mechanisms. Cardiovasc Res *65*, 674-682.

Percival, A.C., and Slack, J.M. (1999). Analysis of pancreatic development using a cell lineage label. Exp Cell Res *247*, 123-132.

Perera, H.K., Caldwell, M.E., Hayes-Patterson, D., Teng, L., Peshavaria, M., Jetton, T.L., and Labosky, P.A. (2006). Expression and shifting subcellular localization of the transcription factor, Foxd3, in embryonic and adult pancreas. Gene Expr Patterns *6*, 971-977.

Peshavaria, M., Larmie, B.L., Lausier, J., Satish, B., Habibovic, A., Roskens, V., Larock, K., Everill, B., Leahy, J.L., and Jetton, T.L. (2006). Regulation of pancreatic beta-cell regeneration in the normoglycemic 60% partial-pancreatectomy mouse. Diabetes *55*, 3289-3298.

Plank, J.L., Frist, A.Y., Legrone, A.W., Magnuson, M.A., and Labosky, P.A. (2011a). Loss of Foxd3 Results in Decreased beta-Cell Proliferation and Glucose Intolerance During Pregnancy. Endocrinology *152*, 4589-4600.

Plank, J.L., Mundell, N.A., Frist, A.Y., LeGrone, A.W., Kim, T., Musser, M.A., Walter, T.J., and Labosky, P.A. (2011b). Influence and timing of arrival of murine neural crest on pancreatic beta cell development and maturation. Developmental biology *349*, 321-330.

Porat, S., Weinberg-Corem, N., Tornovsky-Babaey, S., Schyr-Ben-Haroush, R., Hija, A., Stolovich-Rain, M., Dadon, D., Granot, Z., Ben-Hur, V., White, P., *et al.* (2011). Control of pancreatic beta cell regeneration by glucose metabolism. Cell metabolism *13*, 440-449.

Prado, C.L., Pugh-Bernard, A.E., Elghazi, L., Sosa-Pineda, B., and Sussel, L. (2004). Ghrelin cells replace insulin-producing beta cells in two mouse models of pancreas development. Proc Natl Acad Sci U S A *101*, 2924-2929.

Presnell, J.K., Shreibman, M.P. (1997). Humason's Animal Tissue Techniques (Baltimore, MD, The Johns Hopkins University Press).

Prowse, K.R., and Greider, C.W. (1995). Developmental and tissue-specific regulation of mouse telomerase and telomere length. Proc Natl Acad Sci U S A *92*, 4818-4822.

Radziszewska, A., Schroer, S.A., Choi, D., Tajmir, P., Radulovich, N., Ho, J.C., Wang, L., Liadis, N., Hakem, R., Tsao, M.S., *et al.* (2009). Absence of caspase-3 protects pancreatic {beta}-cells from c-Myc-induced apoptosis without leading to tumor formation. The Journal of biological chemistry *284*, 10947-10956.

Rahl, P.B., Lin, C.Y., Seila, A.C., Flynn, R.A., McCuine, S., Burge, C.B., Sharp, P.A., and Young, R.A. (2010). c-Myc regulates transcriptional pause release. Cell *141*, 432-445.

Rane, S.G., Dubus, P., Mettus, R.V., Galbreath, E.J., Boden, G., Reddy, E.P., and Barbacid, M. (1999). Loss of Cdk4 expression causes insulin-deficient diabetes and Cdk4 activation results in beta-islet cell hyperplasia. Nature genetics *22*, 44-52.

Raum, J.C., Gerrish, K., Artner, I., Henderson, E., Guo, M., Sussel, L., Schisler, J.C., Newgard, C.B., and Stein, R. (2006). FoxA2, Nkx2.2, and PDX-1 regulate islet beta-cell-specific mafA expression through conserved sequences located between base pairs -8118 and -7750 upstream from the transcription start site. Mol Cell Biol *26*, 5735-5743.

Razavi, R., Chan, Y., Afifiyan, F.N., Liu, X.J., Wan, X., Yantha, J., Tsui, H., Tang, L., Tsai, S., Santamaria, P., *et al.* (2006). TRPV1+ sensory neurons control beta cell stress and islet inflammation in autoimmune diabetes. Cell *127*, 1123-1135.

Rhodes, C.J. (2005). Type 2 diabetes-a matter of beta-cell life and death? Science (New York, NY *307*, 380-384.

Rieck, S., and Kaestner, K.H. (2010). Expansion of beta-cell mass in response to pregnancy. Trends Endocrinol Metab *21*, 151-158.

Rieck, S., White, P., Schug, J., Fox, A.J., Smirnova, O., Gao, N., Gupta, R.K., Wang, Z.V., Scherer, P.E., Keller, M.P., *et al.* (2009). The transcriptional response of the islet to pregnancy in mice. Molecular endocrinology (Baltimore, Md *23*, 1702-1712.

Roskoski, R., Jr. (2007). Sunitinib: a VEGF and PDGF receptor protein kinase and angiogenesis inhibitor. Biochem Biophys Res Commun *356*, 323-328.

Rukstalis, J.M., and Habener, J.F. (2007). Snail2, a mediator of epithelial-mesenchymal transitions, expressed in progenitor cells of the developing endocrine pancreas. Gene Expr Patterns *7*, 471-479.

Sabatakos, G., Sims, N.A., Chen, J., Aoki, K., Kelz, M.B., Amling, M., Bouali, Y., Mukhopadhyay, K., Ford, K., Nestler, E.J., *et al.* (2000). Overexpression of DeltaFosB transcription factor(s) increases bone formation and inhibits adipogenesis. Nat Med *6*, 985-990.

Salpeter, S.J., Klein, A.M., Huangfu, D., Grimsby, J., and Dor, Y. (2010). Glucose and aging control the quiescence period that follows pancreatic beta cell replication. Development (Cambridge, England) *137*, 3205-3213.

Sauka-Spengler, T., and Bronner-Fraser, M. (2008). A gene regulatory network orchestrates neural crest formation. Nat Rev Mol Cell Biol *9*, 557-568.

Savage, J., Conley, A.J., Blais, A., and Skerjanc, I.S. (2009). SOX15 and SOX7 differentially regulate the myogenic program in P19 cells. Stem cells (Dayton, Ohio) *27*, 1231-1243.

Saxena, R., Voight, B.F., Lyssenko, V., Burtt, N.P., de Bakker, P.I., Chen, H., Roix, J.J., Kathiresan, S., Hirschhorn, J.N., Daly, M.J., *et al.* (2007). Genome-wide association analysis identifies loci for type 2 diabetes and triglyceride levels. Science (New York, NY *316*, 1331-1336.

Scaglia, L., Cahill, C.J., Finegood, D.T., and Bonner-Weir, S. (1997). Apoptosis participates in the remodeling of the endocrine pancreas in the neonatal rat. Endocrinology *138*, 1736-1741.

Scaglia, L., Smith, F.E., and Bonner-Weir, S. (1995). Apoptosis contributes to the involution of beta cell mass in the post partum rat pancreas. Endocrinology *136*, 5461-5468.

Scheuner, D., Song, B., McEwen, E., Liu, C., Laybutt, R., Gillespie, P., Saunders, T., Bonner-Weir, S., and Kaufman, R.J. (2001). Translational control is required for the unfolded protein response and in vivo glucose homeostasis. Mol Cell *7*, 1165-1176.

Scheuner, D., Vander Mierde, D., Song, B., Flamez, D., Creemers, J.W., Tsukamoto, K., Ribick, M., Schuit, F.C., and Kaufman, R.J. (2005). Control of mRNA translation preserves endoplasmic reticulum function in beta cells and maintains glucose homeostasis. Nat Med *11*, 757-764.

Schilham, M.W., Oosterwegel, M.A., Moerer, P., Ya, J., de Boer, P.A., van de Wetering, M., Verbeek, S., Lamers, W.H., Kruisbeek, A.M., Cumano, A., *et al.* (1996). Defects in cardiac outflow tract formation and pro-B-lymphocyte expansion in mice lacking Sox-4. Nature *380*, 711-714.

Schnutgen, F., Borchers, T., Muller, T., and Spener, F. (1996). Heterologous expression and characterisation of mouse brain fatty acid binding protein. Biol Chem Hoppe Seyler *377*, 211-215.

Schwitzgebel, V.M., Scheel, D.W., Conners, J.R., Kalamaras, J., Lee, J.E., Anderson, D.J., Sussel, L., Johnson, J.D., and German, M.S. (2000). Expression of neurogenin3 reveals an islet cell precursor population in the pancreas. Development (Cambridge, England) *127*, 3533-3542.

Scott, L.J., Mohlke, K.L., Bonnycastle, L.L., Willer, C.J., Li, Y., Duren, W.L., Erdos, M.R., Stringham, H.M., Chines, P.S., Jackson, A.U., *et al.* (2007). A genome-wide association study of type 2 diabetes in Finns detects multiple susceptibility variants. Science (New York, NY *316*, 1341-1345.

Seymour, P.A., Freude, K.K., Tran, M.N., Mayes, E.E., Jensen, J., Kist, R., Scherer, G., and Sander, M. (2007). SOX9 is required for maintenance of the pancreatic progenitor cell pool. Proc Natl Acad Sci U S A *104*, 1865-1870.

Shapiro, A.M., Lakey, J.R., Ryan, E.A., Korbutt, G.S., Toth, E., Warnock, G.L., Kneteman, N.M., and Rajotte, R.V. (2000). Islet transplantation in seven patients with type 1 diabetes mellitus using a glucocorticoid-free immunosuppressive regimen. The New England journal of medicine *343*, 230-238.

Shu, L., Sauter, N.S., Schulthess, F.T., Matveyenko, A.V., Oberholzer, J., and Maedler, K. (2008). Transcription factor 7-like 2 regulates beta-cell survival and function in human pancreatic islets. Diabetes *57*, 645-653.

Slack, J.M. (1995). Developmental biology of the pancreas. Development (Cambridge, England) *121*, 1569-1580.

Smith, C.L., and Tallquist, M.D. (2010). PDGF function in diverse neural crest cell populations. Cell Adh Migr *4*, 561-566.

Song, J., Xu, Y., Hu, X., Choi, B., and Tong, Q. (2010). Brain expression of Cre recombinase driven by pancreas-specific promoters. Genesis *48*, 628-634.

Sorenson, R.L., and Brelje, T.C. (1997). Adaptation of islets of Langerhans to pregnancy: beta-cell growth, enhanced insulin secretion and the role of lactogenic hormones. Hormone and metabolic research Hormon- und Stoffwechselforschung *29*, 301-307.

Soriano, P. (1999). Generalized lacZ expression with the ROSA26 Cre reporter strain. Nature genetics *21*, 70-71.

Southard-Smith, E.M., Kos, L., and Pavan, W.J. (1998). Sox10 mutation disrupts neural crest development in Dom Hirschsprung mouse model. Nature genetics *18*, 60-64.

Srinivas, S., Watanabe, T., Lin, C.S., William, C.M., Tanabe, Y., Jessell, T.M., and Costantini, F. (2001). Cre reporter strains produced by targeted insertion of EYFP and ECFP into the ROSA26 locus. BMC Dev Biol *1*, 4.

Steiner, A.B., Engleka, M.J., Lu, Q., Piwarzyk, E.C., Yaklichkin, S., Lefebvre, J.L., Walters, J.W., Pineda-Salgado, L., Labosky, P.A., and Kessler, D.S. (2006). FoxD3 regulation of Nodal in the Spemann organizer is essential for Xenopus dorsal mesoderm development. Development (Cambridge, England) *133*, 4827-4838.

Steiner, D.J., Kim, A., Miller, K., and Hara, M. (2010). Pancreatic islet plasticity: interspecies comparison of islet architecture and composition. Islets *2*, 135-145.

Stoffel, M., and Duncan, S.A. (1997). The maturity-onset diabetes of the young (MODY1) transcription factor HNF4alpha regulates expression of genes required for glucose transport and metabolism. Proc Natl Acad Sci U S A *94*, 13209-13214.

Stoffers, D.A., Ferrer, J., Clarke, W.L., and Habener, J.F. (1997a). Early-onset type-II diabetes mellitus (MODY4) linked to IPF1. Nature genetics *17*, 138-139.

Stoffers, D.A., Zinkin, N.T., Stanojevic, V., Clarke, W.L., and Habener, J.F. (1997b). Pancreatic agenesis attributable to a single nucleotide deletion in the human IPF1 gene coding sequence. Nature genetics *15*, 106-110.

Sussel, L., Kalamaras, J., Hartigan-O'Connor, D.J., Meneses, J.J., Pedersen, R.A., Rubenstein, J.L., and German, M.S. (1998). Mice lacking the homeodomain transcription factor Nkx2.2 have diabetes due to arrested differentiation of pancreatic beta cells. Development (Cambridge, England) *125*, 2213-2221.

Takahashi, K., and Yamanaka, S. (2006). Induction of pluripotent stem cells from mouse embryonic and adult fibroblast cultures by defined factors. Cell *126*, 663-676.

Tam, P.P. (1981). The control of somitogenesis in mouse embryos. J Embryol Exp Morphol *65 Suppl*, 103-128.

Tapia, R., Huerta, M., Islas, S., Avila-Flores, A., Lopez-Bayghen, E., Weiske, J., Huber, O., and Gonzalez-Mariscal, L. (2009). Zona occludens-2 inhibits cyclin D1 expression and cell proliferation and exhibits changes in localization along the cell cycle. Mol Biol Cell *20*, 1102-1117.

Teng, L., Mundell, N.A., Frist, A.Y., Wang, Q., and Labosky, P.A. (2008). Requirement for Foxd3 in the maintenance of neural crest progenitors. Development (Cambridge, England) *135*, 1615-1624.

Teta, M., Rankin, M.M., Long, S.Y., Stein, G.M., and Kushner, J.A. (2007). Growth and regeneration of adult beta cells does not involve specialized progenitors. Dev Cell *12*, 817-826.

Thomas, A.J., and Erickson, C.A. (2009). FOXD3 regulates the lineage switch between neural crest-derived glial cells and pigment cells by repressing MITF through a non-canonical mechanism. Development (Cambridge, England) *136*, 1849-1858.

Tokuyama, Y., Sturis, J., DePaoli, A.M., Takeda, J., Stoffel, M., Tang, J., Sun, X., Polonsky, K.S., and Bell, G.I. (1995). Evolution of beta-cell dysfunction in the male Zucker diabetic fatty rat. Diabetes *44*, 1447-1457.

Tompers, D.M., Foreman, R.K., Wang, Q., Kumanova, M., and Labosky, P.A. (2005). Foxd3 is required in the trophoblast progenitor cell lineage of the mouse embryo. Developmental biology *285*, 126-137.

Tower, A.M., Trinward, A., Lee, K., Joseph, L., Jacobson, H.I., Bennett, J.A., and Andersen, T.T. (2009). AFPep, a novel drug for the prevention and treatment of breast cancer, does not disrupt the estrous cycle or fertility in rats. Oncol Rep *22*, 49-56.

Tweedie, E., Artner, I., Crawford, L., Poffenberger, G., Thorens, B., Stein, R., Powers, A.C., and Gannon, M. (2006). Maintenance of hepatic nuclear factor 6 in postnatal islets impairs terminal differentiation and function of beta-cells. Diabetes *55*, 3264-3270.

Uchida, T., Nakamura, T., Hashimoto, N., Matsuda, T., Kotani, K., Sakaue, H., Kido, Y., Hayashi, Y., Nakayama, K.I., White, M.F., *et al.* (2005). Deletion of Cdkn1b ameliorates hyperglycemia by maintaining compensatory hyperinsulinemia in diabetic mice. Nat Med *11*, 175-182.

Van Assche, F.A., Aerts, L., and De Prins, F. (1978). A morphological study of the endocrine pancreas in human pregnancy. British journal of obstetrics and gynaecology *85*, 818-820.

van der Vlag, J., and Otte, A.P. (1999). Transcriptional repression mediated by the human polycomb-group protein EED involves histone deacetylation. Nature genetics *23*, 474-478.

van Vliet-Ostaptchouk, J.V., Shiri-Sverdlov, R., Zhernakova, A., Strengman, E., van Haeften, T.W., Hofker, M.H., and Wijmenga, C. (2007). Association of variants of

transcription factor 7-like 2 (TCF7L2) with susceptibility to type 2 diabetes in the Dutch Breda cohort. Diabetologia *50*, 59-62.

Vasavada, R.C., Garcia-Ocana, A., Zawalich, W.S., Sorenson, R.L., Dann, P., Syed, M., Ogren, L., Talamantes, F., and Stewart, A.F. (2000). Targeted expression of placental lactogen in the beta cells of transgenic mice results in beta cell proliferation, islet mass augmentation, and hypoglycemia. The Journal of biological chemistry *275*, 15399-15406.

Voltarelli, J.C., Couri, C.E., Stracieri, A.B., Oliveira, M.C., Moraes, D.A., Pieroni, F., Coutinho, M., Malmegrim, K.C., Foss-Freitas, M.C., Simoes, B.P., *et al.* (2007). Autologous nonmyeloablative hematopoietic stem cell transplantation in newly diagnosed type 1 diabetes mellitus. JAMA *297*, 1568-1576.

Vouriot, M.A., Marchal, A.L., Olive, D., Benz Lemoine, E., Schmitt, M., and Hoeffel, J.C. (1985). [Neuroblastoma of the tail of the pancreas. Apropos of a case]. J Radiol *66*, 547-549.

Wang, I.C., Chen, Y.J., Hughes, D., Petrovic, V., Major, M.L., Park, H.J., Tan, Y., Ackerson, T., and Costa, R.H. (2005). Forkhead box M1 regulates the transcriptional network of genes essential for mitotic progression and genes encoding the SCF (Skp2-Cks1) ubiquitin ligase. Mol Cell Biol *25*, 10875-10894.

Wang, J., Elghazi, L., Parker, S.E., Kizilocak, H., Asano, M., Sussel, L., and Sosa-Pineda, B. (2004). The concerted activities of Pax4 and Nkx2.2 are essential to initiate pancreatic beta-cell differentiation. Developmental biology *266*, 178-189.

Wang, J., Rao, S., Chu, J., Shen, X., Levasseur, D.N., Theunissen, T.W., and Orkin, S.H. (2006). A protein interaction network for pluripotency of embryonic stem cells. Nature *444*, 364-368.

Watt, A.J., Zhao, R., Li, J., and Duncan, S.A. (2007). Development of the mammalian liver and ventral pancreas is dependent on GATA4. BMC Dev Biol *7*, 37.

Wernig, M., Meissner, A., Foreman, R., Brambrink, T., Ku, M., Hochedlinger, K., Bernstein, B.E., and Jaenisch, R. (2007). In vitro reprogramming of fibroblasts into a pluripotent ES-cell-like state. Nature *448*, 318-324.

Wessells, N.K., Cohen, J.H. (1967). Early pancreas organogenesis: Morphogenesis, tissue interactions, and mass effects. Developmental biology *15*, 237-270.

White, P., May, C.L., Lamounier, R.N., Brestelli, J.E., and Kaestner, K.H. (2008). Defining pancreatic endocrine precursors and their descendants. Diabetes *57*, 654-668.

Wicksteed, B., Brissova, M., Yan, W., Opland, D.M., Plank, J.L., Reinert, R.B., Dickson, L.M., Tamarina, N.A., Philipson, L.H., Shostak, A., *et al.* (2010). Conditional gene targeting in mouse pancreatic ss-Cells: analysis of ectopic Cre transgene expression in the brain. Diabetes *59*, 3090-3098.

Xie, T., Chen, M., and Weinstein, L.S. (2010). Pancreas-specific Gsalpha deficiency has divergent effects on pancreatic alpha- and beta-cell proliferation. J Endocrinol *206*, 261-269.

Xu, J., Pope, S.D., Jazirehi, A.R., Attema, J.L., Papathanasiou, P., Watts, J.A., Zaret, K.S., Weissman, I.L., and Smale, S.T. (2007). Pioneer factor interactions and unmethylated CpG dinucleotides mark silent tissue-specific enhancers in embryonic stem cells. Proc Natl Acad Sci U S A *104*, 12377-12382.

Xu, J., Watts, J.A., Pope, S.D., Gadue, P., Kamps, M., Plath, K., Zaret, K.S., and Smale, S.T. (2009). Transcriptional competence and the active marking of tissue-specific enhancers by defined transcription factors in embryonic and induced pluripotent stem cells. Genes & development *23*, 2824-2838.

Ya, J., Schilham, M.W., de Boer, P.A., Moorman, A.F., Clevers, H., and Lamers, W.H. (1998). Sox4-deficiency syndrome in mice is an animal model for common trunk. Circulation research *83*, 986-994.

Yaklichkin, S., Steiner, A.B., Lu, Q., and Kessler, D.S. (2007). FoxD3 and Grg4 physically interact to repress transcription and induce mesoderm in Xenopus. The Journal of biological chemistry *282*, 2548-2557.

Yakovlev, A.G., Di Giovanni, S., Wang, G., Liu, W., Stoica, B., and Faden, A.I. (2004). BOK and NOXA are essential mediators of p53-dependent apoptosis. The Journal of biological chemistry *279*, 28367-28374.

Yamashita, H., Shao, J., Ishizuka, T., Klepcyk, P.J., Muhlenkamp, P., Qiao, L., Hoggard, N., and Friedman, J.E. (2001). Leptin administration prevents spontaneous gestational diabetes in heterozygous Lepr(db/+) mice: effects on placental leptin and fetal growth. Endocrinology *142*, 2888-2897.

Yao, J.C. (2007). Neuroendocrine tumors. Molecular targeted therapy for carcinoid and islet-cell carcinoma. Best Pract Res Clin Endocrinol Metab *21*, 163-172.

Yechoor, V., Liu, V., Espiritu, C., Paul, A., Oka, K., Kojima, H., and Chan, L. (2009). Neurogenin3 is sufficient for transdetermination of hepatic progenitor cells into neo-islets in vivo but not transdifferentiation of hepatocytes. Dev Cell *16*, 358-373.

Yoshitomi, H., and Zaret, K.S. (2004). Endothelial cell interactions initiate dorsal pancreas development by selectively inducing the transcription factor Ptf1a. Development (Cambridge, England) *131*, 807-817.

Young, A.P., and Wagers, A.J. (2010). Pax3 induces differentiation of juvenile skeletal muscle stem cells without transcriptional upregulation of canonical myogenic regulatory factors. J Cell Sci *123*, 2632-2639.

Yu, J., Vodyanik, M.A., Smuga-Otto, K., Antosiewicz-Bourget, J., Frane, J.L., Tian, S., Nie, J., Jonsdottir, G.A., Ruotti, V., Stewart, R., *et al.* (2007). Induced pluripotent stem cell lines derived from human somatic cells. Science (New York, NY *318*, 1917-1920.

Zeggini, E., Weedon, M.N., Lindgren, C.M., Frayling, T.M., Elliott, K.S., Lango, H., Timpson, N.J., Perry, J.R., Rayner, N.W., Freathy, R.M., *et al.* (2007). Replication of genome-wide association signals in UK samples reveals risk loci for type 2 diabetes. Science (New York, NY *316*, 1336-1341.

Zhang, C., Moriguchi, T., Kajihara, M., Esaki, R., Harada, A., Shimohata, H., Oishi, H., Hamada, M., Morito, N., Hasegawa, K., *et al.* (2005). MafA is a key regulator of glucose-stimulated insulin secretion. Mol Cell Biol *25*, 4969-4976.

Zhang, H., Ackermann, A.M., Gusarova, G.A., Lowe, D., Feng, X., Kopsombut, U.G., Costa, R.H., and Gannon, M. (2006). The FoxM1 transcription factor is required to maintain pancreatic beta-cell mass. Molecular endocrinology (Baltimore, Md *20*, 1853-1866.

Zhang, H., Zhang, J., Pope, C.F., Crawford, L.A., Vasavada, R.C., Jagasia, S.M., and Gannon, M. (2010). Gestational diabetes mellitus resulting from impaired beta-cell compensation in the absence of FoxM1, a novel downstream effector of placental lactogen. Diabetes *59*, 143-152.

Zhang, N., Wei, P., Gong, A., Chiu, W.T., Lee, H.T., Colman, H., Huang, H., Xue, J., Liu, M., Wang, Y., *et al.* (2011). FoxM1 Promotes beta-Catenin Nuclear Localization and Controls Wnt Target-Gene Expression and Glioma Tumorigenesis. Cancer Cell *20*, 427-442.

Zhao, L., Guo, M., Matsuoka, T.A., Hagman, D.K., Parazzoli, S.D., Poitout, V., and Stein, R. (2005). The islet beta cell-enriched MafA activator is a key regulator of insulin gene transcription. The Journal of biological chemistry *280*, 11887-11894.

Zhong, L., Georgia, S., Tschen, S.I., Nakayama, K., and Bhushan, A. (2007). Essential role of Skp2-mediated p27 degradation in growth and adaptive expansion of pancreatic beta cells. J Clin Invest *117*, 2869-2876.

Zhou, Q., Brown, J., Kanarek, A., Rajagopal, J., and Melton, D.A. (2008). In vivo reprogramming of adult pancreatic exocrine cells to beta-cells. Nature *455*, 627-632.

Zhou, Q., Law, A.C., Rajagopal, J., Anderson, W.J., Gray, P.A., and Melton, D.A. (2007). A multipotent progenitor domain guides pancreatic organogenesis. Dev Cell *13*, 103-114.